Supporting Information

Selective, rapid and optically switchable regulation of protein function in live mammalian cells

Yu-Hsuan Tsai,[†] Sebastian Essig,[†] John R. James, Kathrin Lang & Jason W. Chin[*]

Medical Research Council Laboratory of Molecular Biology, Francis Crick Avenue, Cambridge CB2 0QH, UK

[†] These authors contributed equally.

[*]Correspondence: chin@mrc-lmb.cam.ac.uk

Table of Contents:

1. Rate Simulation

We use the kinetic simulator, Tenua,[1] to simulate the bioorthogonal tethering under various bioorthogonal reaction rates (k_1 = 10^{-3} to 10^4 $M^{-1}s^{-1}$), k_{on} (k_2 = 10^{-3} to 10^4 $M^{-1}s^{-1}$), K_D (10^{-4} to 10^{-2} M) and effective molarity (1 to 10 M). We set the protein concentration as 1 μM.[2] In order to avoid non-tethering mediated inhibition, we set the inhibitor conjugate concentration as 1 μM, which is at least 100 fold smaller than the K_D in all cases. From the results in Supplementary Table 1, we observe that: (1) when $k_1 << k_{-2}$ (k_{off}), the reaction progress depends mainly on k_1 and k_{-2} (k_{off}); (2) when $k_1 >> k_{-2}$ (k_{off}), k_{-2} (k_{off}) has little effect on the reaction progress; (3) k_2 (k_{on}) only plays a role when $k_1 \geq k_{-2}$ (k_{off}). By comparing **Supplementary Tables 1** and **2**, we noticed the effective molarity has the biggest effect when $k_1 \leq k_{-2}$ (k_{off}). We also performed simulation where the pathway 1 (Figure 1) was ignored (**Supplementary Table S3**), and the results are identical as in **Supplementary Table** 1 when $k_2 >> k_1$. We further simulated the effect of reaction rate (k_1 = 10^{-3} to 10^4 $M^{-1}s^{-1}$) and small molecule concentration (10^{-6} to 10^{-4} M) on pure bioorthogonal tethering (**Supplementary Table 2**), which is exemplified by the Petersson group in inhibiting *E. coli* aminoacyl transferase.[3]

Supplementary Table S1. Percent conversion at different time point without rate enhancement.

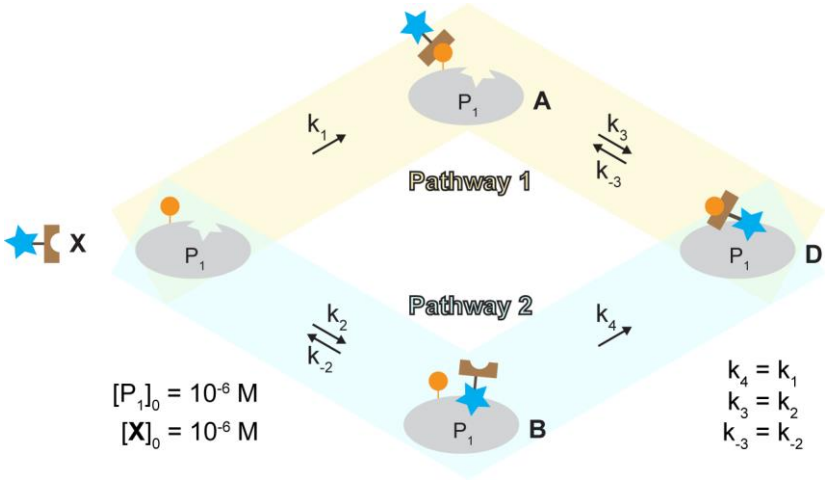

% **D**	k_1	10^{-3}			10^{-2}			10^{-1}			1			10			10^{2}			10^{3}			10^{4}		
Time	k_2 / K_D	10^{-4}	10^{-3}	10^{-2}	10^{-4}	10^{-3}	10^{-2}	10^{-4}	10^{-3}	10^{-2}	10^{-4}	10^{-3}	10^{-2}	10^{-4}	10^{-3}	10^{-2}	10^{-4}	10^{-3}	10^{-2}	10^{-4}	10^{-3}	10^{-2}	10^{-4}	10^{-3}	10^{-2}
5 min	10^4	0.3	0.03	0.003	3	0.3	0.03	21	3	0.3	60	21	3	73	60	21	75	73	60	77	77	74	86	86	85
	10^5	0.3	0.03	0.003	3	0.3	0.03	23	3	0.3	73	23	3	94	73	23	97	94	73	97	97	93	97	97	96
	10^6	0.3	0.03	0.003	3	0.3	0.03	23	3	0.3	74	23	3	97	75	23	99	96	74	100	99	96	100	100	98
10 min	10^4	0.6	0.06	0.006	6	0.6	0.06	35	6	0.6	75	35	6	85	75	35	86	85	75	87	87	85	92	92	91
	10^5	0.6	0.06	0.006	6	0.6	0.06	37	6	0.6	85	37	6	97	85	37	98	97	84	98	98	96	99	98	97
	10^6	0.6	0.06	0.006	6	0.6	0.06	37	6	0.6	86	37	6	98	86	37	100	98	85	100	100	97	100	100	99
30 min	10^4	2	0.2	0.02	15	2	0.2	62	15	2	90	62	15	94	90	62	95	94	89	95	95	94	97	97	96
	10^5	2	0.2	0.02	15	2	0.2	64	15	2	94	64	15	99	94	64	99	99	93	99	99	98	99	99	98
	10^6	2	0.2	0.02	15	2	0.2	64	15	2	95	64	15	99	95	64	100	99	94	100	100	98	100	100	99

Supplementary Table S2. Conversion at different time point with rate enhancement. Values differing less than three percentage points in comparison to **Supplementary Table 1** are highlighted in blue.

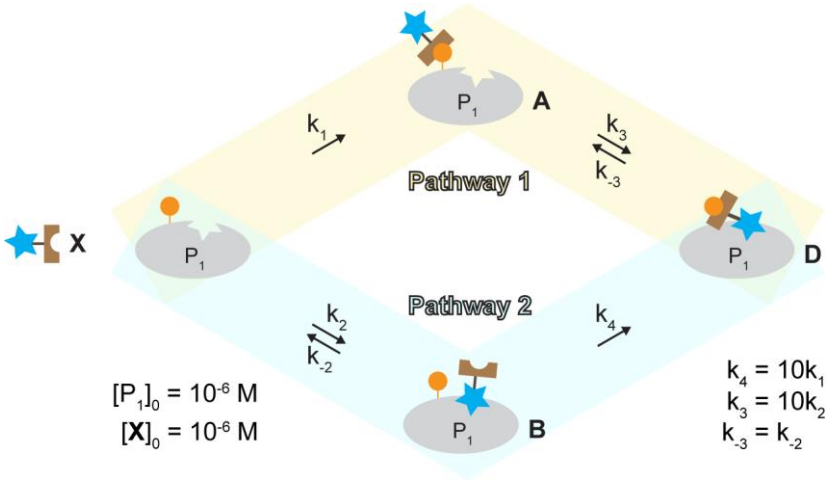

% **D**	k_1	10^{-3}			10^{-2}			10^{-1}			1			10			10^{2}			10^{3}		
Time	k_2 K_D	10^{-4}	10^{-3}	10^{-2}	10^{-4}	10^{-3}	10^{-2}	10^{-4}	10^{-3}	10^{-2}	10^{-4}	10^{-3}	10^{-2}	10^{-4}	10^{-3}	10^{-2}	10^{-4}	10^{-3}	10^{-2}	10^{-4}	10^{-3}	10^{-2}
5 min	10^4	3	0.3	0.03	21	3	0.3	60	21	3	73	60	21	75	73	60	75	75	73	77	77	77
	10^5	3	0.3	0.03	23	3	0.3	73	23	3	94	73	23	96	94	73	97	97	94	97	97	96
	10^6	3	0.3	0.2	23	3	2	75	23	15	96	75	62	99	97	90	100	99	94	100	100	95
10 min	10^4	6	0.6	0.06	35	6	0.6	75	35	6	85	75	35	86	85	75	86	86	85	87	87	87
	10^5	6	0.6	0.06	37	6	0.6	84	37	6	97	84	37	98	97	84	98	98	97	98	98	98
	10^6	6	0.6	0.2	37	6	2	86	37	15	98	86	64	100	98	94	100	100	99	100	100	99
30 min	10^4	15	2	0.2	62	15	2	90	62	15	94	90	62	95	94	90	95	95	94	95	95	95
	10^5	15	2	0.06	64	15	0.6	94	64	6	99	94	37	99	99	86	99	99	98	99	99	100
	10^6	15	2	0.2	64	15	2	95	64	15	99	95	64	100	99	95	100	100	99	100	100	100

Supplementary Table S3. Percent conversion at different time point without rate enhancement and ignoring the pathway 1 (**Figure 1**). Values differing more than three percentage points in comparison to **Supplementary Table 1** are highlighted in red.

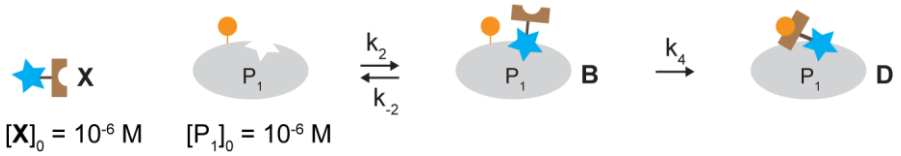

% **D**	k_1	10^{-3}			10^{-2}			10^{-1}			1			10			10^{2}			10^{3}			10^{4}		
Time	k_2 / K_D	10^{-4}	10^{-3}	10^{-2}	10^{-4}	10^{-3}	10^{-2}	10^{-4}	10^{-3}	10^{-2}	10^{-4}	10^{-3}	10^{-2}	10^{-4}	10^{-3}	10^{-2}	10^{-4}	10^{-3}	10^{-2}	10^{-4}	10^{-3}	10^{-2}	10^{-4}	10^{-3}	10^{-2}
5 min	10^4	0.3	0.03	0.003	3	0.3	0.03	21	3	0.3	60	21	3	73	60	21	75	73	60	75	75	73	75	75	75
	10^5	0.3	0.03	0.003	3	0.3	0.03	23	3	0.3	73	23	3	94	73	23	97	94	73	97	97	94	97	97	96
	10^6	0.3	0.03	0.003	3	0.3	0.03	23	3	0.3	74	23	3	97	75	23	99	96	75	100	100	96	100	100	99
10 min	10^4	0.6	0.06	0.006	6	0.6	0.06	35	6	0.6	75	35	6	85	75	35	86	85	75	86	86	85	86	86	86
	10^5	0.6	0.06	0.006	6	0.6	0.06	37	6	0.6	85	37	6	97	85	37	98	97	85	98	98	97	98	98	98
	10^6	0.6	0.06	0.006	6	0.6	0.06	37	6	0.6	86	37	6	98	86	37	100	98	86	100	100	98	100	100	100
30 min	10^4	2	0.2	0.02	15	2	0.2	62	15	2	90	62	15	94	90	62	95	94	90	95	95	94	95	95	95
	10^5	2	0.2	0.02	15	2	0.2	64	15	2	94	64	15	99	94	64	99	99	94	99	99	99	99	99	99
	10^6	2	0.2	0.02	15	2	0.2	64	15	2	95	64	15	99	95	64	100	99	95	100	100	99	100	100	100

Supplementary Table S4. Percent conversion at different time points in pure bioorthogonal tethering. when $[P_1]_0 = 10^{-6}$ M

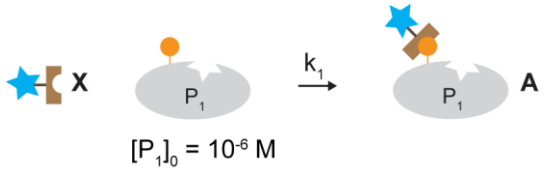

% **A** TIME	$[X]_0$	k_1	10^{-3}	10^{-2}	10^{-1}	1	10	10^2	10^3	10^4
5 min	10^{-6}		0.00003	0.0003	0.003	0.03	0.3	3	23	75
	10^{-5}		0.0003	0.003	0.03	0.3	3	26	94	100
	10^{-4}		0.003	0.03	0.3	3	26	95	100	100
10 min	10^{-6}		0.00006	0.0006	0.006	0.06	0.6	6	38	86
	10^{-5}		0.0006	0.006	0.06	0.6	6	44	100	100
	10^{-4}		0.006	0.06	0.6	6	45	100	100	100
30 min	10^{-6}		0.0002	0.002	0.02	0.2	2	15	64	95
	10^{-5}		0.002	0.02	0.2	2	16	82	100	100
	10^{-4}		0.02*	0.2	2	16	83	100	100	100

* 0.9% conversion after 2

2. Supplementary Figures

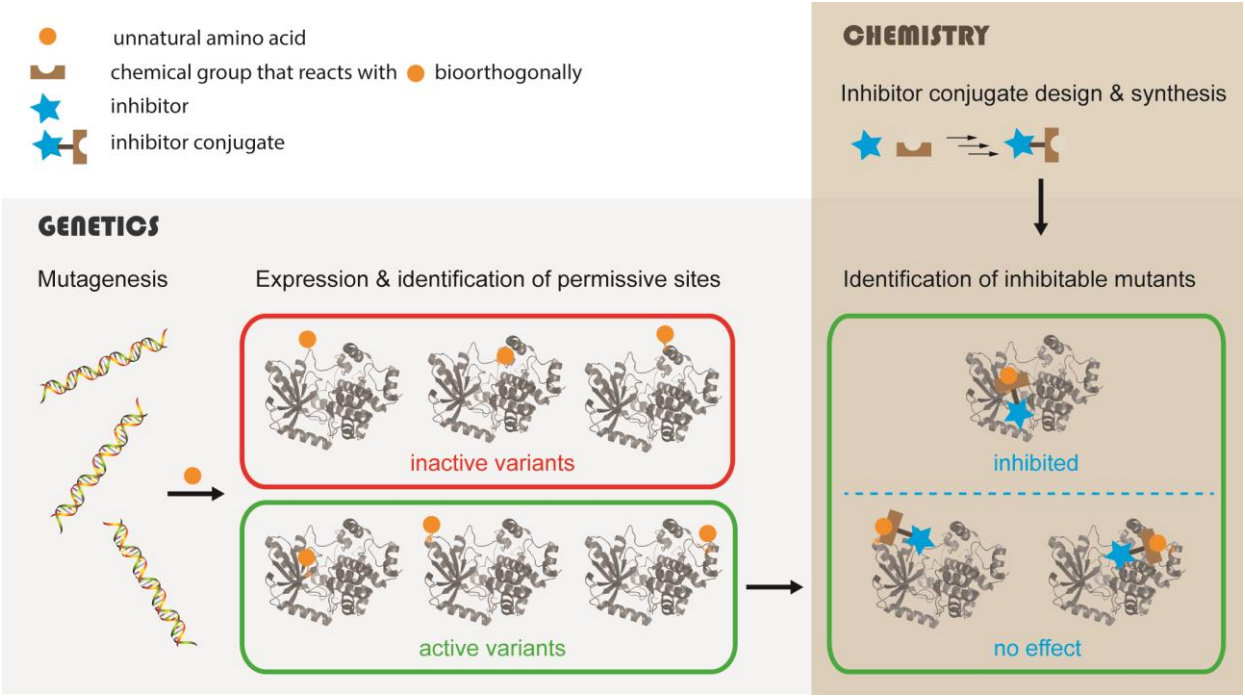

Supplementary Figure S1. Identification of permissive sites for bioorthogonal unnatural amino acid incorporation and the design and synthesis of inhibitor conjugates enable the identification of proteins bearing bioorthogonal groups that can be inhibited by biorthogonal ligand tethering (BOLT).

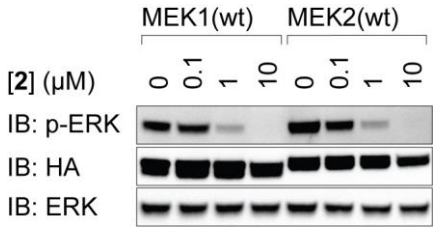

Supplementary Figure S2. Inhibition of MEK1 and MEK2 by **2**. HEK293ET cells were transiently transfected with MEK-HA and EGFP-ERK2 for 24 h in a low serum media. The cells were then incubated with **2** (or DMSO for control) at the indicated concentration for 3 h, followed by western blot analysis. EGFP-ERK2 is detected by immunoblot (IB) for ERK and phosphorylated EGFP-ERK2 is detected by immunoblot for pERK. All MEK variants are HA tagged, contain DD mutations making them constitutively active and are detected by immunoblot for HA.

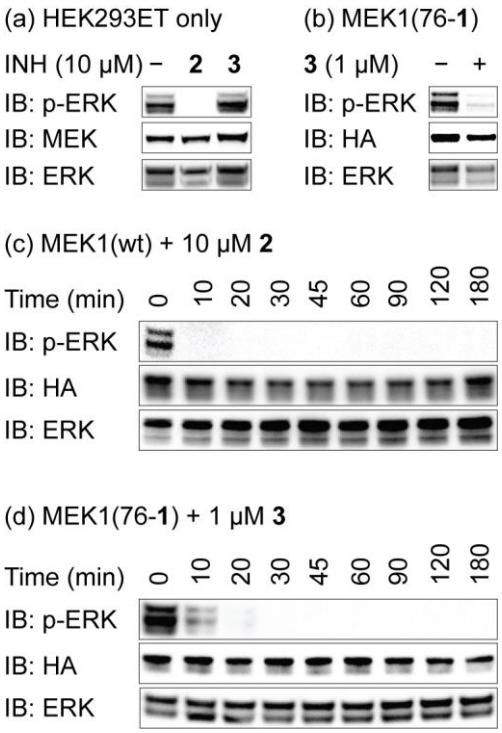

Supplementary Figure S3. Detection of MEK inhibition by monitoring phosphorylation of endogenous ERK1/2. (a) HEK293ET cells were incubated with 10 μM inhibitor (INH) **2** or **3** for 3 h before the addition of EGF (100 ng/ml). Cells were lysed after 15 min for the western blot analysis. (b) HEK293ET cells were transiently transfected with MEK1(76-TAG)-HA and BCNRS/$tRNA_{CUA}$ pair for 24 h in a low serum media containing 0.5 mM **1**, followed by incubation with 1 μM **3** for 3 h before the western blot analysis. (c) Experiment was performed as described in (b) except wild type (wt) MEK1 was expressed and incubated with 10 μM **2** for 0-180 min. (d) Experiment was performed as described in (b) except cells were incubated with 1 μM **3** for 0-180 min. EGFP-ERK2 is detected by immunoblot (IB) for ERK and phosphorylated EGFP-ERK2 is detected by immunoblot for pERK. All MEK variants are HA tagged, contain DD mutations making them constitutively active and are detected by immunoblot for HA.

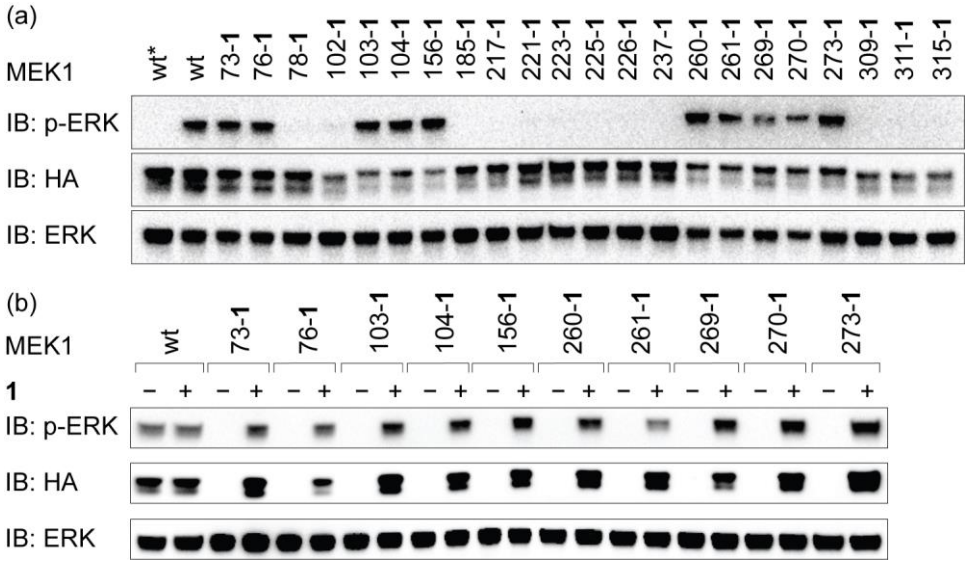

Supplementary Figure S4. Identification of permissive sites in MEK1 (a) and unnatural amino acid dependence of MEK1(XXX-**1**) expression (b). HEK293ET cells were transiently transfected with MEK1-HA, BCNRS/$tRNA_{CUA}$ pair and EGFP-ERK2 for 24 h in a low serum media with or without 0.5 mM **1**, followed by the western blot analysis. Variants 73-**1**, 76-**1**, 103-**1**, 104-**1**, 156-**1**, 260-**1**, 261-**1**, 269-**1**, 270-**1** and 273-**1** retain the kinase activity, and their expression and kinase activity depend on the presence of **1**. EGFP-ERK2 is detected by immunoblot (IB) for ERK and phosphorylated EGFP-ERK2 is detected by immunoblot for pERK. All MEK variants are HA tagged, contain DD mutations making them constitutively active and are detected by immunoblot for HA. The wt* has no DD mutation and hence does not phosphorylate ERK in the low serum media.

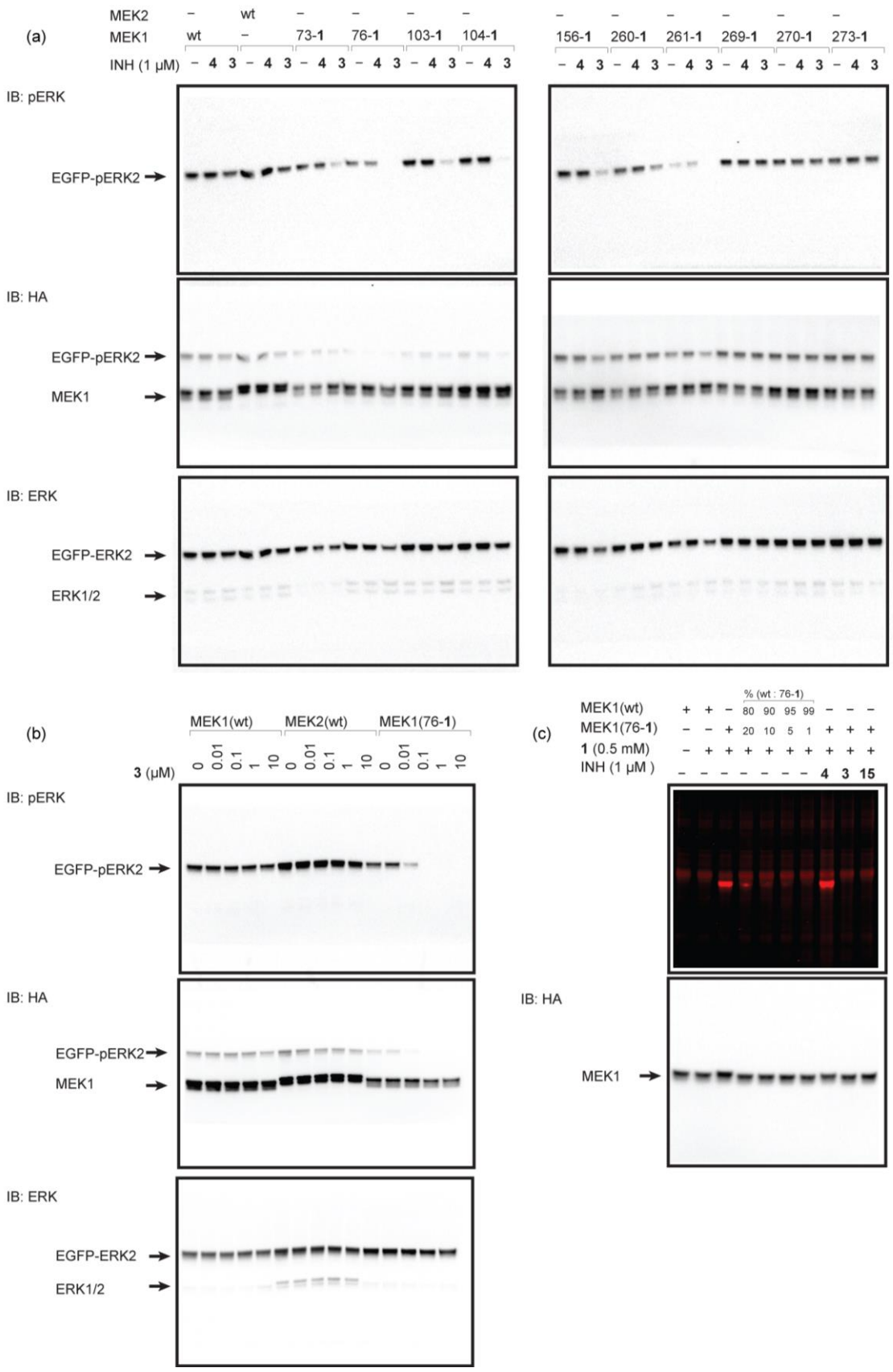
(a)
MEK2
MEK1
INH (1 μM)
wt
73-1
76-1
103-1
104-1
156-1
260-1
261-1
269-1
270-1
273-1
IB: pERK
EGFP-pERK2
IB: HA
EGFP-pERK2
MEK1
IB: ERK
EGFP-ERK2
ERK1/2
(b)
MEK1(wt)
MEK2(wt)
MEK1(76-1)
3 (μM)
0
0.01
0.1
1
10
IB: pERK
EGFP-pERK2
IB: HA
EGFP-pERK2
MEK1
IB: ERK
EGFP-ERK2
ERK1/2
(c)
% (wt : 76-1)
MEK1(wt)
MEK1(76-1)
1 (0.5 mM)
INH (1 μM)
80 90 95 99
20 10 5 1
4 3 15
IB: HA
MEK1

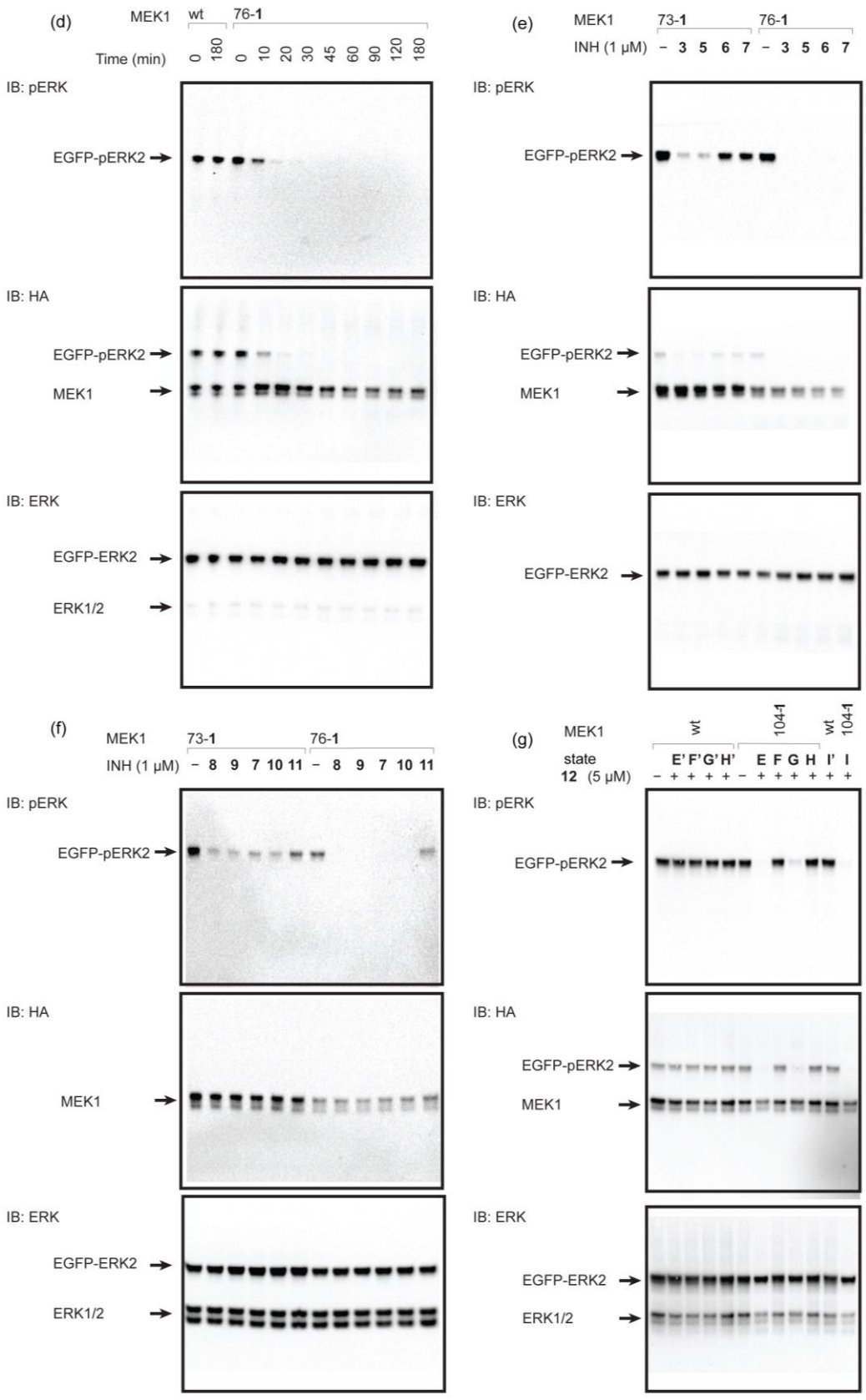
(d)
MEK1
wt
76-1
Time (min)
0 180 0 10 20 30 45 60 90 120 180
IB: pERK
EGFP-pERK2
IB: HA
EGFP-pERK2
MEK1
IB: ERK
EGFP-ERK2
ERK1/2
(e)
MEK1
73-1
76-1
INH (1 μM) – 3 5 6 7 – 3 5 6 7
IB: pERK
EGFP-pERK2
IB: HA
EGFP-pERK2
MEK1
IB: ERK
EGFP-ERK2
(f)
MEK1
73-1
76-1
INH (1 μM) – 8 9 7 10 11 – 8 9 7 10 11
IB: pERK
EGFP-pERK2
IB: HA
MEK1
IB: ERK
EGFP-ERK2
ERK1/2
(g)
MEK1
wt
104-1
wt
104-1
state
E' F' G' H' E F G H I' I
12 (5 μM) – + + + + – + + + + + +
IB: pERK
EGFP-pERK2
IB: HA
EGFP-pERK2
MEK1
IB: ERK
EGFP-ERK2
ERK1/2

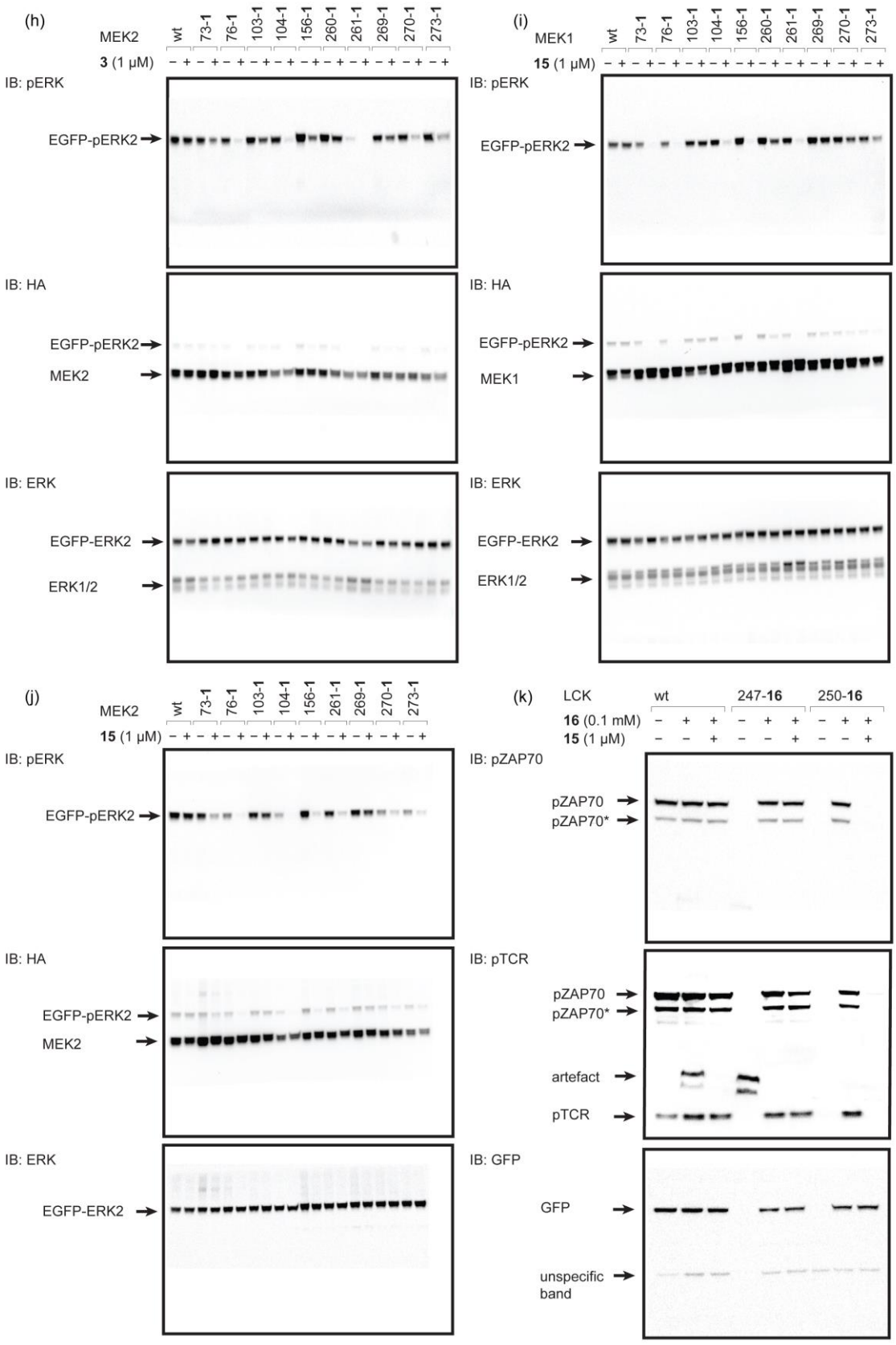

Supplementary Figure S5. Full western blots of all main text experiments with corresponding figure legends. (a) figure 2b; (b) figure 2c; (c) figure 2d; (d) figure 2e; (e) figure 3a; (f) figure 3b; (g) figure 4c; (h) figure 5; (i) figure 6a; (j) figure 6b; (k) figure 7a. For MEK experiments pERK and HA were detected sequentially on the same membrane (see **Methods**), so pERK signal is visible on HA blots.

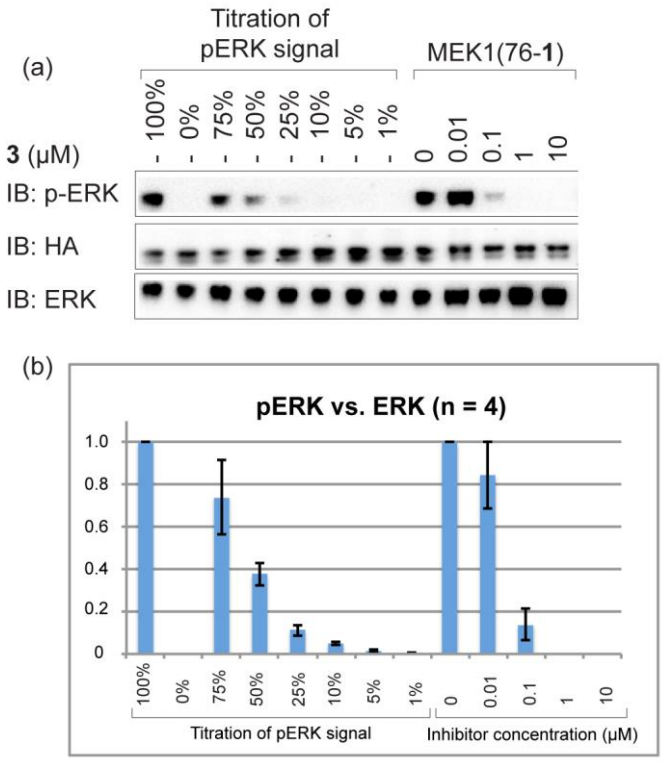

Supplementary Figure S6. Quantifying the concentration dependence of inhibition with **3**. (a) For quantification the MEK1(76-**1**), EGFP-ERK2 sample without inhibitor (in which EGFP-ERK2 is maximally phosphorylated) was mixed in the indicated ratios with a MEK1-wt*, EGFP-ERK2 sample (in which EGFP-ERK2 is not phosphorylated) to titrate the pERK signal. MEK1(76-**1**) was treated with increasing concentrations of the inhibitor **3** (as described in **Figure 2c** and **Methods**). EGFP-ERK2 is detected by immunoblot (IB) for ERK and phosphorylated EGFP-ERK2 is detected by immunoblot for pERK. All MEK variants are HA tagged and are detected by immunoblot for HA. MEK1(76-**1**) contains DD mutations making it constitutively active, MEK1-wt* does not contain DD mutations and does not phosphorylate EGFP-ERK2 in the absence of stimulation. (b) The western blot signals were quantified using the Biorad Image Lab software (version 4.1), with the signal for 100% MEK1(76-**1)**, EGFP-ERK2 sample set to 1 and the signal for 100% MEK1-wt*, EGFP-ERK2 set to 0. This allowed a direct comparison of the western signal arising from different fractions of the maximal phosphorylation signal to the signal arising from different inhibitor concentrations and therefore an estimate of the extent of inhibition observed with different inhibitor concentrations. The data represent the mean of n = 4, the error bars indicate the s.d. At c = 1.0 uM **3** we estimate > 90% inhibition. The sensitivity of the blots does not allow us to resolve higher levels of inhibition.

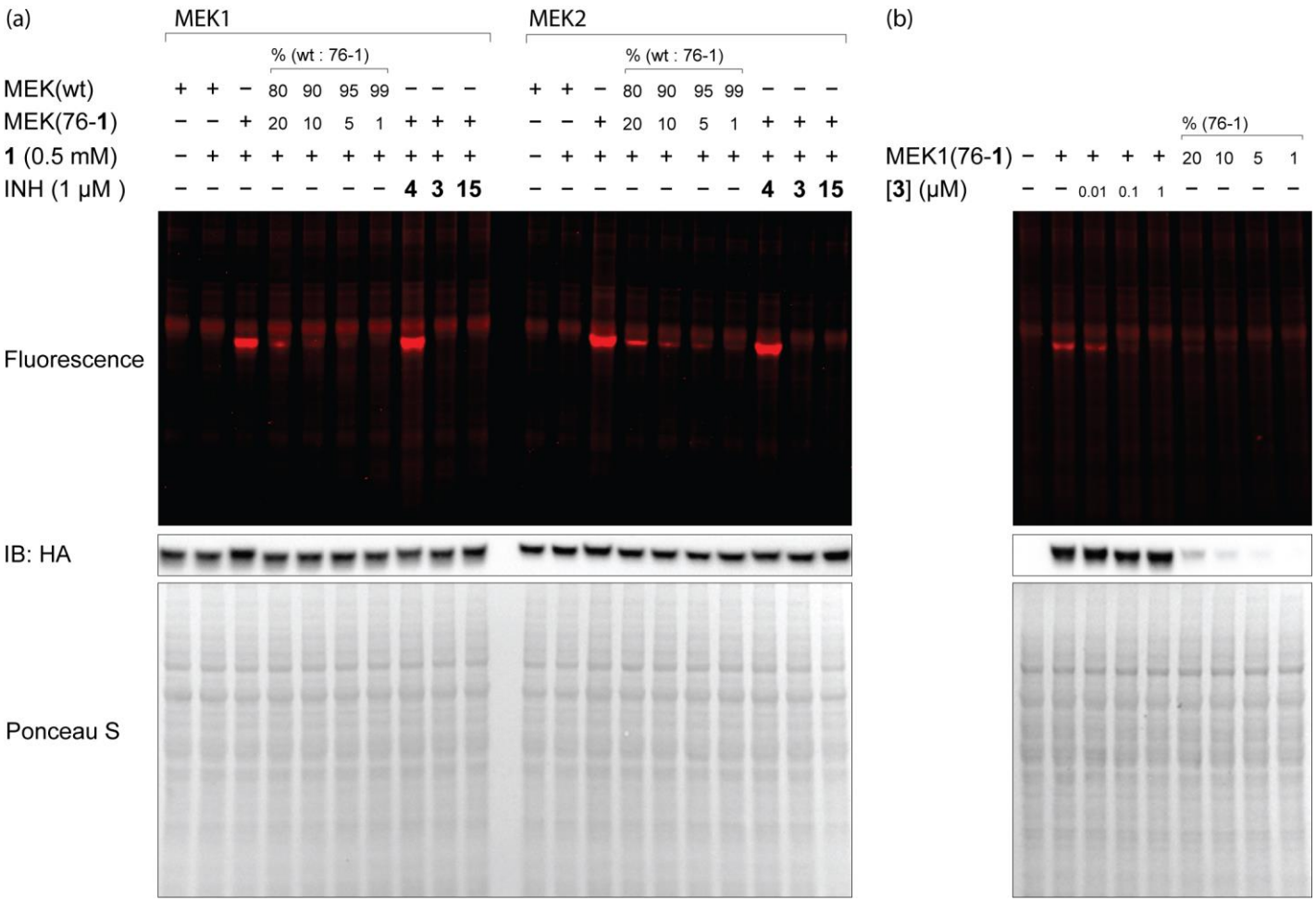

Supplementary Figure S7. Confirmation of quantitative formation of iBOLT product by fluorescent labelling. (a) Tethering of MEK1(76-**1**) and MEK2(76-**1**) with **3** or **15** is at least 99% complete. HEK293ET cells were transiently transfected with the corresponding MEK-DD-HA variant, BCNRS/tRNA$_{CUA}$ pair and EGFP-ERK2 for 24 h in a low serum media with or without 0.5 mM **1**, followed by incubation with the indicated inhibitor (INH) for 3 h before lysing the cells. Lysates were incubated with 10 μM TAMRA tetrazine conjugate **13** for 4 h at 0°C. Samples were then run on SDS-PAGE gels. In gel fluorescence was measured with excitation at 532 nm and emission at 580 nm. Ponceau S stain showed the total amount of protein on the membrane before western blot analysis. Lysates from cells that expressed either wild type MEK or MEK(76-**1**) were mixed in different ratios to compare the fluorescent intensity with the tethered MEK(76-**1**). (b) 1 μM **3** is required for quantitative tethering of MEK1(76-**1**). Experiments were performed as is panel (a). Lysate from cells that expressed MEK1(76-**1**) was mixed with lysate of HEK293ET cells in different ratio to compare the amount of tethering with 100 nM **3**..

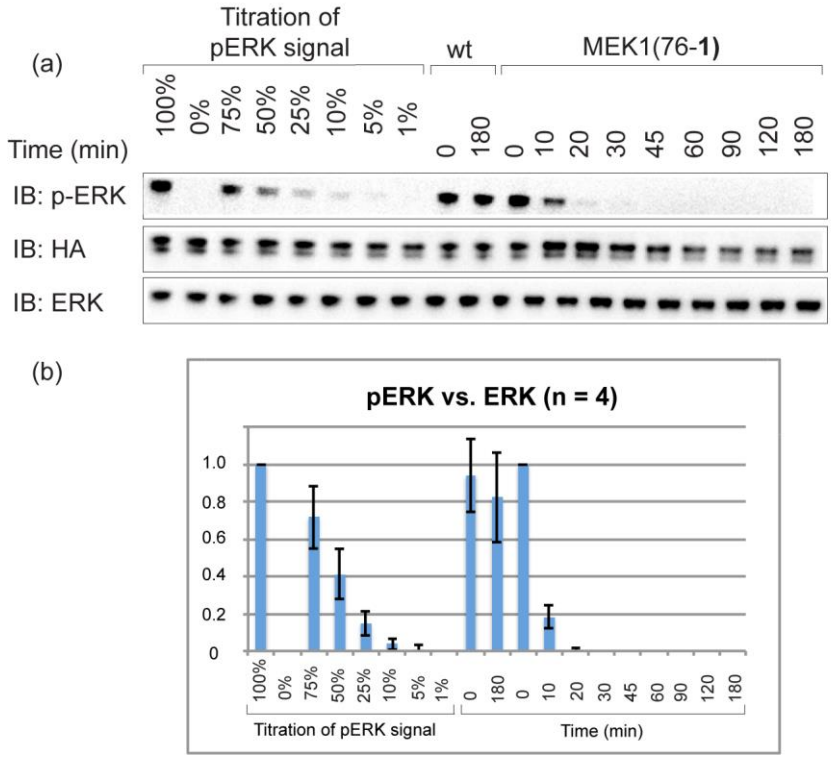

Supplementary Figure S8. Quantifying the time course of inhibition with **3**. (a) For quantification the MEK1(76-**1**), EGFP-ERK2 sample without inhibitor (in which EGFP-ERK2 is maximally phosphorylated) was mixed in the indicated ratios with a MEK1-wt*, EGFP-ERK2 sample (in which EGFP-ERK2 is not phosphorylated) to titrate the pERK signal. The MEK(76-**1**)**,** EGFP-ERK2 sample was treated with inhibitor **3** for increasing times (as described in **Figure 2e** and **Methods**). EGFP-ERK2 is detected by immunoblot (IB) for ERK and phosphorylated EGFP-ERK2 is detected by immunoblot for pERK. All MEK variants are HA tagged and are detected by immunoblot for HA. MEK1(76-**1**) contains DD mutations making it constitutively active, MEK1-wt* does not contain DD mutations and does not phosphorylate EGFP-ERK2 in the absence of stimulation. (b) The western blot signals were quantified using the Biorad Image Lab software (version 4.1), with the signal for 100% MEK(76-**1**), EGFP-ERK2 sample set to 1 and the signal for 100% MEK1-wt*, EGFP-ERK2 set to 0. This allowed a direct comparison of the western signal arising from different fractions of the maximal phosphorylation signal to the signal arising from different time points and therefore an estimate of the extent of inhibition observed as a function of time. The data represent the mean of n = 4, the error bars indicate the s.d. After t = 10 min we estimate > 90% inhibition. The sensitivity of the blots does not allow us to resolve higher levels of inhibition.

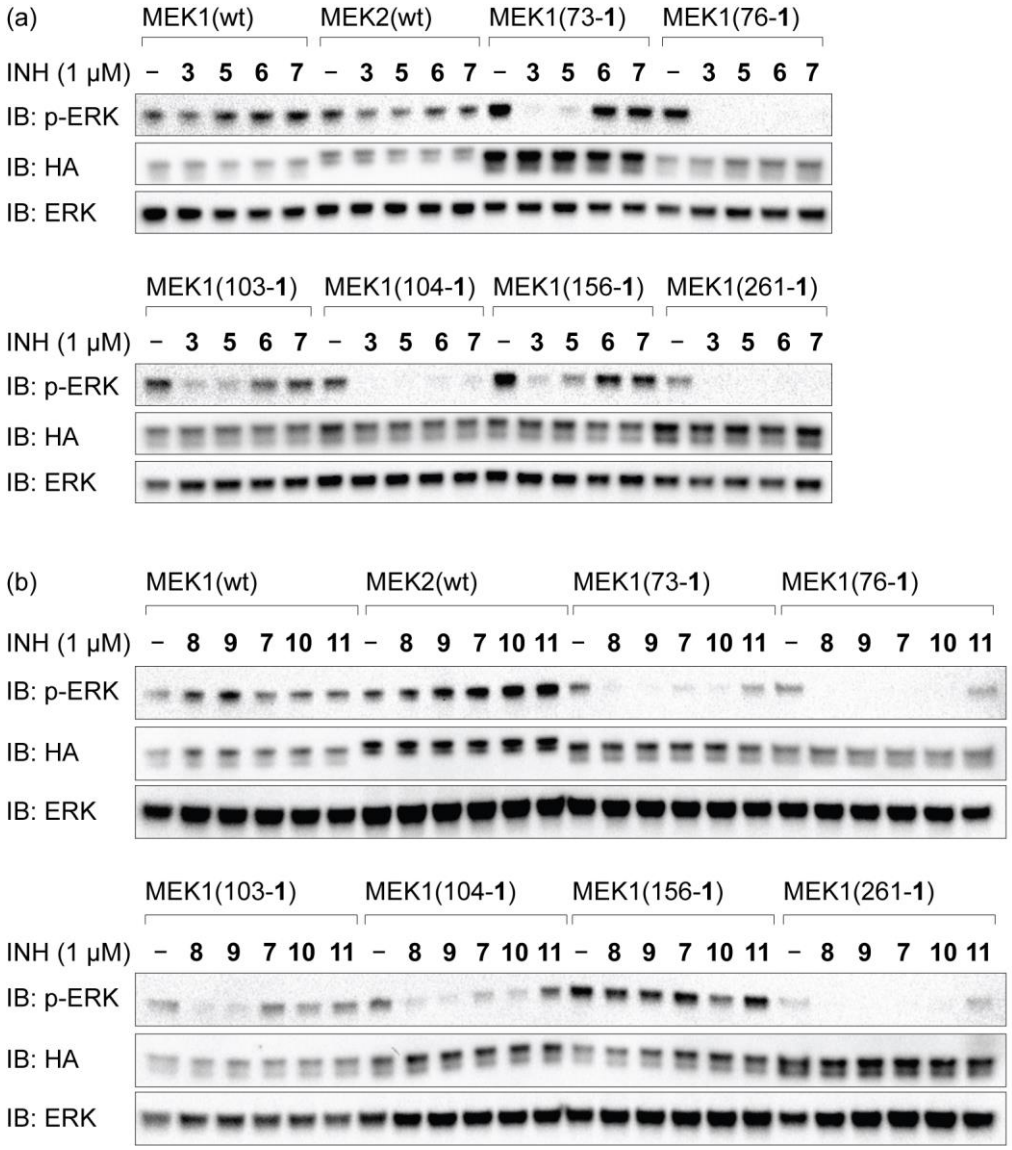

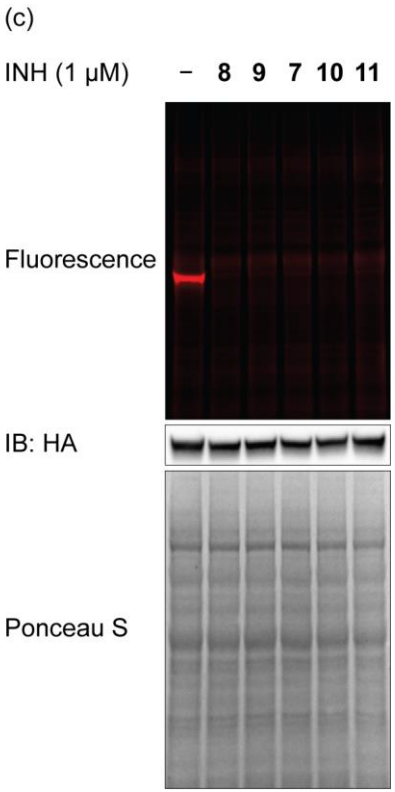

Supplementary Figure S9. Effect of halogen substitutions (a) and linker length (b) on inhibition. HEK293ET cells were transiently transfected with MEK1-DD-HA, BCNRS/$tRNA_{CUA}$ pair and EGFP-ERK2 for 24 h in a low serum media with or without 0.5 mM **1**, followed by incubation with the indicated inhibitor (INH) for 3 h before western blot analysis. EGFP-ERK2 is detected by immunoblot (IB) for ERK and phosphorylated EGFP-ERK2 is detected by immunoblot for pERK. All MEK variants are HA tagged, contain DD mutations making them constitutively active and are detected by immunoblot for HA. (c) Quantitative formation of MEK1(76-**1**) tethered **7**-**11**. Experiment was performed as in Supplementary Figure S7.

(a)

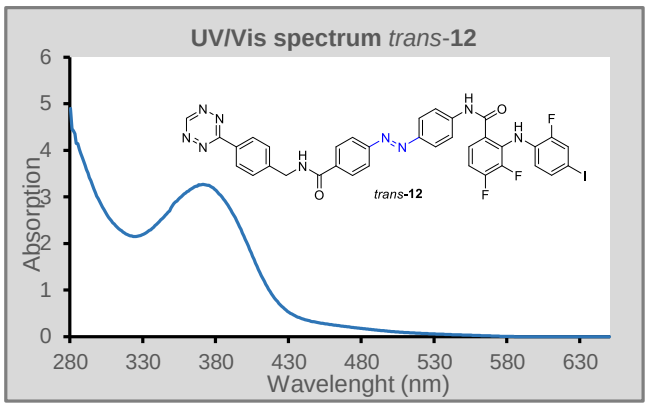

(b)

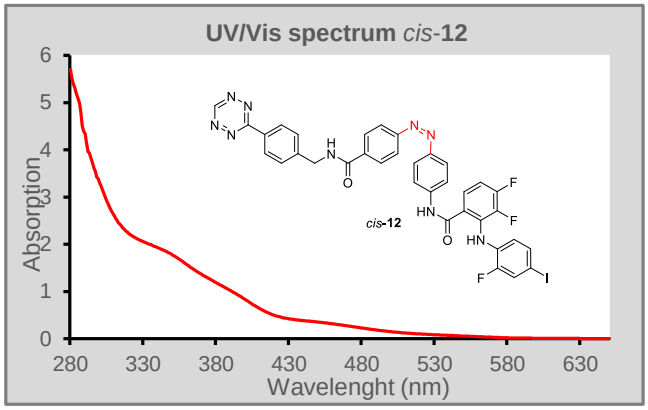

(c)

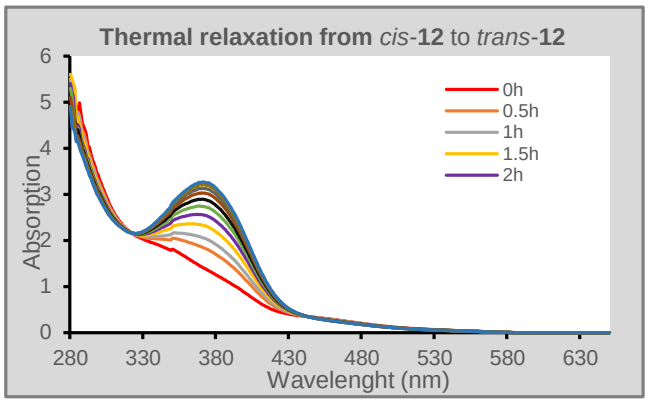

Supplementary Figure S10. (a) UV/Vis spectra of compound *trans*-**12** (0.5 mM, DMSO, 23°C). (b) UV/Vis spectra of compound *cis*-**12** (0.5 mM, DMSO, 23°C) after irradiation with UV light (360 nm, 30 sec). Irradiation of *cis*-**12** with blue light (440 nm, 30 sec) leads to the recovery of the *trans*-**12** spectra. (c) Kinetic scanning of the UV/Vis spectra of compound **12** after irradiation (360 nm, 30 sec, 0.5 mM, DMSO, intervals of 10 min, 23°C). Thermal relaxation leads to the full recovery of the *trans*-state after 3.5 h.

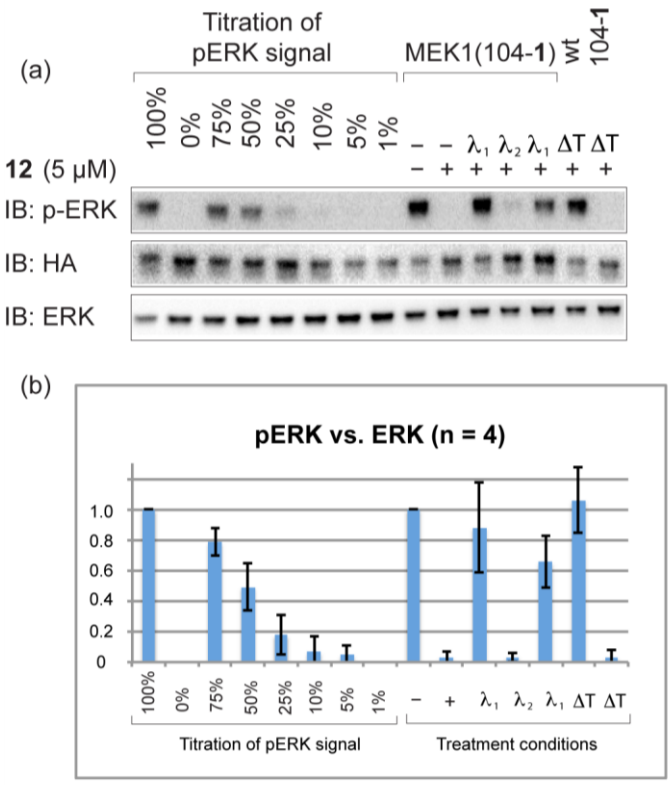

Supplementary Figure S11. A photo-BOLT experiment (see **Figure 4**) with phosphorylation standards. (a) For quantification the MEK1(104-**1**), EGFP-ERK2 sample without inhibitor (in which EGFP-ERK2 is maximally phosphorylated) was mixed in the indicated ratios with a MEK1-wt*, EGFP-ERK2 sample (in which EGFP-ERK2 is not phosphorylated) to titrate the pERK signal. The MEK1(104-**1**), EGFP-ERK2 sample was treated with inhibitor **12** for increasing times (as described in **Figure 4** and **Methods**). EGFP-ERK2 is detected by immunoblot (IB) for ERK and phosphorylated EGFP-ERK2 is detected by immunoblot for pERK. All MEK variants are HA tagged and are detected by immunoblot for HA. MEK1(104-**1**) contains DD mutations making it constitutively active, MEK1-wt* does not contain DD mutations and does not phosphorylate EGFP-ERK2 in the absence of stimulation. (b) The western blot signals were quantified using the Biorad Image Lab software (version 4.1), with the signal for 100% MEK1(104-**1**), EGFP-ERK2 sample set to 1 and the signal for 100% MEK1-wt*, EGFP-ERK2 set to 0. This allowed a direct comparison of the western signal arising from different fractions of the maximal phosphorylation signal to the signal arising from different treatments and therefore an estimate of the extent of inhibition. The data represent the mean of n = 4, the error bars indicate the s.d. We estimate that inhibition in this experiment > 90%. The sensitivity of the blots does not allow us to resolve higher levels of inhibition.

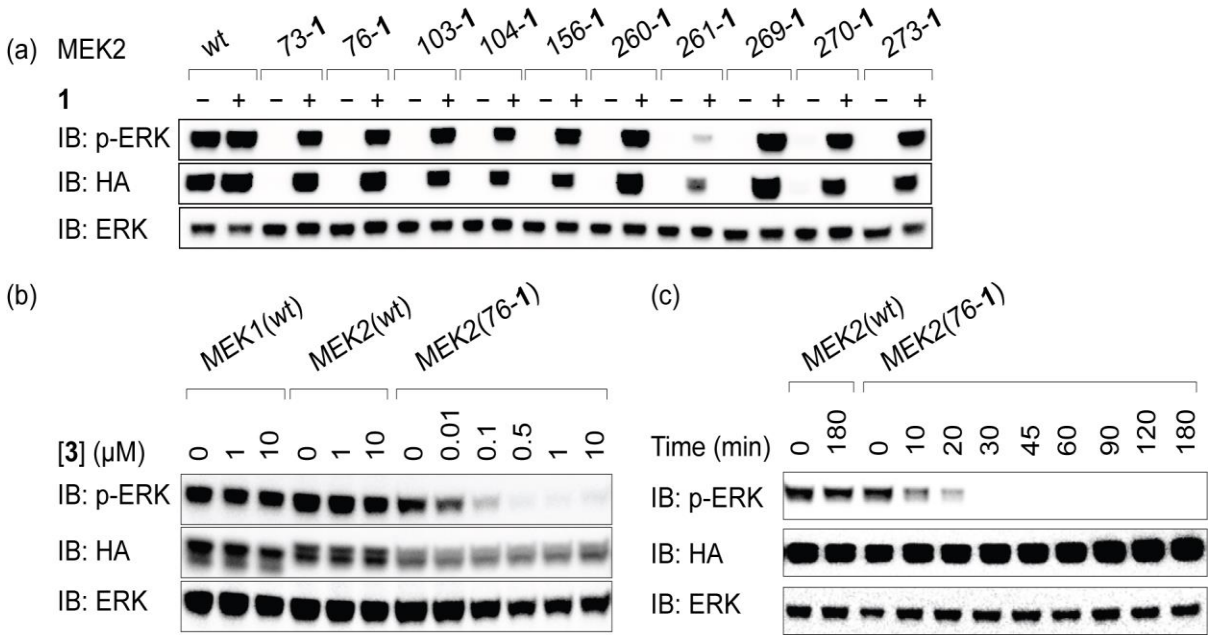

Supplementary Figure S12. (a) Expression of MEK2 variants depends on the presence of unnatural amino acid **1**. HEK293ET cells were transiently transfected with MEK2-DD-HA, BCNRS/tRNA$_{CUA}$ pair and EGFP-ERK2 for 24 h in a low serum media with or without 0.5 mM **1**, followed by western blot analysis. EGFP-ERK2 is detected by immunoblot (IB) for ERK and phosphorylated EGFP-ERK2 is detected by immunoblot for pERK. All MEK variants are HA tagged, contain DD mutations making them constitutively active and are detected by immunoblot for HA. MEK2 mutants using MEK1 numbering. (b) Concentration dependence of inhibiting MEK2(76-**1**). Experiment was performed as in (a), except cells were treated with **3** for 3 h at different concentrations before western blot analysis. (c) Time dependence of inhibiting MEK2(76-**1**) by 1 μM **3**. Experiment was performed as in (a), except cells were incubated with 1 μM **3** for 0-180 min before western blot analysis.

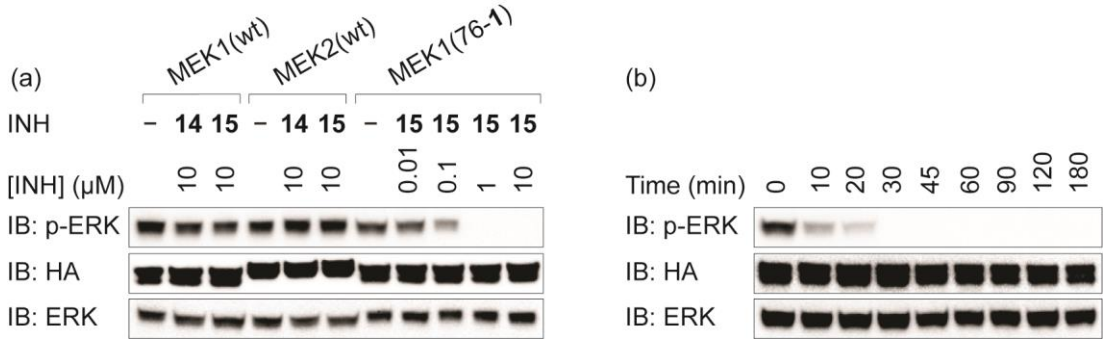

Supplementary Figure S13. Concentration (a) and time (b) dependence of MEK1(76-**1**) inhibition by **15**. HEK293ET cells were transiently transfected with MEK-DD-HA, BCNRS/tRNA$_{CUA}$ pair and EGFP-ERK2 for 24 h in a low serum media with 0.5 mM **1**, followed by incubation with the inhibitor (INH) before western blot analysis. EGFP-ERK2 is detected by immunoblot (IB) for ERK and phosphorylated EGFP-ERK2 is detected by immunoblot for pERK. All MEK variants are HA tagged, contain DD mutations making them constitutively active and are detected by immunoblot for HA. (a) Cells were incubated with the indicated inhibitor for 3 h. (b) Cells expressing MEK1(76-**1**) were incubated with 1 μM **15** for 0-180 min.

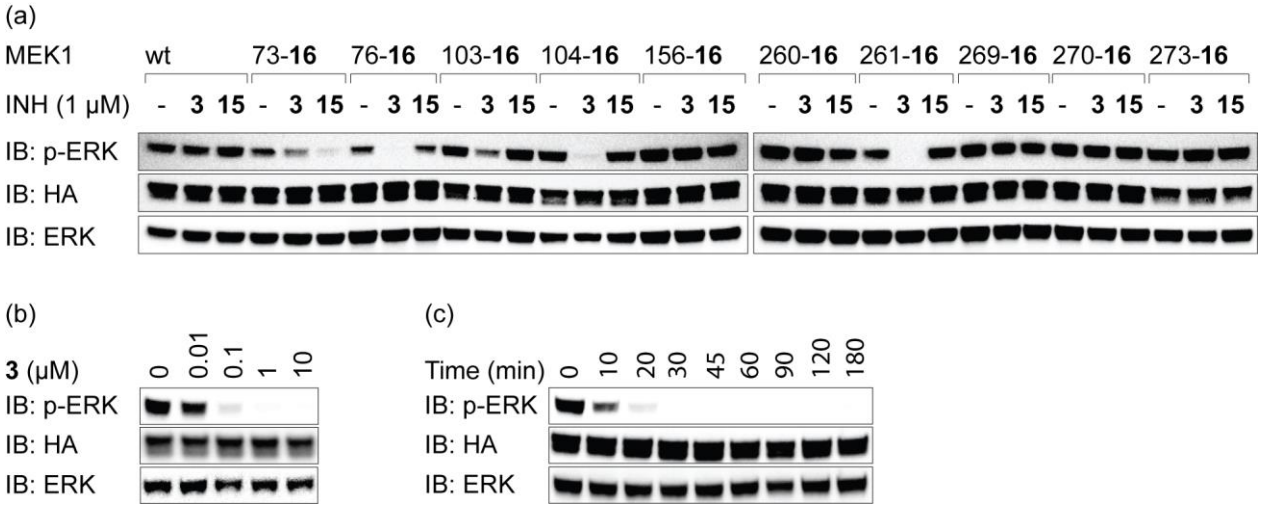

Supplementary Figure S14. (a) iBOLT of MEK1(XXX-**16**) variants by conjugates **3** and **15**. HEK293ET cells were transiently transfected with MEK1-DD-HA, PylS/$tRNA_{CUA}$ pair and EGFP-ERK2 for 24 h in a low serum media with 0.1 mM **16**, followed by incubation with 1 μM **3** or **15** for 3 h before western blot analysis. EGFP-ERK2 is detected by immunoblot (IB) for ERK and phosphorylated EGFP-ERK2 is detected by immunoblot for pERK. All MEK variants are HA tagged, contain DD mutations making them constitutively active and are detected by immunoblot for HA. (b) Concentration dependence of inhibiting MEK1(76-**16**). Experiment was performed as in a, except cells were incubated with **3** at different concentrations for 3 h. (c) Time dependence of inhibiting MEK1(76-**16**) by 1 μM **3**. Experiment was performed as in (a), except cells were incubated with 1 μM **3** for 0-180 min.

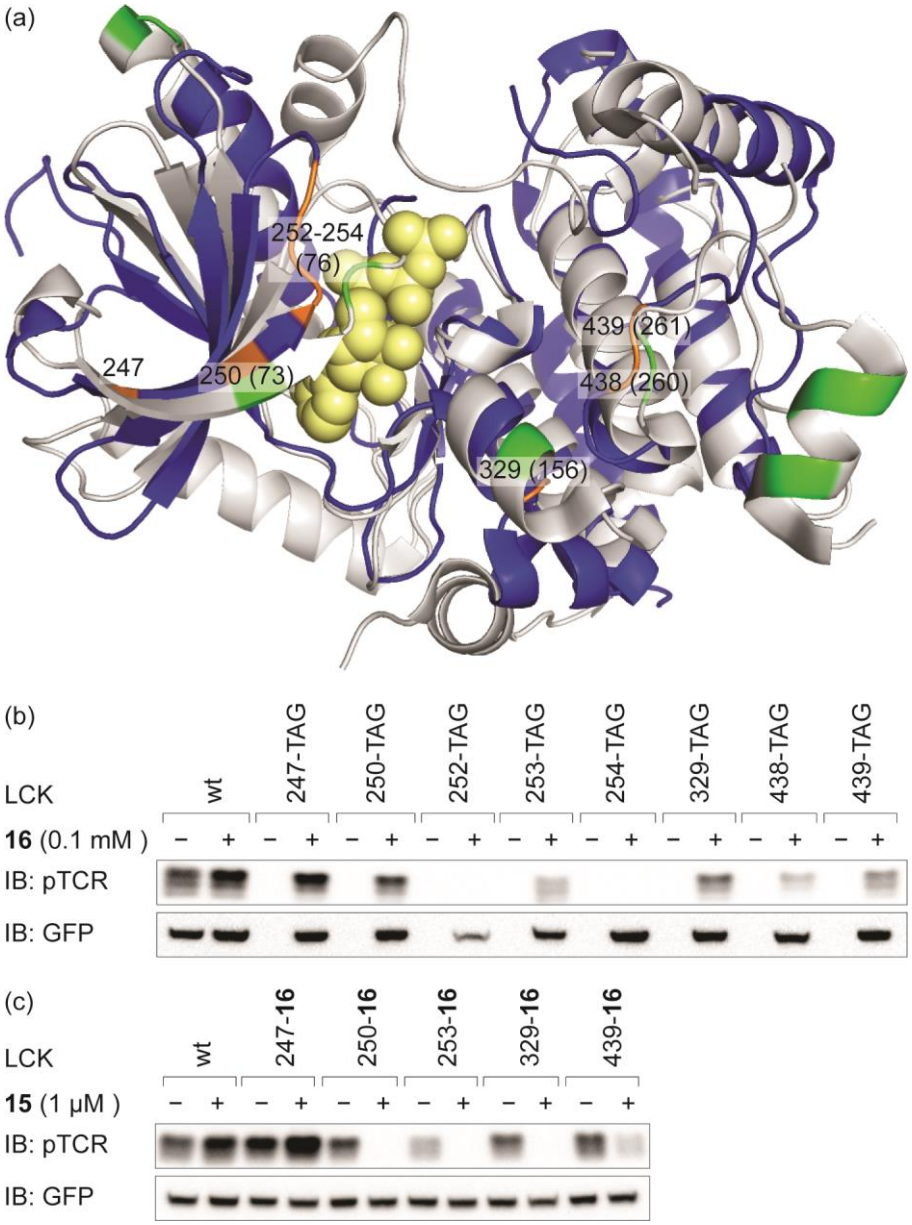

Supplementary Figure S15. Expanding iBOLT to LCK. (a) Sites for substitution with unnatural amino acid in LCK. LCK (blue) and MEK1 (grey) are aligned. The substitution sites in LCK are highlighted in orange and labeled. The active sites of MEK1 are highlighted in green and labeled in parenthesis. ATP is shown as yellow spheres. (b) Expression of LCK(XXX-**16**)-GFP variants depends on the presence of unnatural amino acid **16**. HEK-TCR cells were transiently transfected with LCK-GFP and PylS/$tRNA_{CUA}$ pair with or without 0.1 mM **16** for 24 h, followed by western blot analysis. The activity of LCK(438-**16**)-GFP is weaker in comparison to other active variants. (c) Inhibition of LCK(XXX-**16**)-GFP variants by conjugate **15**. Experiment was performed as in (a), and cells were incubated with 1 μM **15** for 3 h before western blot analysis.

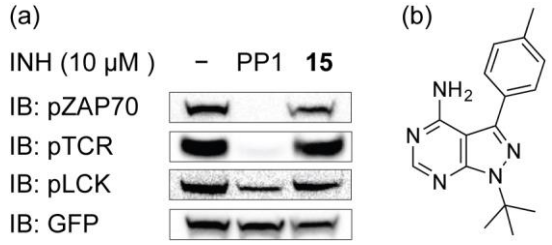

Supplementary Figure S16. Effect of inhibitors PP1 and **15** on LCK activity. (a) HEK-TCR cells were transiently transfected with LCK-GFP and ZAP70-mCherry for 24 h, followed by incubation with 10 μM of the corresponding inhibitor for 3 h before western blot analysis. (b) Chemical structure of PP1.

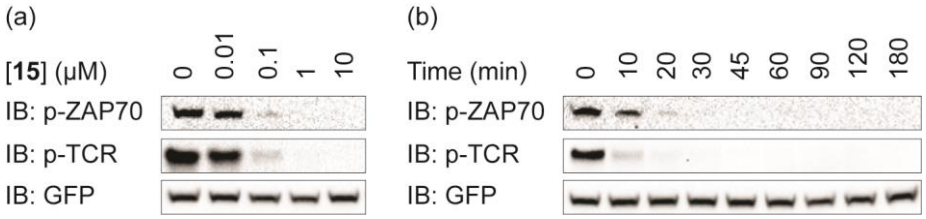

Supplementary Figure S17. Inhibition of LCK(250-**16**)-GFP by conjugate **15** at different concentrations (a) and time points (b). HEK-TCR cells were transiently transfected with LCK-GFP, PylS/tRNA$_{CUA}$ pair and ZAP70-mCherry with 0.1 mM **16** for 24 h, followed by incubation with conjugate **15** before western blot analysis. (a) Cells were incubated with **15** at different concentrations for 3 h. (b) Cells were incubated with 1 μM **15** for 0-180 minutes.

3. Molecular Biology Methods

3.1 Construction of the Plasmids

The plasmids pCMV-EGFP-ERK2[4], pEF1a-FLAG-PylRS-4xU6-PylT^{U25C} (for the expression of pyrrolysyl tRNA synthetase and pyrrolysyl tRNA$_{CUA}$ that directs the incorporation of **16**)[5] and pHR-ZAP70-mCherry[6] were described previously. pEF1a-FLAG-MbBCNRS-4xU6-PylT^{U25C} (for the pyrrolysyl tRNA synthetase and pyrrolysyl tRNA$_{CUA}$ that directs the incorporation of **1**) was constructed from pEF1a-FLAG-PylRS-4xU6-PylT^{U25C} by replacement of the PylRS gene with MbBCNRS.[7]

Construction of pCMV-FLAG-MbBCNRS-CMV-MEK1-DD-HA for the expression of constitutively active MEK1 wt and mutants

The plasmid pCMV-FLAG-MbBCNRS-CMV-EGFR(128TAG)-GFP-HA[8] was digested with BmtI-HF, PflMI and MluI, and the digested vector containing FLAG-MbBCNRS (6.1 kb) was purified by gel extraction. The plasmid pCMV-FLAG-MbPCKRS-CMV-MEK1(wt)-DD-HA[4] was digested with BmtI-HF and AscI, and the digested insert containing MEK1-DD-HA (1.2 kb) was purified by gel extraction. The plasmid pCMV-FLAG-MbBCNRS-CMV-MEK1(wt)-DD-HA was obtained by ligation of the vector and the insert by T4 ligase.

Mutants MEK1(78TAG), MEK1(156TAG), MEK1(223TAG), MEK1(225TAG), MEK1(226TAG), MEK1(260TAG) and MEK1(261TAG) were prepared by site-directed mutagenesis using the plasmid pCMV-FLAG-MbBCNRS-CMV-MEK1(wt)-DD-HA as the template.

For mutants containing amber codon at the site E72, A76, E102, I103, K104, K185, D217, N221, G237, K269, E270 or L273, the fragment of MEK1(15-299, 72TAG, S218D, S222D), MEK1(15-299, 76TAG, S218D, S222D), MEK1(15-299, 102TAG, S218D, S222D), MEK1(15-299, 103TAG, S218D, S222D), MEK1(15-299, 104TAG, S218D, S222D), MEK1(15-299, 185TAG, S218D, S222D), MEK1(15-299, 217TAG, S218D, S222D), MEK1(15-299, 221TAG, S218D, S222D), MEK1(15-299, 237TAG, S218D, S222D), MEK1(15-299, 269TAG, S218D, S222D), MEK1(15-299, 270TAG, S218D, S222D) and MEK1(15-299, 273TAG, S218D, S222D) were purchased (GeneArt String DNA Fragments, Life Technologies). These fragments were cloned into pCMV-FLAG-MbBCNRS-CMV-MEK1(wt)-DD-HA using HpaI and XmaI sites to afford the mutant plasmids.

For mutants containing an amber codon at the site A309, F311 or D315, the fragment of MEK1(288-372, 309TAG), MEK1(288-372, 311TAG) and MEK1(288-372, 315TAG) were purchased (GeneArt String DNA Fragments, Life Technologies). These fragments were cloned into pCMV-FLAG-MbBCNRS-CMV-MEK1(wt)-DD-HA using XmaI and BbvCI sites to afford the mutant plasmids.

Construction of pEF1a-MEK1-DD-HA-4xU6-PylT^{U25C} for the expression of constitutively active MEK1 wt and mutants

The plasmid pEF1a-FLAG-MbBCNRS-4xU6-PylT^{U25C} was digested with NheI-HF and EcoRI-HF, and the digested vector containing 4xU6-PylT^{U25C} (8.1 kb) was purified by gel extraction. The genes MEK1(wt)-DD-HA, MEK1(73TAG)-DD-HA, MEK1(76TAG)-DD-HA, MEK1(103TAG)-DD-HA, MEK1(104TAG)-DD-HA, MEK1(156TAG)-DD-HA, MEK1(260TAG)-DD-HA, MEK1(261TAG)-DD-HA, MEK1(269TAG)-DD-HA, MEK1(270TAG)-DD-HA and MEK1(273TAG)-DD-HA were amplified from the corresponding plasmid pCMV-FLAG-MbBCNRS-CMV-MEK1-DD-HA by the forward (TGACCGGCGCCTACTCTAGAGCTAGCGTTTAAACTTAAGCTTGCCACCATGCCCAAGAAGA AGC) and reverse (CACTGTGCTGGATATCTGCAGAATTCCACCACACTGGACTAGTGGATCCTT ATCATTAAGCGTAATCTGGAACATCG) primers (1.2 kb). Gibson assembly of the vector and the corresponding PCR fragment afforded the corresponding MEK1 plasmid.

Construction of pEF1a-MEK2-DD-HA-4xU6-PylT^{U25C} for the expression of constitutively active MEK2 wt and mutants

The plasmid pEF1a-MEK1-DD-HA-4xU6-PylT^{U25C} was digested with AflII and BamHI-HF, and the digested vector containing 4xU6-PylT^{U25C} (8.1 kb) was purified by gel extraction. The gene MEK2(wt)-DD-HA was obtained by PCR mutagenesis of MEK2 gene (Origene SC110003) with primers CTCTAGAGCTAGCGTTTAAACTTAAGCTTGCCACCATGCTGGCCCGGAGGAAG and GTCGAT GAGCTGGCCGCTCAC (0.7 kb) and TGAGCGGCCAGCTCATCGACGACATGGCCAACGACTT CGTGGGCACGCGCTCCTAC and TTCCACCACACTGGACTAGTGGATCCT TATCATTAAGCGT AATCTGGAACATCGTATGGGTACATCACGGCGGTGCGCGTG (0.6 kb). The plasmid pEF1a-MEK2(wt)-DD-HA-4xU6-PylT^{U25C} was obtained by Gibson assembly of the vector and the two PCR fragments. MEK2 mutant plasmids were prepared by site-directed mutagenesis using the plasmid pEF1a-MEK2(wt)-DD-HA-4xU6-PylT^{U25C} as the template.

Construction of pEF1a-LCK-GFP-4xU6-PylT^{U25C} for the expression of LCK wt and mutants

The plasmid pEF1a-MEK1-DD-HA-4xU6-PylT^{U25C} was digested with NheI and SalI-HF, and the digested vector containing 4xU6-PylT^{U25C} (5.9 kb) was purified by gel extraction. The gene LCK-GFP was PCR amplified with primers TGACCGGCGCCTACTCTAGAGCTAGCGTTTAAACTTAAGCTTGCCA CCATGGGCTGTGGCTGC and TTGTAATCCAGAGGTTGATTGTCGACGCGGCCGCTTTACTTG TACAG (2.3 kb) from pHR-LCK-GFP.[6] The plasmid pEF1a-LCK-GFP-4xU6-PylT^{U25C} was obtained by Gibson assembly of the vector and the PCR fragment. LCK mutant plasmids were prepared by site-directed mutagenesis using the plasmid pEF1a-LCK-GFP-4xU6-PylT^{U25C} as the template.

3.2 Cell Culture

The HEK-TCR cell line was created in a similar manner to that used previously.[6] Briefly, lentivirus was produced from a plasmid that expresses the CD3γ, δ, ε, ξ genes and another that expresses the 1G4 TCR clone before being combined and used to infect HEK293T cells. TCR-positive HEK cells were confirmed by flow cytometry, single-cell sorted and a clone expressing physiological levels was grown up for subsequent experiments.

HEK293ET and HEK-TCR cells were grown at 37°C in 5% CO_2 atmosphere in DMEM + GlutaMAX medium (Gibco) supplemented with 10% fetal bovine serum (FBS) for 24 hours before transfection.

4. Chemical Synthesis

4.1 General Remarks

Solvents and Reagents: Unless stated otherwise, solvents and dry solvents like dichloromethane, tetrahydrofuran (THF), toluene, acetonitrile, dimethylformamide (DMF) and diethyl ether were purchased from Sigma-Aldrich. Unless stated otherwise all of these chemicals were used without further purification. The following reagents and building blocks were prepared according to literature procedures: inhibitor **2**,[9] (4-(1,2,4,5-tetrazin-3-yl)phenyl)methanamine hydrochloride,[8, 10] methyl 3-aminopropanoate hydro-chloride **9a**,[11] TAMRA-conjugate **13**,[12] methyl 6-aminohexanoate hydro-chloride **15j**,[11] 1,3-cyclopropene containing amino acid **16**.[13]

Reaction Handling: Unless stated otherwise all non-aqueous reactions were performed in flame-dried glassware under an atmosphere of argon. All flasks were equipped with rubber septa and reactants were handled using standard Schlenk techniques. Temperatures above the room temperature refer to oil bath temperatures which were controlled by a thermostat. Reactions were magnetically stirred and monitored by thin layer chromatography **(**TLC) unless otherwise noted.

Analytical Thin Layer Chromatography was carried out with "LuxPlate® silica gel 60 F254" sheets from Merck. Detection was carried out using UV light (254 nm and 366 nm) or permanganate (0.6% $KMnO_4$ in water with 1.0% K_2CO_3). Concentrations under reduced pressure were performed by rotary evaporation at 40°C at the appropriated pressure, unless otherwise noted. **Flash column chromatography** was accomplished using silica gel S (pore size 60 Å, 0.040-0.063 mm) from Sigma-Aldrich. The yields given refer to the isolated yields.

^{1}H-NMR spectra were recorded at room temperature on Bruker AVB-400 spectrometer with ^{1}H operating frequency of 400 MHz. Unless stated otherwise all spectra were recorded at room temperature in $CDCl_3$, d^3-MeOD, d^6-DMSO and all chemical shifts are given in δ units relative to $CHCl_3$ (central line of singlet: δH = 7.27), MeOH (central line of quintet: δH = 3.31) or DMSO (central line of quintet: δH = 2.50).[14] Analyses followed first order and the following abbreviations were used throughout: s = singlet, br. s. = broad singlet, d = doublet, t = triplet, q = quartet, quin = quintet, sxt = sextet, sept = spt, dd = doublet of doublet, dt = doublet of triplet, m = multiplet, m_c = centered multiplet. Coupling constants through n bonds (^nJ) are given in Hertz [Hz].

^{13}C-NMR spectra were recorded at room temperature on Bruker AVB-400 spectrometer with ^{13}C operating frequency of 101 MHz. Unless stated otherwise all spectra were recorded at room temperature in $CDCl_3$, d^3-MeOD, d^6-DMSO and all chemical shifts are given in δ units relative to $CHCl_3$ (central line of triplet: δC = 77.00), MeOH (central line of quintet: δC = 49.51) or DMSO (central line of quintet: δC = 39.51). The following abbreviation was used throughout: s = singlet, d = doublet, dd = doublet of doublet. If no coupling constants are given, the multiplicity refers to the ^{1}H-decoupled spectra.

* chem. shifts associated with the major rotamer are marked with an asterisk.
# chem. shifts associated with the minor rotamer are marked with a hash.

Mass spectra (MS) were recorded on an Agilent 1200 LC-MS system with a 6130 Quadrupole spectrometer for ESI-MS. The solvent system consisted of 0.2 % formic acid in H_2O as buffer A, and 0.2 % formic acid in MeCN as buffer B. Small molecule LC-MS was carried out using a Phenomenex Jupiter C18 column (150 x 2 mm, 5 µm). Variable wavelengths were used and MS acquisitions were carried out in positive and negative ion modes.

IUPAC names and atom numbering of the compounds described in the experimental section were determined with the program ChemDraw ultra 13.0.

4.2 Synthesis of Compound 3

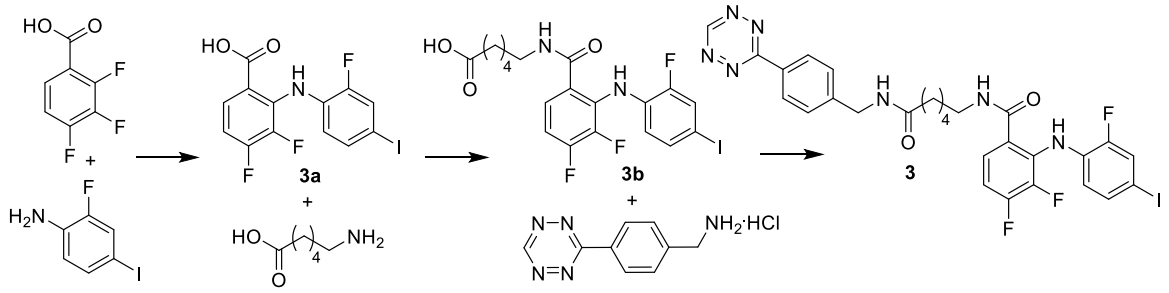

Scheme S1. Synthesis of compound **3**.

3,4-Difluoro-2-((2-fluoro-4-iodophenyl)amino)benzoic acid (3a)

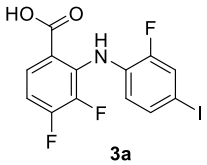

Representative procedure for the nucleophilic substitution:

2,3,4-Trifluorobenzoic acid (1.00 g, 5.68 mmol, 1.0 eq) and 2-fluoro-4-iodoaniline (1.31 g, 5.96 mmol, 1.05 eq) were dissolved in THF (5 mL). 10% of this mixture was slowly added to a stirring slurry of $LiNH_2$ (456 mg, 19.9 mmol, 3.5 eq) in THF (5 mL) at 50°C. After stirring for 30 min the rest of the mixture was slowly added over a period of 1 h and stirring was continued while maintaining the temperature at 50°C until the reaction was completed (1.5 h). The reaction mixture was then cooled to rt and quenched by the addition of 6N HCl (5 mL), followed by the addition of Et_2O (15 mL). The aqueous phase was separated, the organic phase was washed with 3 x 5 mL brine and dried over $MgSO_4$. After evaporation of the solvent *in vacuo* product **3a** (2.17 g, 5.52 mmol, 97% yield) was obtained as a grey solid without any further purification.

TLC: R_f = 0.28 (hexane/ethyl acetate = 1:1). **^{1}H NMR** (d^3-MeOD, 400 MHz): δ = 6.74 (1 H, d, *J* = 5.4 Hz), 6.90 (1 H, d, *J* = 7.8 Hz), 7.40 (1 H, d, *J* = 7.9 Hz), 7.47 (1 H, d, *J* = 8.8 Hz), 7.89 (1 H, br). **^{13}C NMR** (d^3-MeOD, 101 MHz): δ = 84.18 (d, $J_{C,F}$ = 7.3 Hz), 109.49 (d, $J_{C,F}$ = 18.3 Hz), 116.47, 123.08 (d, $J_{C,F}$ = 5.1 Hz), 125.44 (d, $J_{C,F}$ = 22.1 Hz), 129.29 (dd, $J_{C,F}$ = 9.2, 3.3 Hz), 131.69 (d, $J_{C,F}$ = 10.3 Hz), 134.57 (d, $J_{C,F}$ = 2.9 Hz), 137.14 (dd, $J_{C,F}$ = 9.5, 1.9 Hz), 143.45 (dd, $J_{C,F}$ = 248.0, 14.7 Hz), 155.46 (d, $J_{C,F}$ = 253.0 Hz), 155.58 (dd, $J_{C,F}$ = 250.0, 3.9 Hz), 170.20. **ESI-MS** $[M-H]^-$ calculated for $C_{13}H_6O_2NF_3I$: 391.9; found: 391.8.

6-(2-((4-Iodo-2-fluorophenyl)amino)-3,4-difluorobenzamido)hexanoic acid (3b)

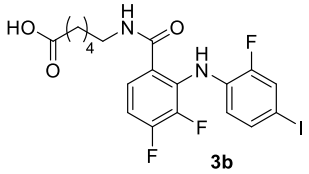

Representative procedure for the amide coupling:

A solution of 3,4-difluoro-2-((2-fluoro-4-iodophenyl)amino)benzoic acid **3a** (400 mg, 1.02 mmol, 1.0 eq) in THF (15 mL) under argon atmosphere was cooled down to -30 °C, treated with *N*-methylmorpholine (151 µL, 1.37 mmol, 1.35 eq) and isobutyl chloroformate (158 µL, 1.20 mmol, 1.2 eq). The resulting mixture was stirred at this temperature for 15 min, before 6-aminohexanoic acid (189 µL, 2.00 mmol, 1.0 eq) in THF (5 mL) was added. Afterwards the reaction mixture was slowly warmed up to rt and stirred overnight. The solvent was removed *in vacuo*, the residue was slurrying in ethyl acetate (50 mL), filtrated and washed exhaustively with ethyl acetate, before the solution was dried with $MgSO_4$, filtrated. After evaporation of the solvent *in vacuo*, the obtained crude product was purified by flash column chromatography on silica gel (ethyl acetate/n-hexane 3:1 to 1:1) to give amide **3b** (272 mg, 0.540 mmol, 53% yield) in form of white crystals.

TLC: R_f = 0.53 (hexane/ethyl acetate = 1:1). **^{1}H NMR** (d^3-MeOD $_3$, 400 MHz): δ = 1.27 - 1.43 (2 H, m), 1.44 - 1.56 (2 H, m), 1.61 (2 H, dq, *J* = 15.0, 7.3 Hz), 2.26 (2 H, t, *J* = 7.4 Hz), 3.27 (2 H, t, *J* = 7.0 Hz), 6.57 (1 H, td, *J* = 8.7, 4.5 Hz), 7.03 (1 H, td, *J* = 9.3, 7.2 Hz), 7.26 - 7.38 (1 H, m), 7.38 - 7.46 (2 H, m). **^{13}C NMR** (d^3-MeOD $_3$, 101 MHz):[15] δ = 25.9, 27.7, 30.1, 35.0, 40.8, 81.9, 111.7 (d, $J_{C,F}$ = 18.3 Hz), 116.4, 120.5, 125.2, 125.4, 133.1 (d, $J_{C,F}$ = 10.3 Hz), 134.6, 142.1, 145.3 (d, $J_{C,F}$ = 246.8 Hz), 154.3 (d, $J_{C,F}$ = 259.0 Hz), 155.6 (d, $J_{C,F}$ = 252.0 Hz), 169.4, 177.7. **ESI-MS** $[M-H]^-$ calculated for $C_{19}H_{17}O_3N_2F_3I$: 505.0; found: 505.3.

***N*-(6-((4-(1,2,4,5-Tetrazin-3-yl)benzyl)amino)-6-oxohexyl)-2-((2-fluoro-4-iodophenyl)amino)-3,4-difluorobenzamide (3)**

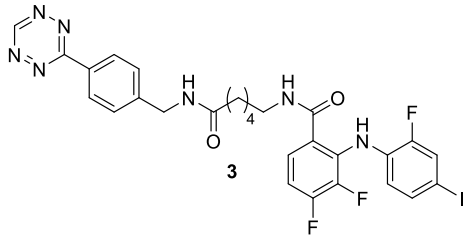

3

Representative procedure for the tetrazine-coupling:

Amide **3b** (18.0 mg, 35.5 µmol, 1.0 eq), (4-(1,2,4,5-tetrazin-3-yl)phenyl)methanamine hydrochloride (12.0 mg, 53.3 µmol, 1.5 eq), EDCI hydrochloride (17.0 mg, 88.9 µmol, 2.5 eq) and BtOH (1.1 mg, 7.1 µmol, 0.2 eq) were dissolved in dry DMF (2.5 mL). Then pyridine (14 µL, 177 µmol, 5.0 eq), was added dropwise and the mixture was stirred for 18 h at rt. After the addition of water (5 mL) the pink reaction mixture was extracted with 3 x 10 mL EtOAc, dried over $MgSO_4$, filtered off and the solvent was removed under reduced pressure. The crude product was then purified by flash column chromatography on silica gel (hexane/ethyl acetate 1:1 to pure ethyl acetate) to afford the pink tetrazine conjugate **3** (15.8 mg, 23.3 µmol, 66% yield).

TLC: R_f = 0.35 (ethyl acetate). **^{1}H NMR** (d^6-DMSO, 400 MHz): δ = 1.21 - 1.34 (2 H, m), 1.39 - 1.52 (2 H, m), 1.52 - 1.63 (2 H, m), 2.17 (2 H, t, *J* = 7.4 Hz), 3.19 (2 H, q, *J* = 6.3 Hz), 4.38 (2 H, d, *J* = 5.7 Hz), 6.68 (1 H, d, *J* = 5.3 Hz), 7.18 (1 H, d, *J* = 7.5 Hz), 7.37 (1 H, d, *J* = 8.5 Hz), 7.52 (2 H, d, *J* = 8.1 Hz), 7.49 - 7.55 (1 H, m), 7.58 (1 H, dd, *J* = 10.8, 1.8 Hz), 8.40 - 8.44 (1 H, m), 8.45 (2 H, d, *J* = 8.3 Hz), 8.70 (1 H, t, *J* = 5.5 Hz), 9.28 (1 H, s), 10.58 (1 H, s). **^{13}C NMR** (d^6-DMSO, 101 MHz):[15] δ = 25.0, 26.1, 28.5, 35.2, 38.9, 41.8, 82.2 (d, $J_{C,F}$ = 7.8 Hz), 109.6 (d, $J_{C,F}$ = 17.6 Hz), 120.0, 122.2, 123.6 (d, $J_{C,F}$ = 21.0 Hz), 124.6 (dd, $J_{C,F}$ = 11.8, 2.9 Hz), 127.8 (2 C), 128.0 (2 C), 130.3, 130.7 (dd, $J_{C,F}$ = 10.5, 2.2 Hz), 131.7, 133.1 (d, $J_{C,F}$ = 2.9 Hz), 142.7 (d, $J_{C,F}$ = 257.0 Hz), 145.1, 151.6 (d, $J_{C,F}$ = 253.0 Hz), 152.6 (d, $J_{C,F}$ = 247.4 Hz), 158.1, 165.4, 166.7, 172.2. **ESI-MS** $[M+H]^+$ calculated for $C_{28}H_{26}O_2N_7F_3I$: 676.1; found: 675.8.

4.3 Synthesis of Compound 4

***N*-(6-(([1,1'-Biphenyl]-4-ylmethyl)amino)-6-oxohexyl)-2-((4-bromo-2-chlorophenyl)amino)-3,4-difluorobenzamide (4)**

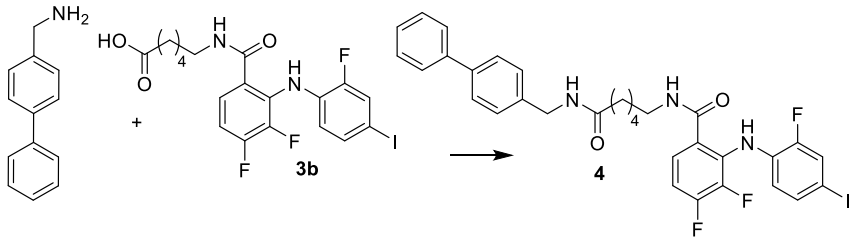

Scheme S2. Synthesis of compound **4**.

The representative procedure given for tetrazine conjugate **3** was carried out with compound **3b** (100 mg, 198 µmol, 1.0 eq) and 4-phenylbenzylamine (56.8 mg, 296 µmol, 1.5 eq) to afford the conjugate **4** (110 mg, 163 µmol, 83% yield) after flash column chromatography on silica gel (hexane/ethyl acetate 2:1 to pure ethyl acetate).

TLC: R_f = 0.41 (ethyl acetate). **^{1}H NMR** (d^6-DMSO, 400 MHz): δ = 1.20 - 1.33 (2 H, m), 1.43 - 1.62 (4 H, m), 2.14 (2 H, t, *J* = 7.4 Hz), 3.15 - 3.24 (2 H, m), 4.28 (2 H, d, *J* = 5.9 Hz), 6.67 (1 H, td, *J* = 8.8, 5.3 Hz), 7.17 (1 H, td, *J* = 9.2, 7.6 Hz), 7.28 - 7.34 (2 H, m), 7.34 - 7.39 (2 H, m), 7.41 - 7.47 (2 H, m), 7.51 - 7.57 (1 H, m), 7.57 - 7.64 (5 H, m), 8.27 - 8.34 (1 H, m), 8.69 (1 H, t, *J* = 5.6 Hz), 9.29 (1 H, s). **^{13}C NMR** (d^6-DMSO, 101 MHz):[15] δ = 25.0, 26.2, 28.5, 35.3, 38.9, 41.7, 82.2 (d, $J_{C,F}$ = 7.3 Hz), 109.6 (d, $J_{C,F}$ = 17.6 Hz), 120.0 (d, $J_{C,F}$ = 2.9 Hz), 122.2, 123.5 (d, $J_{C,F}$ = 20.5 Hz), 124.6 (d, $J_{C,F}$ = 8.8 Hz), 126.5 (2 C), 126.6 (2 C), 127.3, 127.8 (2 C), 128.9 (2 C), 130.8 (d, $J_{C,F}$ = 11.0 Hz), 131.8 (d, $J_{C,F}$ = 8.1 Hz), 133.2 (d, $J_{C,F}$ = 2.2 Hz), 138.6, 139.0, 140.0, 142.6 (dd, $J_{C,F}$ =250.0, 13.9 Hz), 151.7 (dd, $J_{C,F}$ = 249.0, 11.7 Hz), 152.6 (d, $J_{C,F}$ = 247.0 Hz), 166.7, 172.1. **ESI-MS** $[M+H]^+$ calculated for $C_{32}H_{30}O_2N_3BrClF_2$: 640.1; found: 640.4.

4.4 Synthesis of Compound 5

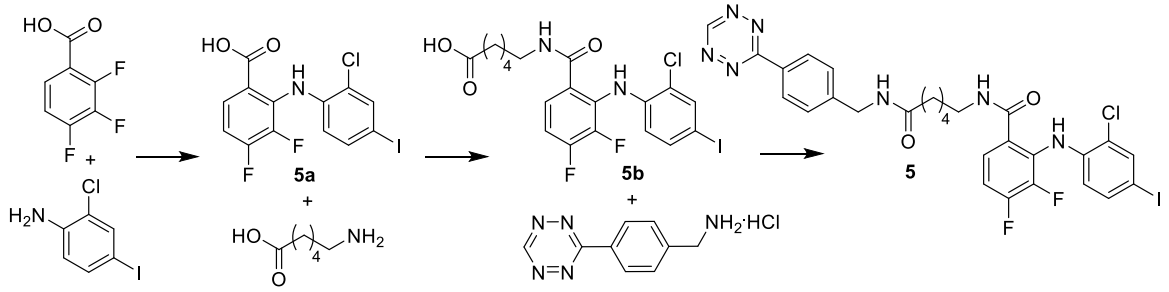

Scheme S3. Synthesis of compound **5**.

3,4-Difluoro-2-((2-chloro-4-iodophenyl)amino)benzoic acid (5a)

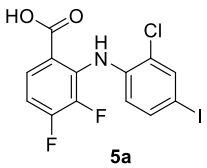

The representative procedure given for **3a** was carried out with 2-chloro-4-iodoaniline (1.51 g, 5.96 mmol, 1.05 eq) to afford **5a** (2.07 g, 5.05 mmol, 89% yield) as a brown solid.

TLC: R_f = 0.34 (hexane/ethyl acetate = 1:1). **^{1}H NMR** (d^3-MeOD, 400 MHz): δ = 6.66 (1 H, dd, *J* = 8.6, 7.1 Hz), 6.97 (1 H, td, *J* = 9.3, 7.1 Hz), 7.50 (1 H, dd, *J* = 8.6, 1.9 Hz), 7.72 (1 H, d, *J* = 1.9 Hz), 7.92 (1 H, ddd, *J* = 9.0, 5.9, 2.1 Hz). **^{13}C NMR** (d^3-MeOD, 101 MHz): δ = 84.0, 110.3 (d, $J_{C,F}$ = 18.3 Hz), 117.5, 121.2, 121.2, 126.0, 129.4 (dd, $J_{C,F}$ = 9.2, 4.0 Hz), 137.5, 138.5, 140.2, 143.3 (d, $J_{C,F}$ = 256.4 Hz), 155.4 (d, $J_{C,F}$ = 245.1 Hz), 170.0. **ESI-MS** $[M-H]^-$ calculated for $C_{13}H_6O_2NClF_2I$: 407.9; found: 408.1.

6-(2-((4-Iodo-2-chlorophenyl)amino)-3,4-difluorobenzamido)hexanoic acid (5b)

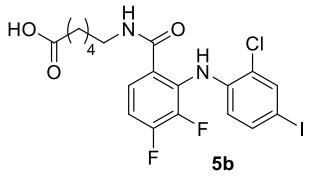

5b

The representative procedure given for amide **3b** was carried out with 3,4-difluoro-2-((2-chloro-4-iodophenyl)amino)benzoic acid **5a** (400 mg, 977 µmol, 1.0 eq) to afford **5b** (209 mg, 400 µmol, 41% yield) as a white solid after flash column chromatography on silica gel (hexane/ethyl acetate 3:1 to 1:1).

TLC: R_f = 0.51 (hexane/ethyl acetate = 1:1). **^{1}H NMR** (d^3-MeOD, 400 MHz): δ = 1.27 - 1.38 (2 H, m), 1.48 - 1.67 (4 H, m), 2.25 (2 H, t, *J* = 7.4 Hz), 3.26 - 3.29 (2 H, m), 6.49 (1 H, dd, *J* = 8.6, 5.6 Hz), 7.04 - 7.13 (1 H, m), 7.44 (1 H, dd, *J* = 8.4, 1.8 Hz), 7.45 - 7.49 (1 H, m), 7.68 (1 H, d, *J* = 1.9 Hz). **^{13}C NMR** (d^3-MeOD, 101 MHz):**[15]** δ = 25.9, 27.6, 30.1, 34.9, 40.8*, 41.0#, 82.2, 112.3 (d, $J_{C,F}$ = 17.6 Hz), 118.9, 119.0, 124.3, 125.6 (dd, $J_{C,F}$ = 8.4, 4.8 Hz), 126.1, 132.3, 137.6, 138.5, 141.2, 145.2 (d, $J_{C,F}$ = 233.9 Hz), 154.1 (dd, $J_{C,F}$ = 249.3, 11.9 Hz), 169.3, 177.6. **ESI-MS** $[M-H]^-$ calculated for $C_{19}H_{17}O_3N_2ClF_2I$: 521.0; found: 521.2.

***N*-(6-((4-(1,2,4,5-Tetrazin-3-yl)benzyl)amino)-6-oxohexyl)-2-((2-chloro-4-iodophenyl)amino)-3,4-difluorobenzamide (5)**

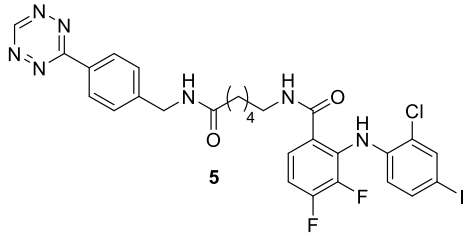

5

The representative procedure given for tetrazine conjugate **3** was carried out with compound **5b** (18.7 mg, 35.7 µmol, 1.0 eq) to afford the tetrazine conjugate **5** (14.9 mg, 22.6 µmol, 63% yield) after flash column chromatography on silica gel (hexane/ethyl acetate 1:1 to pure ethyl acetate).

TLC: R_f = 0.31 (ethyl acetate). **^{1}H NMR** (d^6-DMSO, 400 MHz): δ = 1.25 - 1.35 (2 H, m), 1.45 - 1.52 (2 H, m), 1.52 - 1.61 (2 H, m), 2.17 (2 H, t, *J* = 7.4 Hz), 3.14 - 3.24 (2 H, m), 4.38 (2 H, d, *J* = 5.9 Hz), 6.60 (1 H, dd, *J* = 8.4, 7.0 Hz), 7.23 (1 H, ddd, *J* = 9.7, 9.2, 7.0 Hz), 7.46 - 7.50 (1 H, m), 7.52 (2 H, d, *J* = 8.5 Hz), 7.54 - 7.59 (1 H, m), 7.76 (1 H, d, *J* = 1.9 Hz), 8.39 - 8.44 (1 H, m), 8.45 (2 H, d, *J* = 8.3 Hz), 8.75 (1 H, t, *J* = 5.5 Hz), 9.42 (1 H, s), 10.58 (1 H, s). **^{13}C NMR** (d^6-DMSO, 101 MHz):**[15]** δ = 25.0, 26.1, 28.5, 35.2, 38.9, 41.8, 82.6, 110.2 (d, $J_{C,F}$ = 19.1 Hz), 118.4, 122.6, 122.8, 125.3 (m), 126.4, 127.8 (2 C), 128.0 (2 C), 130.3, 136.1, 136.5, 137.2 (d, $J_{C,F}$ = 241.0 Hz), 138.9, 145.1, 151.6 (d, $J_{C,F}$ = 249.0 Hz), 158.1, 165.4, 166.6, 172.2. **ESI-MS** $[M+H]^+$ calculated for $C_{28}H_{26}O_2N_7ClF_2I$: 691.1; found: 690.7.

4.5 Synthesis of Compound 6

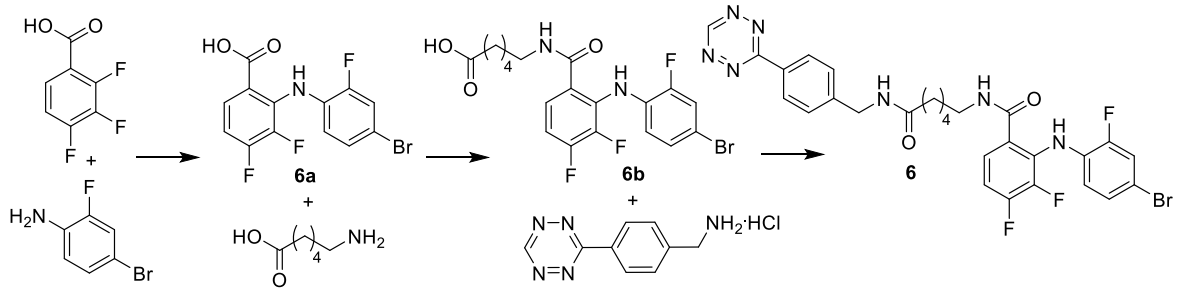

Scheme S4. Synthesis of compound **6**.

3,4-Difluoro-2-((4-bromo-2-fluorophenyl)amino)benzoic acid (6a)

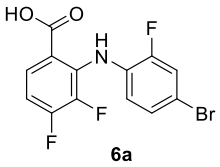

The representative procedure given for **3a** was carried out with 4-bromo-2-fluoroaniline (1.13 g, 5.96 mmol, 1.05 eq) to afford **6a** (1.89 g, 5.46 mmol, 96% yield) as a brown solid.

TLC: R_f = 0.30 (hexane/ethyl acetate = 1:1). **^{1}H NMR** (d^3-MeOD, 400 MHz): δ = 6.84 - 6.96 (2 H, m), 7.19 - 7.27 (1 H, m), 7.34 (1 H, dd, *J* = 10.7, 2.2 Hz), 7.89 (1 H, ddd, *J* = 9.0, 6.0, 2.2 Hz). **^{13}C NMR** (d^3-MeOD, 101 MHz): δ = 109.4 (d, $J_{C,F}$ = 18.3 Hz), 115.3 (d, $J_{C,F}$ = 8.8 Hz), 116.4, 119.8 (d, *J* = 23.0 Hz), 123.0 (d, *J* = 3.7 Hz), 128.5 (d, *J* = 3.7 Hz), 129.3 (dd, *J* = 9.9, 4.0 Hz), 131.1, 134.7, 137.4, 140.9 (d, $J_{C,F}$ = 235.4 Hz), 155.5 (dd, $J_{C,F}$ = 253.0, 11.0 Hz), 155.8 (d, $J_{C,F}$ = 249.0 Hz), 170.2. **ESI-MS** $[M-H]^-$ calculated for $C_{13}H_6O_2NF_3Br$: 344.0; found: 344.2.

6-(2-((4-Bromo-2-fluorophenyl)amino)-3,4-difluorobenzamido)hexanoic acid (6b)

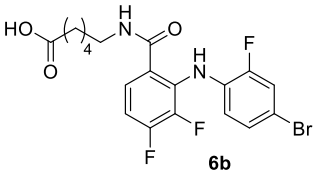

The representative procedure given for amide **3b** was carried out with 3,4-difluoro-2-((4-bromo-2-fluorophenyl)amino)benzoic acid **6a** (400 mg, 1.16 mmol, 1.0 eq) to afford **6b** (241 mg, 525 µmol, 45% yield) as a brown solid after flash column chromatography on silica gel (hexane/ethyl acetate 3:1 to 1:1).

TLC: R_f = 0.49 (hexane/ethyl acetate = 1:1). **^{1}H NMR** (d^3-MeOD, 400 MHz): δ = 1.13 - 1.32 (m), 1.41 (dd, *J* = 14.6, 7.3 Hz), 1.47 - 1.58 (m), 2.16[#] (t, *J* = 7.3 Hz), 2.20[*] (t, *J* = 7.2 Hz), 3.00 - 3.13[*] (m), 3.15 - 3.19[#] (m), 7.18 - 7.26 (m), 7.26 - 7.37 (m). **^{13}C NMR** (d^3-MeOD, 101 MHz):[15] δ = 25.9, 27.7, 30.0, 34.9, 40.9, 111.5, 117.6 (d, $J_{C,F}$ = 19.8 Hz), 119.9, 120.9 (d, $J_{C,F}$ = 17.5 Hz), 124.9 (d, $J_{C,F}$ = 13.2 Hz), 128.5, 128.9, 131.7, 134.0, 145.0 (d, $J_{C,F}$ = 246.0 Hz), 153.2 (d, $J_{C,F}$ = 210.1 Hz), 153.8 (d, $J_{C,F}$ = 237.0 Hz), 167.9, 177.6. **ESI-MS** $[M-H]^-$ calculated for $C_{19}H_{17}O_3N_2BrF_3$: 457.0; found: 456.9.

***N*-(6-((4-(1,2,4,5-Tetrazin-3-yl)benzyl)amino)-6-oxohexyl)-2-((2-fluoro-4-bromophenyl)amino)-3,4-difluorobenzamide (6)**

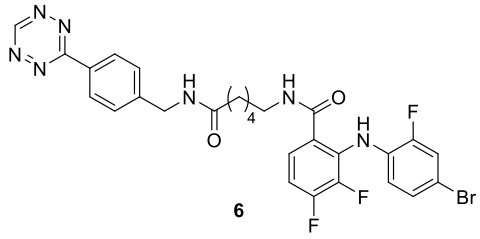

The representative procedure given for tetrazine conjugate **3** was carried out with compound **6b** (16.4 mg, 35.8 µmol, 1.0 eq) to afford the tetrazine conjugate **6** (16.1 mg, 25.6 µmol, 71% yield) after flash column chromatography on silica gel (hexane/ethyl acetate 1:1 to pure ethyl acetate).

TLC: R_f = 0.38 (ethyl acetate). **^{1}H NMR** (d^6-DMSO, 400 MHz): δ = 1.25 - 1.34 (2 H, m), 1.41 - 1.51 (2 H, m), 1.56 (2 H, t, *J* = 7.5 Hz), 2.17 (2 H, t, *J* = 7.3 Hz), 3.14 - 3.24 (2 H, m), 4.38 (2 H, d, *J* = 5.9 Hz), 6.84 (1 H, ddd, *J* = 9.0, 8.8, 5.2 Hz), 7.08 - 7.19 (1 H, m), 7.23 (1 H, d, *J* = 8.8 Hz), 7.52 (2 H, d, *J* = 8.1 Hz), 7.47 - 7.58 (2 H, m), 8.45 (2 H, d, *J* = 8.4 Hz), 8.41 - 8.50 (1 H, m), 8.70 (1 H, t, *J* = 5.6 Hz), 9.29 (1 H, s), 10.58 (1 H, s). **^{13}C NMR** (d^6-DMSO, 101 MHz):[15] δ = 24.9, 26.1, 28.5, 35.2, 38.9, 41.8, 110.8 (d, $J_{C,F}$ = 22.6 Hz), 115.6, 118.3, 119.7 (d, $J_{C,F}$ = 19.8 Hz), 124.6 (d, $J_{C,F}$ = 8.1 Hz), 127.3, 127.7 (2 C), 128.0 (2 C), 128.1, 130.3, 132.0, 133.0, 143.7 (d, $J_{C,F}$ = 241.0 Hz), 145.0, 152.8 (d, $J_{C,F}$ = 254.0 Hz), 153.1 (d, $J_{C,F}$ = 251.0 Hz), 158.1, 165.4, 166.4, 172.2. **ESI-MS** $[M+H]^+$ calculated for $C_{28}H_{26}O_2N_7BrF_3$: 628.1; found: 628.4.

4.6 Synthesis of Compound 7

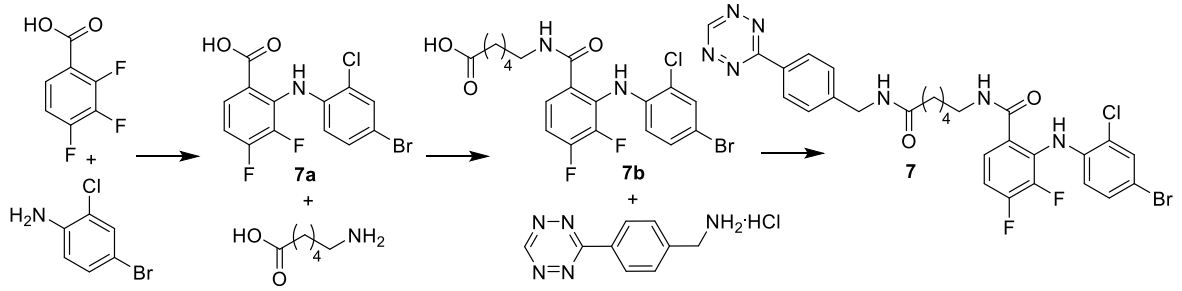

Scheme S5. Synthesis of compound **7**.

3,4-Difluoro-2-((4-bromo-2-chlorophenyl)amino)benzoic acid (7a)

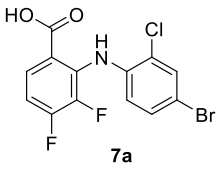

The representative procedure given for **3a** was carried out with 4-bromo-2-chloroaniline (1.23 g, 5.96 mmol, 1.05 eq) to afford **7a** (1.96 g, 5.41 mmol, 95% yield) as a brown solid.

TLC: R_f = 0.31 (hexane/ethyl acetate = 1:1). **^{1}H NMR** (d^3-MeOD, 400 MHz): δ = 6.81 (1 H, dd, *J* = 8.6, 7.0 Hz), 6.97 (1 H, td, *J* = 9.3, 7.2 Hz), 7.34 (1 H, dd, *J* = 8.8, 2.2 Hz), 7.58 (1 H, d, *J* = 2.2 Hz), 7.92 (1 H, ddd, *J* = 8.7, 6.2, 2.0 Hz). **^{13}C NMR** (d^3-MeOD, 101 MHz): δ = 110.2 (d, $J_{C,F}$ = 18.3 Hz), 114.9, 117.4, 121.0, 121.0, 126.1, 129.4 (dd, $J_{C,F}$ = 9.5, 3.7 Hz), 131.5, 132.8, 139.6, 143.5 (d, $J_{C,F}$ = 241.3 Hz), 155.5 (d, $J_{C,F}$ = 253.6 Hz), 170.0. **ESI-MS** $[M-H]^-$ calculated for $C_{13}H_6O_2NBrClF_2$: 359.9; found: 358.7.

6-(2-((4-Bromo-2-chlorophenyl)amino)-3,4-difluorobenzamido)hexanoic acid (7b)

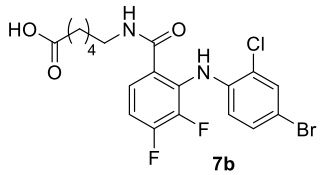

7b

The representative procedure given for amide **3b** was carried out with 3,4-difluoro-2-((4-bromo-2-chlorophenyl)amino)benzoic acid **7a** (400 mg, 1.10 mmol, 1.0 eq) to afford **7b** (245 mg, 515 µmol, 47% yield) as a white solid after flash column chromatography on silica gel (hexane/ethyl acetate 3:1 to 1:1).

TLC: R_f = 0.53 (hexane/ethyl acetate = 1:1). **^{1}H NMR** (d^3-MeOD, 400 MHz): δ = 1.27 - 1.45 (2 H, m), 1.47 - 1.59 (2 H, m), 1.60 - 1.70 (2 H, m), 2.25 (2 H, t, *J* = 7.4 Hz), 3.11 - 3.23 (2 H, m), 6.63 (1 H, dd, *J* = 8.8, 5.6 Hz), 7.05 - 7.14 (1 H, m), 7.28 (1 H, dd, *J* = 8.8, 2.3 Hz), 7.44 - 7.49 (1 H, m), 7.55 (1 H, d, *J* = 2.2 Hz). **^{13}C NMR** (d^3-MeOD, 101 MHz):[15] δ = 25.9, 27.7, 30.1, 34.9, 41.0, 112.2 (d, $J_{C,F}$ = 18.3 Hz), 113.4, 118.7, 118.7, 124.3, 124.9 (dd, $J_{C,F}$ = 7.3, 5.1 Hz), 126.0, 131.6, 132.8, 140.7, 145.1 (d, $J_{C,F}$ = 264.8 Hz), 154.4 (d, $J_{C,F}$ = 245.2 Hz), 169.3, 177.6. **ESI-MS** $[M-H]^-$ calculated for $C_{19}H_{17}O_3N_2BrClF_2$: 473.0; found: 473.0.

***N*-(6-((4-(1,2,4,5-Tetrazin-3-yl)benzyl)amino)-6-oxohexyl)-2-((2-chloro-4-bromophenyl)amino)-3,4-difluorobenzamide (7)**

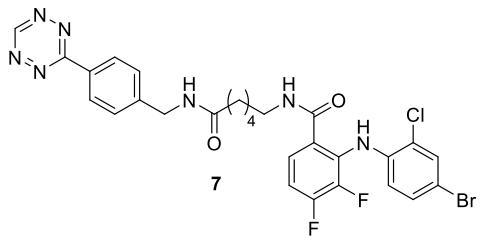

7

The representative procedure given for tetrazine conjugate **3** was carried out with compound **7b** (17.4 mg, 36.6 µmol, 1.0 eq) to afford tetrazine conjugate **7** (14.1 mg, 22.4 µmol, 61% yield) after flash column chromatography on silica gel (hexane/ethyl acetate 1:1 to pure ethyl acetate).

TLC: R_f = 0.33 (ethyl acetate). **^{1}H NMR** (d^6-DMSO, 400 MHz):): δ = 1.25 - 1.35 (2 H, m), 1.43 - 1.53 (2 H, m), 1.53 - 1.60 (2 H, m), 2.17 (2 H, t, *J* = 7.4 Hz), 3.21 (2 H, q, *J* = 6.7 Hz), 4.38 (2 H, d, *J* = 6.0 Hz), 6.75 (1 H, dd, *J* = 8.6, 6.7 Hz), 7.16 - 7.29 (1 H, m), 7.36 (1 H, dd, *J* = 8.8, 2.3 Hz), 7.52 (2 H, d, *J* = 8.5 Hz), 7.54 - 7.60 (1 H, m), 7.67 (1 H, d, *J* = 2.3 Hz), 8.38 - 8.43 (1 H, m), 8.45 (2 H, d, *J* = 8.3 Hz), 8.74 (1 H, t, *J* = 5.5 Hz), 9.43 (1 H, s), 10.58 (1 H, s). **^{13}C NMR** (d^6-DMSO, 101 MHz):[15] δ = 24.9, 26.1, 28.5, 35.2, 38.9, 41.8, 110.2 (d, $J_{C,F}$ = 17.7 Hz), 111.7, 118.1, 118.2, 122.6 (2 C), 124.8, 127.7 (2 C), 128.0 (2 C), 130.3, 130.4, 131.1, 138.5, 141.9 (d, $J_{C,F}$ = 239.0 Hz), 145.0, 149.6 (d, $J_{C,F}$ = 249.0 Hz), 158.1, 165.4, 166.6, 172.2. **ESI-MS** $[M+H]^+$ calculated for $C_{28}H_{26}O_2N_7BrClF_2$: 643.1; found: 642.7.

4.7 Synthesis of Compound 8

***N*-(4-(1,2,4,5-Tetrazin-3-yl)benzyl)-2-((4-bromo-2-chlorophenyl)amino)-3,4-difluorobenzamide (8)**

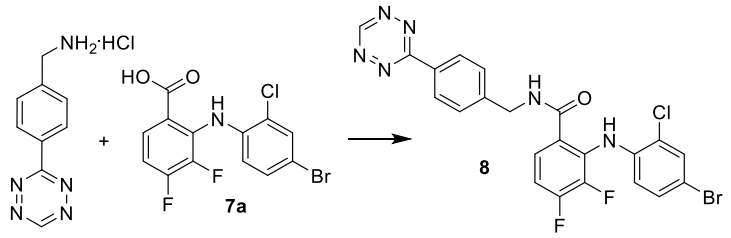

Scheme S6. Synthesis of compound **8**.

The representative procedure given for tetrazine conjugate **3** was carried out with 3,4-difluoro-2-((4-bromo-2-chlorophenyl)amino)benzoic acid **7a** (29.2 mg, 80.5 µmol, 1.0 eq) to afford tetrazine conjugate **8** (33.4 mg, 63 µmol, 78% yield) after flash column chromatography on silica gel (hexane/ethyl acetate 2:1 to pure ethyl acetate).

TLC: R_f = 0.45 (ethyl acetate). **^{1}H NMR** (d^6-DMSO, 400 MHz): δ = 4.58 (2 H, d, *J* = 5.4 Hz), 6.78 (1 H, dd, *J* = 8.6, 6.6 Hz), 7.30 (1 H, q, *J* = 8.8 Hz), 7.37 (1 H, dd, *J* = 8.8, 2.2 Hz), 7.58 (2 H, d, *J* = 8.3 Hz), 7.67 (1 H, d, *J* = 2.0 Hz), 7.71 (1 H, dd, *J* = 7.3, 6.0 Hz), 8.44 (2 H, d, *J* = 8.2 Hz), 9.37 (1 H, s), 9.45 (1 H, t, *J* = 5.9 Hz), 10.58 (1 H, s). **^{13}C NMR** (d^6-DMSO, 101 MHz):[15] δ = 42.5, 110.5 (d, $J_{C,F}$ = 18.2 Hz), 111.8, 118.2, 118.2, 122.3, 122.6, 124.9 (dd, $J_{C,F}$ = 9.3, 4.1 Hz), 127.8 (2 C), 128.1 (2 C), 130.4, 130.5, 131.2, 138.6, 142.7 (d, $J_{C,F}$ = 234.0 Hz), 144.1, 151.9 (d, $J_{C,F}$ = 250.6 Hz), 158.1, 165.4, 167.0. **ESI-MS** $[M+H]^+$ calculated for $C_{22}H_{15}ON_6BrClF_2$: 531.0; found: 531.3.

4.8 Synthesis of Compound 9

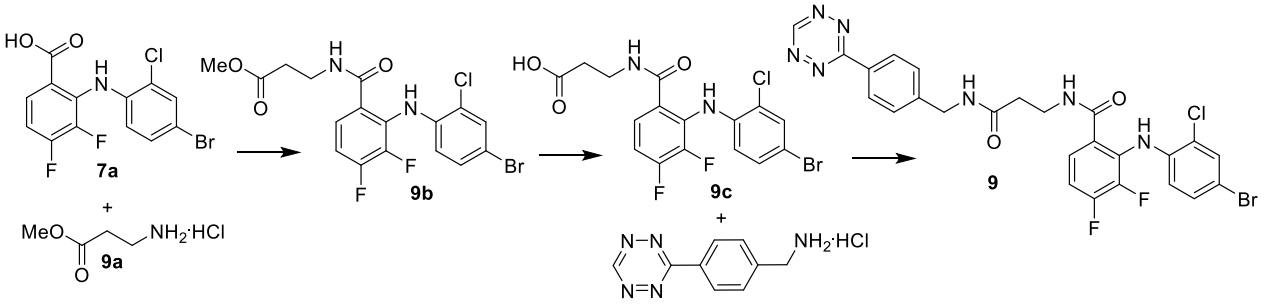

Scheme S7. Synthesis of Compound **9**.

Methyl 3-(2-((4-bromo-2-chlorophenyl)amino)-3,4-difluorobenzamido)propanoate (9b)

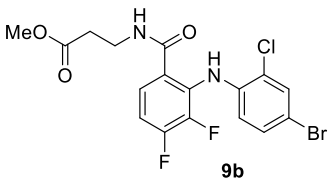

3,4-Difluoro-2-((4-bromo-2-chlorophenyl)amino)benzoic acid **7a** (200 mg, 552 µmol, 1.0 eq), methyl 3-aminopropanoate hydrochloride **9a** (104 mg, 744 µmol, 1.35 eq), EDCI hydrochloride (158 mg, 827 µmol, 1.5 eq) and BtOH (12.6 mg, 82.8 µmol, 0.15 eq) were dissolved in dry DMF (4.0 mL). Then triethylamine (147 µL, 1.10 mmol, 2.0 eq), was added dropwise and the mixture was stirred for 14 h at rt. Subsequently,

water (10 mL) was added and the mixture was extracted with 3 x 10 mL EtOAc, dried over $MgSO_4$ and filtered off. The solvent was then evaporated under reduced pressure and the crude product was purified by flash column chromatography on silica gel (hexane/ethyl acetate 3:1 to - 1:1) to afford amide **9b** (192 mg, 428 µmol, 78% yield) as a colourless oil.

TLC: R_f = 0.47 (hexane/ethyl acetate = 3:1). **^{1}H NMR** ($CDCl_3$, 400 MHz): δ = 2.58 (2 H, t, *J* = 5.9 Hz), 3.66 (2 H, dd, *J* = 11.7, 5.9 Hz), 3.70 (3 H, s), 6.62 (1 H, dd, *J* = 8.7, 6.1 Hz), 6.87 - 6.96 (1 H, m), 7.02 - 7.08 (1 H, m), 7.24 (1 H, dd, *J* = 8.8, 2.2 Hz), 7.33 - 7.40 (1 H, m), 7.51 (1 H, d, *J* = 2.2 Hz), 8.68 (1 H, s). **^{13}C NMR** ($CDCl_3$, 101 MHz):[15] δ = 33.3, 35.2, 51.9, 110.4 (d, $J_{C,F}$ = 17.6 Hz), 112.9, 117.6, 117.7, 122.2, 123.6 (dd, $J_{C,F}$ = 8.8, 3.7 Hz), 123.8, 130.0, 131.7, 138.4, 143.5 (dd, $J_{C,F}$ = 251.0, 13.9 Hz), 153.0 (dd, $J_{C,F}$ = 254.0, 11.0 Hz), 166.7, 173.2. **ESI-MS** $[M+H]^+$ calculated for $C_{17}H_{15}O_3N_2BrClF_2$: 447.0; found: 447.1.

3-(2-((4-Bromo-2-chlorophenyl)amino)-3,4-difluorobenzamido)propanoic acid (9c)

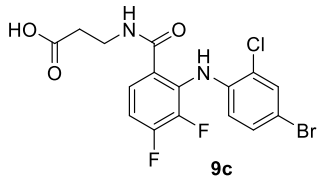

9c

Ester **9b** (90.0 mg, 201 µmol, 1.0 eq) was treated with $LiOH{\cdot}H_2O$ (169 mg, 4.02 mmol, 20 eq) in a 2:1:1 mixture of MeOH/THF/H_2O (4 mL, 2 mL, 2 mL), heated up to 60 °C and stirred for 5 h. The organic solvents were then evaporated *in vacuo*, water was added (10 mL) and the pH value was adjusted to pH = 2 by the dropwise addition of 1M HCl. Subsequently the mixture was extracted with 3 x 10 mL EtOAc, dried over $MgSO_4$ and evaporated under reduced pressure to yield carboxylic acid **9c** (84.7 mg, 195 µmol, 97% yield) as a white solid.

TLC: R_f = 0.32 (petroleum ether/ethyl acetate = 1:1). **^{1}H NMR** (d^3-MeOD, 400 MHz): δ = 2.56 (2 H, t, *J* = 6.8 Hz), 3.55 (2 H, t, *J* = 6.8 Hz), 6.65 (1 H, dd, *J* = 8.6, 5.9 Hz), 7.07 (1 H, td, *J* = 9.3, 7.2 Hz), 7.29 (1 H, dd, *J* = 8.8, 2.2 Hz), 7.45 - 7.51 (1 H, m), 7.54 (1 H, d, *J* = 2.2 Hz). **^{13}C NMR** (d^3-MeOD, 101 MHz):[15] δ = 34.5, 37.0, 111.9 (d, $J_{C,F}$ = 18.3 Hz), 113.5, 118.9, 119.0, 124.6, 125.0, 125.8 (dd, $J_{C,F}$ = 8.4, 4.0 Hz), 131.5, 132.8, 140.5, 145.2 (dd, $J_{C,F}$ = 250.4, 14.8 Hz), 154.2 (dd, $J_{C,F}$ = 253.0, 10.0 Hz), 169.4, 175.5. **ESI-MS** $[M-H]^-$ calculated for $C_{16}H_{11}O_3N_2BrClF_2$: 431.0; found: 430.8.

***N*-(3-((4-(1,2,4,5-Tetrazin-3-yl)benzyl)amino)-3-oxopropyl)-2-((4-bromo-2-chlorophenyl)amino)-3,4-difluorobenzamide (9)**

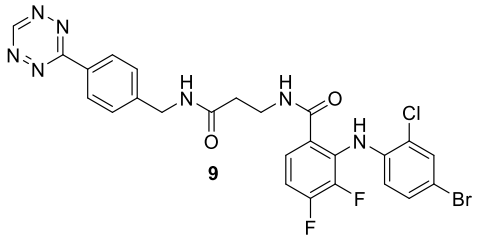

9

The representative procedure given for tetrazine conjugate **3** was carried out with compound **9c** (22.3 mg, 51.4 µmol, 1.0 eq) to afford tetrazine conjugate **9** (23.9 mg, 39.6 µmol, 77% yield) after flash column chromatography on silica gel (hexane/ethyl acetate 1:1 to pure ethyl acetate).

TLC: R_f = 0.29 (ethyl acetate). **^{1}H NMR** (d^6-DMSO, 400 MHz): δ = 2.45 - 2.48 (2 H, m), 3.45 - 3.53 (2 H, m), 4.39 (2 H, d, *J* = 4.5 Hz), 6.76 (1 H, dd, *J* = 8.6, 7.0 Hz), 7.15 - 7.27 (1 H, m), 7.36 (1 H, dd, *J* = 8.6, 2.2 Hz), 7.51 (2 H, d, *J* = 7.9 Hz), 7.54 - 7.60 (1 H, m), 7.68 (1 H, d, *J* = 2.2 Hz), 8.40 (2 H, d, *J* = 8.1

Hz), 8.57 (1 H, t, *J* = 5.9 Hz), 8.89 (1 H, t, *J* = 5.4 Hz), 9.56 (1 H, s), 10.59 (1 H, s). **^{13}C NMR** (d^6-DMSO, 101 MHz):[15] δ = 34.9, 36.1, 41.8, 110.0 (d, $J_{C,F}$ = 17.6 Hz), 111.8, 118.3, 118.4, 121.8, 122.8, 124.9 (dd, $J_{C,F}$ = 8.4, 3.3 Hz), 127.7 (2 C), 128.1 (2 C), 130.3, 130.4, 131.1, 138.4, 142.5 (d, $J_{C,F}$ = 249.0 Hz), 144.8, 151.9 (d, $J_{C,F}$ = 261.0 Hz), 158.1, 165.4, 166.8, 170.4. **ESI-MS** $[M+H]^+$ calculated for $C_{25}H_{20}O_2N_7BrClF_2$: 602.1; found: 601.8.

4.9 Synthesis of Compound 10

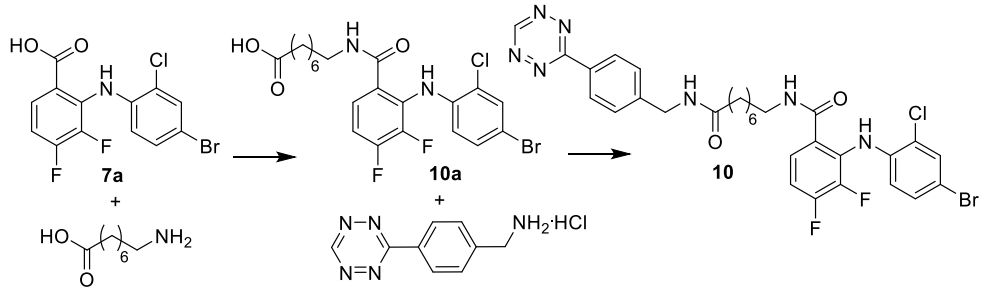

Scheme S8. Synthesis of compound **10**.

8-(2-((4-Bromo-2-chlorophenyl)amino)-3,4-difluorobenzamido)octanoic acid (10a)

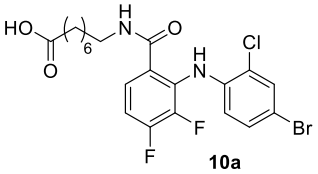

The representative procedure given for amide **3b** was carried out with 3,4-difluoro-2-((4-bromo-2-chlorophenyl)amino)benzoic acid **7a** (250 mg, 690 µmol, 1.0 eq) and 8-aminooctanoic acid (131 mg, 827 µmol, 1.2 eq) to afford **10a** (225 mg, 446 µmol, 65% yield) as a brown solid after flash column chromatography on silica gel (hexane/ethyl acetate 3:1 to 1:1).

TLC: R_f = 0.39 (hexane/ethyl acetate = 3:1). **^{1}H NMR** (d^3-MeOD, 400 MHz): δ = 1.24 - 1.40 (6 H, m), 1.46 - 1.54 (2 H, m), 1.54 - 1.64 (2 H, m), 2.26 (2 H, t, *J* = 7.4 Hz), 3.25 - 3.29 (2 H, m), 6.62 (1 H, dd, *J* = 8.7, 5.5 Hz), 7.09 (1 H, td, *J* = 9.3, 7.2 Hz), 7.28 (1 H, dd, *J* = 8.8, 2.2 Hz), 7.46 (1 H, ddd, *J* = 8.7, 5.5, 2.0 Hz), 7.54 (1 H, d, *J* = 2.2 Hz). **^{13}C NMR** ($CDCl_3$, 101 MHz):[15] δ = 26.2, 28.0, 30.2, 30.3, 30.4, 35.1, 40.9*, 41.2#, 112.4 (d, $J_{C,F}$ = 18.3 Hz), 113.3, 118.6, 118.6, 124.3, 125.6 (dd, $J_{C,F}$ = 8.8, 4.4 Hz), 126.2, 131.6, 132.8, 140.7, 144.5 (d, $J_{C,F}$ = 242.0 Hz), 154.1 (dd, $J_{C,F}$ = 252.0, 11.2 Hz), 169.3, 177.8. **ESI-MS** $[M-H]^-$ calculated for $C_{21}H_{21}O_3N_2BrClF_2$: 501.0; found: 501.4.

***N*-(8-((4-(1,2,4,5-tetrazin-3-yl)benzyl)amino)-8-oxooctyl)-2-((4-bromo-2-chlorophenyl)amino)-3,4-difluorobenzamide (10)**

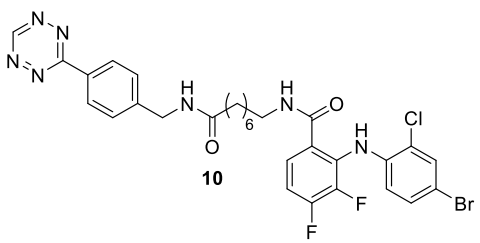

The representative procedure given for tetrazine conjugate **3** was carried out with compound **10a** (22.5 mg, 44.7 µmol, 1.0 eq) to afford the pink tetrazine conjugate **10** (18.9 mg, 28.1 µmol, 63% yield) after flash column chromatography on silica gel (hexane/ethyl acetate 2:1 to pure ethyl acetate).

TLC: R_f = 0.42 (ethyl acetate). **^{1}H NMR** (d^6-DMSO, 400 MHz): 1.18 - 1.30 (6 H, m), 1.41 - 1.49 (2 H, m), 1.49 - 1.57 (2 H, m), 2.16 (2 H, t, *J* = 7.4 Hz), 3.20 (2 H, q, *J* = 6.2 Hz), 4.39 (2 H, d, *J* = 5.7 Hz), 6.73 (1 H, dd, *J* = 8.6, 6.6 Hz), 7.20 - 7.29 (1 H, m), 7.36 (1 H, dd, *J* = 8.7, 2.3 Hz), 7.52 (2 H, d, *J* = 8.3 Hz), 7.55 - 7.58 (1 H, m), 7.68 (1 H, d, *J* = 2.2 Hz), 8.41 - 8.44 (1 H, m), 8.45 (2 H, d, *J* = 8.3 Hz), 8.73 (1 H, t, *J* = 5.6 Hz), 9.37 (1 H, s), 10.58 (1 H, s). **^{13}C NMR** (d^6-DMSO, 101 MHz):[15] δ = 25.2, 26.3, 28.4, 28.6, 28.7, 35.3, 38.9, 41.8, 110.4 (d, $J_{C,F}$ = 16.9 Hz), 111.6, 118.0, 118.0, 122.5, 122.9, 124.7 (dd, $J_{C,F}$ = 11.3, 4.3 Hz), 127.8 (2 C), 128.0 (2 C), 130.3, 130.4, 131.1, 138.6, 142.8 (d, $J_{C,F}$ = 253.0 Hz), 145.1, 151.6 (d, $J_{C,F}$ = 251.0 Hz), 158.1, 165.4, 166.6, 172.3. **ESI-MS** $[M+H]^+$ calculated for $C_{30}H_{30}O_2N_7BrClF_2$: 672.1; found: 672.2.

4.10 Synthesis of Compound 11

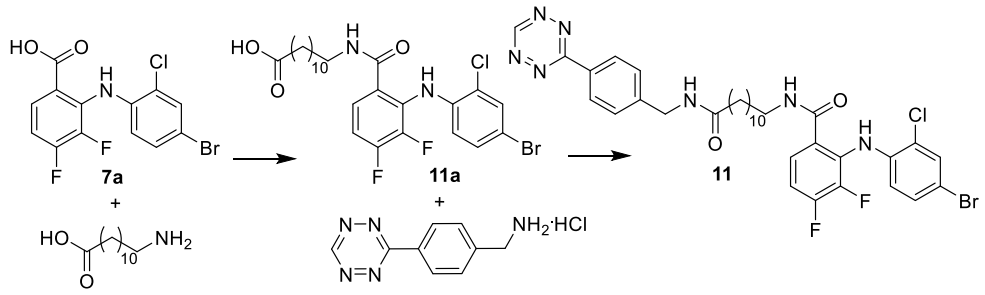

Scheme S9. Synthesis of compound **11**.

12-(2-((4-Bromo-2-chlorophenyl)amino)-3,4-difluorobenzamido)dodecanoic acid (11a)

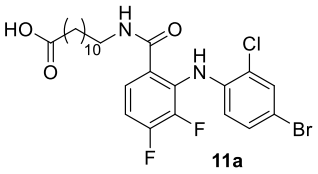

The representative procedure given for amide **3b** was carried out with 3,4-difluoro-2-((4-bromo-2-chlorophenyl)amino)benzoic acid **7a** (250 mg, 690 µmol, 1.0 eq) and 12-aminododecanoic acid (178 mg, 827 mmol, 1.2 eq) to afford **11a** (237 mg, 423 µmol, 61% yield) as a brown solid after flash column chromatography on silica gel (hexane/ethyl acetate 5:1 to 2:1).

TLC: R_f = 0.36 (hexane/ethyl acetate = 5:1). **^{1}H NMR** (d^3-MeOD, 400 MHz): δ = 1.15 - 1.39 (14 H, m), 1.44 - 1.54 (2 H, m), 1.55 - 1.64 (2 H, m), 2.27 (2 H, t, *J* = 7.5 Hz), 3.09-3.20[#] (2 H, m), 3.26 - 3.29[*] (2 H, m), 6.61 (1 H, dd, *J* = 8.7, 5.5 Hz), 7.08 (1 H, ddd, *J* = 9.3, 9.2, 7.2 Hz), 7.26 (1 H, dd, *J* = 8.8, 2.2 Hz), 7.43 - 7.48 (1 H, m), 7.52 (1 H, d, *J* = 2.2 Hz). **^{13}C NMR** (d^3-MeOD, 101 MHz):[15] δ = 26.2, 28.1, 30.4, 30.4, 30.6, 30.7, 30.8, 30.8, 30.8, 35.1, 41.0[*], 41.3[#], 112.3 (d, $J_{C,F}$ = 18.3 Hz), 113.3, 118.5, 118.6, 124.3, 125.6 (dd, $J_{C,F}$ = 8.8, 3.7 Hz), 126.2, 131.6, 132.8, 140.7, 145.5 (dd, $J_{C,F}$ = 250.0, 14.7 Hz), 154.1 (dd, $J_{C,F}$ = 251.0, 11.0 Hz), 169.3, 177.8. **ESI-MS** $[M-H]^-$ calculated for $C_{25}H_{29}O_3N_2BrClF_2$: 557.1; found: 556.8.

***N*-(12-((4-(1,2,4,5-Tetrazin-3-yl)benzyl)amino)-12-oxododecyl)-2-((4-bromo-2-chlorophenyl)amino)-3,4-difluorobenzamide (11)**

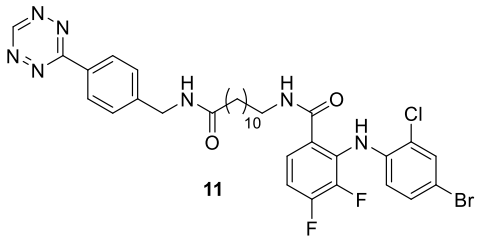

The representative procedure given for tetrazine conjugate **3** was carried out with compound **11a** (21.9 mg, 39.1 µmol, 1.0 eq) to afford tetrazine conjugate **11** (20.3 mg, 27.8 µmol, 71% yield) after flash column chromatography on silica gel (hexane/ethyl acetate 3:1 to pure ethyl acetate).

TLC: R_f = 0.51 (ethyl acetate). **^{1}H NMR** (d^6-DMSO, 400 MHz): δ = 1.13 - 1.30 (14 H, m), 1.39 - 1.49 (2 H, m), 1.50 - 1.58 (2 H, m), 2.17 (2 H, t, *J* = 7.3 Hz), 3.20 (2 H, q, *J* = 6.1 Hz), 4.39 (2 H, d, *J* = 5.9 Hz), 6.73 (1 H, dd, *J* = 8.5, 6.7 Hz), 7.19 - 7.31 (1 H, m), 7.36 (1 H, dd, *J* = 8.8, 2.0 Hz), 7.53 (2 H, d, *J* = 8.1 Hz), 7.55 - 7.58 (1 H, m), 7.66 (1 H, d, *J* = 2.2 Hz), 8.39 - 8.43 (1 H, m), 8.45 (2 H, d, *J* = 8.2 Hz), 8.71 (1 H, t, *J* = 5.5 Hz), 9.33 (1 H, s), 10.57 (1 H, s). **^{13}C NMR** (d^6-DMSO, 101 MHz):[15] δ = 25.3, 26.3, 28.6, 28.7, 28.7, 28.9, 28.9, 29.0, 35.3, 38.9, 41.8, 110.5, 111.6, 117.9, 118.0, 122.4, 123.1, 124.7, 127.7 (2 C), 128.0 (2 C), 130.3, 130.4, 131.1, 138.6, 142.8 (d, $J_{C,F}$ = 249.0 Hz), 145.1, 151.8 (d, $J_{C,F}$ = 258.0 Hz), 158.1, 165.4, 166.7, 172.3. **ESI-MS** $[M+H]^+$ calculated for $C_{34}H_{38}O_2N_7BrClF_2$: 728.1; found: 727.8.

4.11 Synthesis of Compound 12

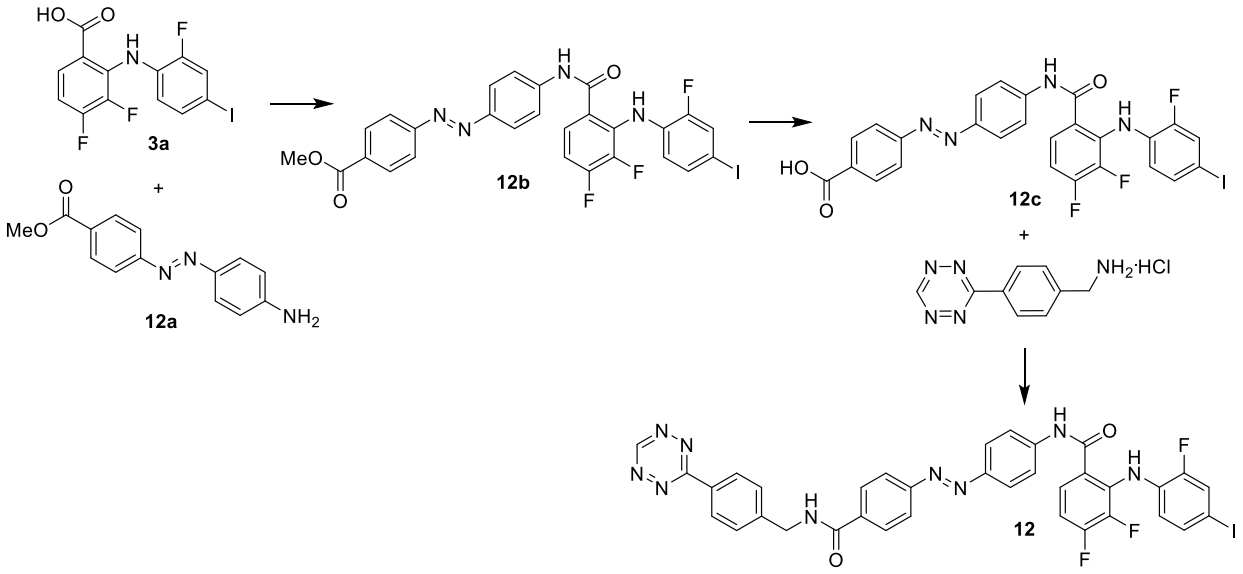

Scheme S10. Synthesis of compound **12**.

Methyl (*E*)-4-((4-aminophenyl)diazenyl)benzoate (12a)

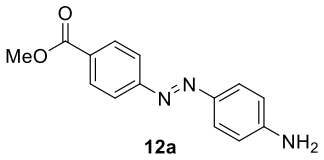

12a

To a stirring solution of methyl 4-aminobenzoate (7.50 g, 49.6 mmol, 1.0 eq) in CH_2Cl_2 was added a solution of Oxone® (48.8 g, 79.4 mmol, 1.6 eq) in water (250 mL). The reaction mixture was then stirred for 4.5 h at rt. Subsequently, the deep green coloured organic layer was separated, the aqueous solution was neutralized by the addition of saturated solution of $NaHCO_3$ (150 mL) and extraceted with CH_2Cl_2 (3 x 125 mL). The combined organic layers were tried with $MgSO_4$, filtered off and the solvent was removed *in vacuo*. The crude nitroso-compound was then dissolved in a mixture of dry CH_2Cl_2 (120 mL) and dry THF (30 mL). To this solution p-phenylenediamine (5.37 g, 49.6 mmol, 1.0 eq) and glacial acetic acid (14.2 mL, 248 mmol, 5.0 eq) was added. The mixture was finally stirred overnight (14 h) in the absence of light, the solvent was evaporated under reduced pressure and the residue was purified by column chromatography (hexane/ethyl acetate 3:1 to 1:1, 1% NEt_3) to yield azobenzene linker **12a** (8.30 g, 32.5 mmol, 66% yield) as an orange solid.

TLC: R_f = 0.52 (hexane/ethyl acetate 3:1). **^{1}H NMR** (d^6-DMSO, 400 MHz): δ = 3.88 (3 H, s), 6.32 (2 H, br. s), 6.69 (2 H, d, *J* = 8.9 Hz), 7.71 (2 H, d, *J* = 8.8 Hz), 7.82 (2 H, d, *J* = 8.5 Hz), 8.08 (2 H, d, *J* = 8.6 Hz). **^{13}C NMR** (d^6-DMSO, 101 MHz): δ = 52.2, 113.4 (2 C), 121.7 (2 C), 125.9 (2 C), 129.4, 130.4 (2 C), 142.9, 153.8, 155.3, 165.8. **ESI-MS** $[M+H]^+$ calculated for $C_{14}H_{13}N_3O_2$: 256.3; found: 256.3.

Methyl (*E*)-4-((4-(3,4-difluoro-2-((2-fluoro-4-iodophenyl)amino)benzamido)phenyl)diazenyl) benzoate (12b)

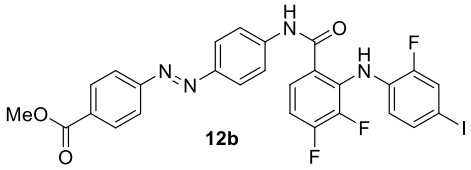

12b

3,4-Difluoro-2-((2-fluoro-4-iodophenyl)amino)benzoic acid **3a** (311 mg, 793 µmol, 1.35 eq) was dissolved in dry CH_2Cl_2 (3 mL) and one drop of DMF was added. The resulting mixture was then cooled to 0°C, followed by the dropwise addition of a solution of oxalyl chloride (73 µL, 852 µL, 1.45 eq) in CH_2Cl_2 (0.5 mL). The mixture was further stirred at 0°C for 15 min, warmed up to rt and the stirring was continued for additional 2 h. Subsequently the solvent and excess of oxalyl chloride was removed under reduced pressure, the residue was dissolved in CH_2Cl_2 (1 mL) and added dropwise to a mixture of azobenzene linker **12a** (150 mg, 587 µmol, 1.0 eq) and NEt_3 (523 µL, 2.94 mmol, 5.0 eq) in CH_2Cl_2 (5 mL) at 0°C. The reaction mixture was then warmed up to rt and stirred overnight (15 h). After the addition of water the pH was adjusted to pH = 10 by the dropwise addition of NaOH (1 M). The layers were the separated, the organic layer was washed with water (2 x 10 mL) and the aqueous layer was extracted with CH_2Cl_2 (3 x 10 mL). The combined organic layers were dried over $MgSO_4$, filtered off and the solvent was removed *in vacuo*. Column chromatography (hexane/ethyl acetate 9:1 to 5:1 to 1:1) affords azobenzene conjugate **12b** (235 mg, 372 µmol, 63% yield) as a yellow solid.

TLC: R_f = 0.56 (hexane/ethyl acetate 3:1). **^{1}H NMR** (d^6-DMSO, 400 MHz): δ = 3.97 (3 H, s), 6.59 (1 H, ddd, *J* = 8.6, 8.5, 4.0 Hz), 6.97 - 7.08 (1 H, m), 7.29 - 7.36 (1 H, m), 7.39 - 7.45 (1 H, m), 7.59 - 7.68 (1 H, m), 7.72 (2 H, d, *J* = 8.9 Hz), 7.94 (2 H, d, *J* = 8.7 Hz), 7.98 (2 H, d, *J* = 8.6 Hz), 7.99 (1 H, br.s), 8.19 (2 H, d, *J* = 8.8 Hz), 8.61 (1 H, s). **^{13}C NMR** (d^6-DMSO, 101 MHz):[15] δ = 52.3, 83.1, 111.0 (d, $J_{C,F}$ = 18.0 Hz), 119.8, 120.3 (2 C), 122.4, 122.6 (2 C), 124.2, 124.5 (2 C), 124.6, 130.6 (2 C), 130.9, 131.7, 133.3,

140.3, 144.0 (d, $J_{C,F}$ = 237.0 Hz), 149.3, 152.1, 153.3 (d, $J_{C,F}$ = 257.0 Hz), 153.7 (d, $J_{C,F}$ = 247.0 Hz), 155.1, 164.6, 166.5. **ESI-MS** $[M+H]^+$ calculated for $C_{27}H_{19}F_3IN_4O_3$: 631.0; found: 631.1.

(*E*)-4-((4-(3,4-Difluoro-2-((2-fluoro-4-iodophenyl)amino)benzamido)phenyl)diazenyl)benzoic acid (12c)

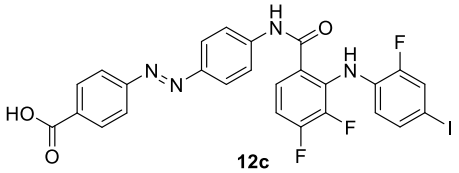

12c

Azobenzene ester **12b** (44.0 mg, 69.8 µmol, 1.0 eq) was treated with $LiOH \cdot H_2O$ (8.80 mg, 209 µmol, 3.0 eq) in a 2:1:1 mixture of MeOH/THF/H_2O (0.5 mL, 0.25 mL, 0.25 mL) at rt and stirred for 4 h. The organic solvents were then evaporated *in vacuo*, water was added (3 mL) and the pH value was adjusted to pH = 4 by the dropwise addition of 1M HCl. Subsequently, the reaction product was filtered off, repetitively washed with water (3 x 10 mL) and ethyl acetate (3 x 10 mL) and dried *in vacuo* to afford acid **12c** (38.0 mg, 61.6 µmol, 88% yield) as a yellow solid which was used in the following reaction without further purification.

(*E*)-*N*-(4-((4-((4-(1,2,4,5-Tetrazin-3-yl)benzyl)carbamoyl)phenyl)diazenyl)phenyl)-3,4-difluoro-2-((2-fluoro-4-iodophenyl)amino)benzamide (12)

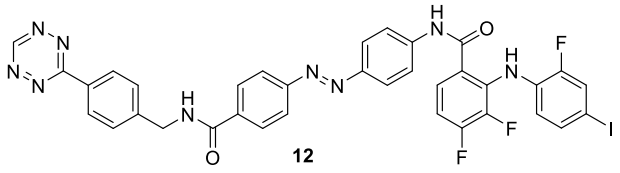

12

Acid **12c** (33.0 mg, 53.5 µmol, 1.35 eq), (4-(1,2,4,5-tetrazin-3-yl)phenyl)methanamine hydrochloride (8.87 mg, 39.6 µmol, 1.0 eq), EDCI hydrochloride (13.7 mg, 71.4 µmol, 1.8 eq) and BtOH (1.52 mg, 9.92 µmol, 0.25 eq) were dissolved in dry DMF (1.5 mL). Then pyridine (32 µL, 397 µmol, 10.0 eq) was added dropwise and the mixture was stirred for 16 h at rt. After removal of the solvent by freeze drying the crude product was purified by column chromatography (hexane/ethyl acetate 3:1 to 1:1 to pure ethyl acetate) to yield tetrazine azobenzene conjugate **12** (15.2 mg, 19.4 µmol, 49% yield) as a red orange solid.

TLC: R_f = 0.21 (hexane/ethyl acetate 1:1). **^{1}H NMR** (d^6-DMSO, 400 MHz): δ = 4.66 (2 H, d, *J* = 5.7 Hz), 6.72 (1 H, td, *J* = 8.8, 3.8 Hz), 7.25 - 7.33 (1 H, m), 7.35 (1 H, d, *J* = 8.5 Hz), 7.53 (1 H, dd, *J* = 10.8, 1.8 Hz), 7.60 (1 H, d, *J* = 8.6 Hz), 7.65 (2 H, d, *J* = 8.3 Hz), 7.86 - 7.92 (3 H, m), 7.93 - 7.98 (3 H, m), 8.13 (2 H, d, *J* = 8.6 Hz), 8.49 (2 H, d, *J* = 8.3 Hz), 8.60 (1 H, s), 9.31 - 9.41 (1 H, m), 10.57 (1 H, s), 10.78 - 10.83 (1 H, m). **^{13}C NMR** (d^6-DMSO, 101 MHz):[15] δ = 42.7, 82.0, 110.4, 120.3, 120.5 (2 C), 122.3 (2 C), 123.6 (2 C), 123.8, 125.4, 127.9 (2 C), 128.2 (2 C), 128.6 (2 C), 130.5, 131.3, 133.2, 135.9, 138.5, 138.7, 143.4 (d, $J_{C,F}$ = 256.0 Hz), 144.8, 148.0, 152.1, 152.3 (d, $J_{C,F}$ = 234.0 Hz), 152.7 (d, $J_{C,F}$ = 237.0 Hz), 153.6, 158.1, 165.5, 165.7, 169.4. **ESI-MS** $[M+H]^+$ calculated for $C_{35}H_{24}F_3IN_9O_2$: 786.1; found: 786.3.

4.12 Synthesis of Compound 15i

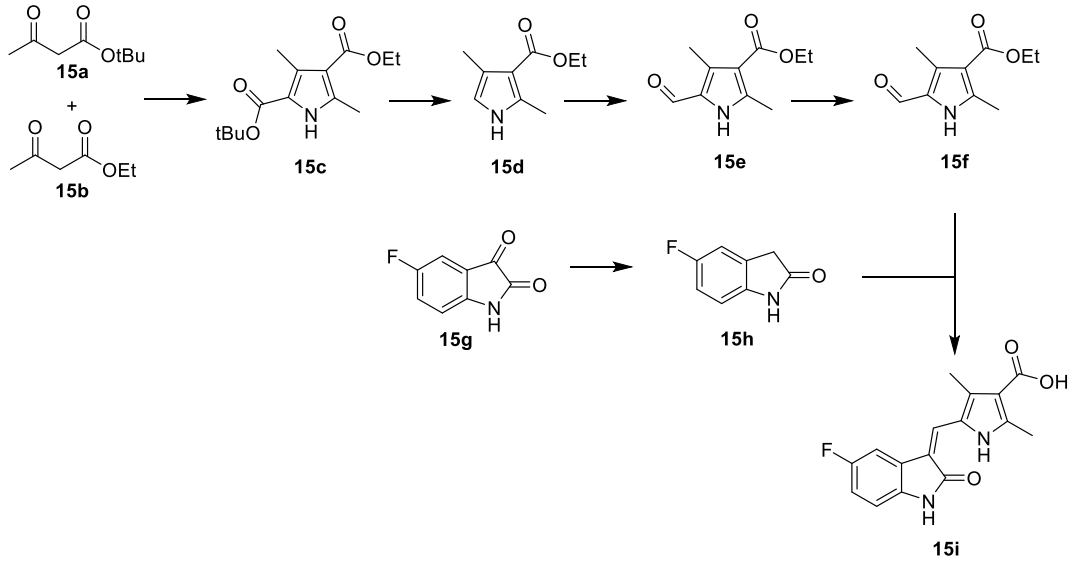

Scheme S11. Synthesis of compound **15i**.

2-(*tert*-Butyl) 4-ethyl 3,5-dimethyl-1H-pyrrole-2,4-dicarboxylate (15c)

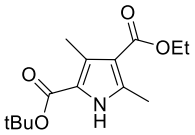

To an ice-cooled mixture of *tert*-butyl acetoacetate **15a** (10.0 g, 126.4 mmol, 1.0 eq) and glacial acetic acid (20 mL) was slowly added an aqueous solution of $NaNO_2$ (3 M, 21 mL, 126.4 mmol, 1.0 eq). The resulting solution was warmed to rt and stirring was continued at this temperature for 4 h. A solution of ethyl acetoacetate **15b** (14.4 g, 126.4 mmol, 1.0 eq) in glacial acetic acid (50 mL) was added in one portion to the mixture and the resulting solution warmed up to 65°C. Then zinc dust (8.2 g, 126.4 mmol, 1.0 eq) was added to the warm solution in small portions. The mixture was stirred at 65°C for 2 h and subsequently poured into 600 mL of cold water and stirred for 30 min. The resulting precipitate was filtered off, washed with water and dried under vacuum to afford **15c** as a pale yellow solid (18.3 g, 68.5 mmol, 54% yield).

TLC: R_f = 0.51 (hexane/ethyl acetate = 1:1). **^{1}H NMR** ($CDCl_3$, 400 MHz): δ = 1.36 (3 H, t, *J* = 7.1 Hz), 1.58 (9 H, s), 2.51 (3 H, s), 2.54 (3 H, s), 4.29 (2 H, q, *J* = 7.2 Hz), 9.03 (1 H, br. s.). **^{13}C NMR** ($CDCl_3$, 101 MHz): δ = 11.9, 14.3, 14.4, 28.5 (3 C), 59.4, 81.1, 113.4, 119.1, 129.9, 138.2, 161.1, 165.6. **ESI-MS** $[M+H]^+$ calculated for $C_{14}H_{21}O_4N$: 268.2; found: 268.3.

Ethyl 2,4-dimethyl-1*H*-pyrrole-3-carboxylate (15d)

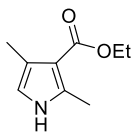

To a stirred solution of 3,5-dimethyl-1H-pyrrole-2,4-dicarboxylic acid 2-tert-butyl ester 4-ethyl ester **15c** (9.0 g, 33.7 mmol, 1.0 eq) in ethanol (300 mL) at 0°C was added slowly HCl (10 M, 17 mL, 168 mmol, 1.0 eq). The reaction mixture was then stirred at 65°C for 4 h. After cooling to rt the mixture was poured into ice water (1 L) and was extracted with 3 x 100 mL CH_2Cl_2. The combined organic extracts were washed with brine (50 mL) and water (50 mL), dried over anhydrous $MgSO_4$, filtered off and concentrated *in vacuo* to afford **15d** (5.52 g, 33.0 mmol, 98% yield) as a light brown solid.

TLC: R_f = 0.46 (hexane/ethyl acetate = 1:1). **^{1}H NMR** ($CDCl_3$, 400 MHz): δ = 1.36 (3 H, t, *J* = 7.2 Hz), 2.25 (3 H, s), 2.50 (3 H, s), 4.28 (2 H, q, *J* = 7.1 Hz), 6.36 (1 H, br. s), 7.92 (1 H, br. s.). **^{13}C NMR** ($CDCl_3$, 101 MHz): δ = 14.0, 14.5, 59.0, 110.8, 114.2, 121.6, 135.9, 166.3. **ESI-MS** $[M+H]^+$ calculated for $C_9H_{14}O_2N$: 168.1; found: 168.3.

Ethyl 5-formyl-2,4-dimethyl-1*H*-pyrrole-3-carboxylate (15e)

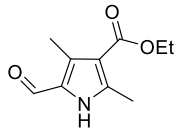

15e

To an ice-cooled solution of DMF (2.54 mL, 32.9 mmol, 1.1 eq) in CH_2Cl_2 (8 mL) was added drop wise $POCl_3$ (3.07 mL, 32.9 mmol, 1.1 eq). The reaction mixture was then warmed up to rt and stirring was continued for 15 min before it was cannulated over a period of 10 min to a solution of ethyl 2,4-dimethyl-1H-pyrrole-3-carboxylate **15c** (5.00 g, 29.9 mmol, 1.0 eq) in CH_2Cl_2 (60 mL) at 0°C. The reaction mixture was then stirred for additional 15 min and subsequently heated to reflux for 2.0 h. After cooling to rt an aqueous solution of $NaHCO_3$ (1 M, 150 mL, 150 mmol, 5.0 eq) was added and the reaction mixture was refluxed for 1 h. The organic layer was than separated and the aqueous layer was extracted with 3 x 50 mL CH_2Cl_2. The combined organic layers were washed with brine (50 mL) and water (2 x 50 mL), dried with $MgSO_4$, filtered of and the solvents were evaporated under reduced pressure to yield **15e** as a yellow solid (4.13 g, 21.2 mmol, 71% yield).

TLC: R_f = 0.56 (hexane/ethyl acetate = 1:1). **^{1}H NMR** ($CDCl_3$, 400 MHz): δ = 1.37 (3 H, t, *J* = 7.1 Hz), 2.56 (3 H, s), 2.59 (3 H, s), 4.31 (2 H, q, *J* = 7.1 Hz), 9.61 (1 H, s), 10.37 (1 H, br. s.). **^{13}C NMR** ($CDCl_3$, 101 MHz): δ = 10.6, 14.3, 14.4, 59.7, 114.2, 128.3, 136.3, 143.8, 165.0, 177.3. **ESI-MS** $[M+H]^+$ calculated for $C_{10}H_{14}O_3N$: 196.1; found: 196.1.

5-Formyl-2,4-dimethyl-1*H*-pyrrole-3-carboxylic acid (15f)

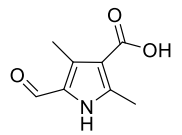

15f

To a solution of ethyl 5-formyl-2,4-dimethyl-1*H*-pyrrole-3-carboxylate **15e** (3.40 g, 17.4 mmol, 1.0 eq) in MeOH (60 mL) was added a solution of potassium hydroxide (1 M, 34.8 mL, 1.95 g, 34.8 mmol, 1.0 eq) in water and the reaction mixture was heated to reflux for 16 h. After cooling to rt the clear solution was diluted with water (30 mL) and washed with dichloromethane (40 mL). Subsequently, the pH was adjusted to pH = 3 by the slowly addition of concentrated HCl to recover **15f** as a red precipitate (2.59 g, 15.6 mmol, 89% yield). SE30

TLC: R_f = 0.33 (hexane/ethyl acetate = 1:1). **^{1}H NMR** (d^3-MeOD, 400 MHz): δ = 2.50 (3 H, s), 2.53 (3 H, s), 9.59 (1 H, s). **^{13}C NMR** (d^3-MeOD, 101 MHz): δ = 10.9, 14.0, 101.2, 115.0, 130.0, 145.2, 168.5, 179.3. **ESI-MS** $[M-H]^-$ calculated for $C_8H_8O_3N$: 166.1; found: 166.3.

5-Fluoroindolin-2-one (15h)

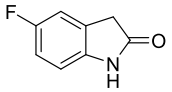

15h

5-Fluoroisatin **15g** (8.00 g, 48.5 mmol, 1.0 eq) and hydrazine monohydrate (3.41 g, 63.0 mmol, 1.3 eq) were suspended in *n*-butanol (60 mL) and stirred at rt for 30 min. After heating to 80°C for 3 h, triethylamine (9.0 mL, 67.8 mmol, 1.4 eq) was added and the suspension was stirred further 12 h at 100°C. Upon cooling to rt the solvent was removed *in vacuo*, the crude mixture was dissolved in ethyl acetate (50 mL) and washed with a solution of 10% $KHSO_4$ in water (50 mL). The aqueous layer was then extracted with ethyl acetate (3 x 100 mL), the combined organic phases were washed with brine (50 mL) and the solvents were evaporated under reduced pressure. Afterwards the residue was dissolved in hot ethyl acetate (50 mL) and petroleum ether was added until the solution became slightly cloudy. After filtration and cooling to rt **15h** was obtained as light brown crystals (6.1 g, 40.3 mmol, 83% yield).

TLC: R_f = 0.31 (ethyl acetate). **^{1}H NMR** (d^3-MeOD, 400 MHz): δ = 4.30 (2 H, s), 7.59 (1 H, dd, *J* = 8.5, 4.4 Hz), 7.75 - 7.83 (1 H, m), 7.90 (1 H, dd, *J* = 8.5, 2.3 Hz), 11.17 (1 H, br. s.). **^{13}C NMR** (d^3-MeOD, 101 MHz): δ = 45.8, 119.2 (d, $J_{C,F}$ =8.1 Hz), 121.8 (d, $J_{C,F}$ =25.0 Hz), 123.2 (d, $J_{C,F}$ =22.0 Hz), 137.3 (d, $J_{C,F}$ =8.8 Hz), 149.5, 167.4 (d, $J_{C,F}$ =234.0 Hz), 185.8. **ESI-MS** $[M+H]^+$ calculated for C_8H_7ONF: 152.1; found: 152.3.

(*Z*)-5-((5-Fluoro-2-oxoindolin-3-ylidene)methyl)-2,4-dimethyl-1*H*-pyrrole-3-carboxylic acid (15i)

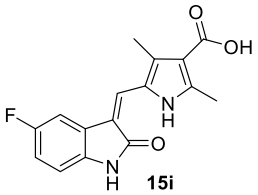

15i

A solution of 5-fluoro-1,3-dihydro-2H-indol-2-one **15h** (1.36 g, 8.97 mmol, 1.0 eq), 5-formyl-2,4-dimethyl-1H-pyrrole-3-carboxylic acid **15f** (1.50 g, 8.97 mmol, 1.0 eq), and pyrrolidine (1.47 mL, 18.0 µmol, 2.0 eq) in ethanol (130 mL) was heated to reflux for 3 h. Upon cooling to rt HCl (2 M, 15 mL) was added to the suspension and the resulted crude precipitate was recovered by suction filtration, washed with ethanol (20 mL) and petroleum ether (20 mL) to afford **15i** as a yellow powder (2.19 g, 7.29 mmol, 81% yield).

TLC: R_f = 0.11 (ethyl acetate). **^{1}H NMR** (d^6-DMSO, 400 MHz): δ = 2.50 (3 H, s), 2.53 (3 H, s), 3.33 (1 H, br. s.), 6.84 (1 H, dd, *J* = 8.5, 4.5 Hz), 6.88 - 6.98 (1 H, m), 7.74 (1 H, s), 7.77 (1 H, dd, *J* = 9.5, 2.5 Hz), 10.92 (1 H, br. s.), 13.85 (1 H, br. s.). **^{13}C NMR** (d^6-DMSO, 101 MHz):[15] δ = 11.5, 14.5, 106.2 (d, $J_{C,F}$ =25.0 Hz), 110.1 (d, $J_{C,F}$ =9.5 Hz), 112.7 (d, $J_{C,F}$ =24.0 Hz), 114.7, 115.5, 124.8, 126.0, 127.0 (d, $J_{C,F}$ =9.0 Hz), 133.5, 134.7, 140.8, 158.2 (d, $J_{C,F}$ =235.0 Hz), 166.0, 169.6. **ESI-MS** $[M-H]^-$ calculated for $C_{16}H_{12}O_3N_2F$: 299.1; found: 299.2.

4.13 Synthesis of Compound 15

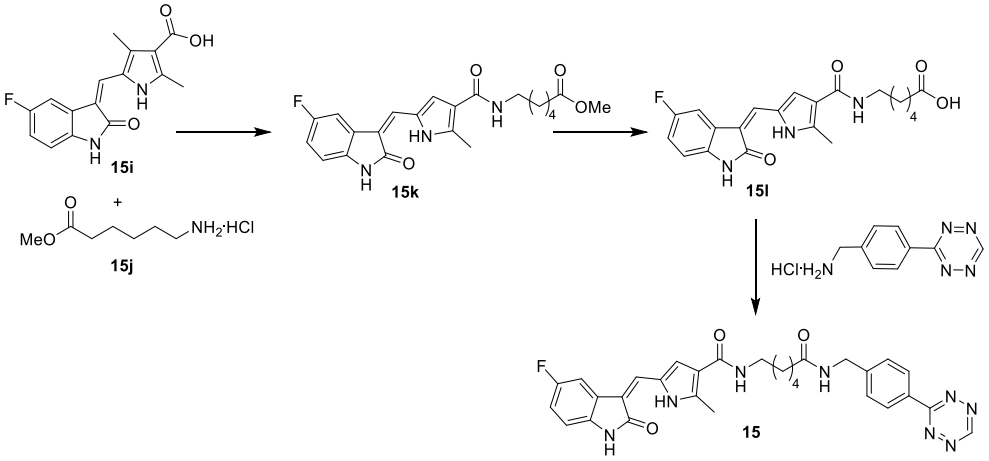

Scheme S12. Synthesis of compound **15**.

Methyl (Z)-6-(5-((5-fluoro-2-oxoindolin-3-ylidene)methyl)-2,4-dimethyl-1H-pyrrole-3-carboxamido)hexanoate (15k)

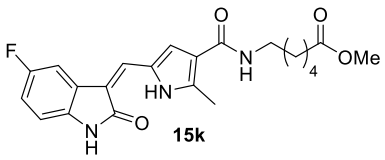

Sunitinib Acid **15i** (100 mg, 333 µmol, 1.0 eq), methyl 6-aminohexanoate hydrochloride **15j** (76 mg, 416 µmol, 1.25 eq), EDCI hydrochloride (96 mg, 500 µmol, 1.5 eq) and BtOH (7.6 mg, 82.8 µmol, 0.15eq) were dissolved in dry DMF (2.0 mL). Then triethylamine (89 µL, 662 µmol, 2.0 eq), was added dropwise and the mixture was stirred at rt for 14 h. Subsequently, DMF was removed *in vacuo*, the residue was resuspended in water (10 mL) and ethyl acetate (10 mL) and filtered off. The crude filtrate was washed repetitively with water (3 x 10 mL) and ethyl acetate (3 x 10 mL) and dried *in vacuo* to afford amide **15k** (119 mg, 278 µmol, 84% yield) as a yellow solid which was used in the following reaction without further purification.

TLC: R_f = 0.25 (ethyl acetate/MeOH = 9:1). **^{1}H NMR** (d^6-DMSO, 400 MHz): δ = 1.26 - 1.38 (2 H, m), 1.43 - 1.52 (2 H, m), 1.57 (2 H, dd, *J* = 15.1, 7.5 Hz), 2.32 (1 H, t, *J* = 7.3 Hz), 2.40 (3 H, s), 2.42 (3 H, s), 3.20 (2 H, q, *J* = 6.7 Hz), 3.32 (1 H, s), 3.59 (3 H, s), 6.80 - 6.87 (1 H, m), 6.88 - 6.95 (1 H, m), 7.63 (1 H, t, *J* = 5.6 Hz), 7.71 (1 H, s), 7.76 (1 H, dd, *J* = 9.4, 2.2 Hz), 10.88 (1 H, s), 13.67 (1 H, br. s.). **^{13}C NMR** (d^6-DMSO, 101 MHz):[15] δ = 10.5, 13.2, 24.2, 26.0, 29.0, 33.3, 38.5, 51.2, 105.9 (d, $J_{C,F}$ = 25.0 Hz), 110.0 (d, $J_{C,F}$ = 9.4 Hz), 112.4 (d, $J_{C,F}$ = 24.0 Hz), 114.5, 121.2, 124.9, 125.8, 127.2 (d, $J_{C,F}$ = 9.2 Hz), 130.3, 134.5, 136.3, 158.2 (d, $J_{C,F}$ = 235.0 Hz), 164.7, 169.6, 173.4. **ESI-MS** $[M+H]^+$ calculated for $C_{23}H_{27}O_4N_3F$: 428.2; found: 428.3.

(*Z*)-6-(5-((5-Fluoro-2-oxoindolin-3-ylidene)methyl)-2,4-dimethyl-1*H*-pyrrole-3-carboxamido)hexanoic acid (15l)

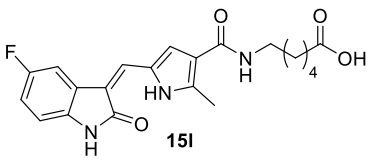

Ester **15k** (60.0 mg, 140 µmol, 1.0 eq) was treated with $LiOH \cdot H_2O$ (118 mg, 2.81 mmol, 20 eq) in a 2:1:1 mixture of MeOH/THF/H_2O (5 mL, 2.5 mL, 2.5 mL), heated up to 60 °C and stirred for 5 h. The organic solvents were then evaporated *in vacuo*, water was added (10 mL) and the pH value was adjusted to pH = 1 by the dropwise addition of 1M HCl. Subsequently, the reaction product was filtered off, repetitively washed with water (3 x 10 mL) and ethyl acetate (3 x 10 mL) and dried *in vacuo* to afford acid **15l** (53.7 mg, 128 µmol, 91% yield) as a yellow solid which was used in the following reaction without further purification.

(*Z*)-*N*-(6-((4-(1,2,4,5-Tetrazin-3-yl)benzyl)amino)-6-oxohexyl)-5-((5-fluoro-2-oxoindolin-3-ylidene)methyl)-2,4-dimethyl-1*H*-pyrrole-3-carboxamide (15)

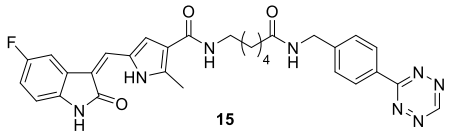

15

Acid **15l** (30.0 mg, 72.5 µmol, 1.3 eq), (4-(1,2,4,5-tetrazin-3-yl)phenyl)methanamine hydrochloride (12.4 mg, 55.8 µmol, 1.0 eq), EDCI hydrochloride (21.4 mg, 111.6 µmol, 2.0 eq) and BtOH (1.28 mg, 8.37 µmol, 0.15 eq) were dissolved in dry DMF (2.5 mL). Then pyridine (45 µL, 558 µmol, 10.0 eq) was added dropwise and the mixture was stirred for 16 h at rt. After removal of the solvent by freeze drying the reaction mixture was purified by reversed phase column chromatography (C-18, H_2O/MeCN 70:30) and freeze dried again to afford the tetrazine conjugate **15** (23.7 mg, 40.7 µmol, 73% yield) as a red solid.

TLC: R_f = 0.22 (H_2O/MeCN 70:30). **^{1}H NMR** (d^6-DMSO, 400 MHz): δ = 1.29 - 1.40 (2 H, m), 1.46 - 1.55 (2 H, m), 1.55 - 1.64 (2 H, m), 2.21 (2 H, t, *J* = 7.3 Hz), 2.38 (3 H, s), 2.41 (3 H, s), 3.22 (2 H, q, *J* = 6.6 Hz), 4.40 (2 H, d, *J* = 5.9 Hz), 6.80 - 6.87 (1 H, m), 6.87 - 6.96 (1 H, m), 7.52 (2 H, d, *J* = 8.8 Hz), 7.63 (1 H, t, *J* = 5.6 Hz), 7.67 (1 H, s), 7.74 (1 H, dd, *J* = 9.4, 2.5 Hz), 8.44 (2 H, d, *J* = 8.3 Hz), 8.48 (1 H, t, *J* = 6.0 Hz), 10.55 (1 H, s), 10.92 (1 H, br. s.), 13.63 (1 H, s). **^{13}C NMR** (d^6-DMSO, 101 MHz):[15] δ = 10.5, 13.2, 25.0, 26.2, 29.1, 35.3, 38.6, 41.8, 105.9 (d, $J_{C,F}$ = 24.4 Hz), 110.0 (d, $J_{C,F}$ = 9.4 Hz), 112.3 (d, $J_{C,F}$ = 24.0 Hz), 114.4, 121.2, 124.8, 125.7, 127.2 (d, $J_{C,F}$ = 9.5 Hz), 127.8 (2 C), 128.0 (2 C), 130.2, 134.5, 136.3, 145.1, 158.0, 158.2 (d, $J_{C,F}$ = 235.0 Hz), 162.3, 164.6, 165.4, 169.5, 172.3. **ESI-MS** $[M+H]^+$ calculated for $C_{31}H_{32}O_3N_8F$: 583.3; found: 583.4.

5. References

1. http://bililite.com/tenua/
2. Lu, P., Vogel, C., Wang, R., Yao, X. & Marcotte, E. M. Absolute protein expression profiling estimates the relative contributions of transcriptional and translational regulation. *Nat. Biotech.* **25**, 117-124 (2007).
3. Warner, J. B., Muthusamy, A. K. & Petersson, E. J. Specific Modulation of Protein Activity by Using a Bioorthogonal Reaction. *ChemBioChem* **15**, 2508-2514 (2014).
4. Gautier, A., Deiters, A. & Chin, J. W. Light-activated kinases enable temporal dissection of signaling networks in living cells. *J. Am. Chem. Soc.* **133**, 2124-2127 (2011).
5. Schmied, W. H., Elsässer, S. J., Uttamapinant, C. & Chin, J. W. Efficient Multisite Unnatural Amino Acid Incorporation in Mammalian Cells via Optimized Pyrrolysyl tRNA Synthetase/tRNA Expression and Engineered eRF1. *J. Am. Chem. Soc.* **136**, 15577-15583 (2014).
6. James, J. R. & Vale, R. D. Biophysical mechanism of T-cell receptor triggering in a reconstituted system. *Nature* **487**, 64-69 (2012).
7. Lang, K., Davis, L., Torres-Kolbus, J., Chou, C., Deiters, A. & Chin, J. W. Genetically encoded norbornene directs site-specific cellular protein labelling via a rapid bioorthogonal reaction. *Nat. Chem.* **4**, 298-304 (2012).
8. Lang, K., Davis, L., Wallace, S., Mahesh, M., Cox, D. J., Blackman, M. L., Fox, J. M. & Chin, J. W. Genetic Encoding of Bicyclononynes and trans-Cyclooctenes for Site-Specific Protein Labeling in Vitro and in Live Mammalian Cells via Rapid Fluorogenic Diels-Alder Reactions. *J. Am. Chem. Soc.* **134**, 10317-10320 (2012).
9. Rice, K. D., Aay, N., Anand, N. K., Blazey, C. M., Bowles, O. J., Bussenius, J., Costanzo, S., Curtis, J. K., Defina, S. C., Dubenko, L., Engst, S., Joshi, A. A., Kennedy, A. R., Kim, A. I., Koltun, E. S., Lougheed, J. C., Manalo, J.-C. L., Martini, J.-F., Nuss, J. M., Peto, C. J., Tsang, T. H., Yu, P. & Johnston, S. Novel Carboxamide-Based Allosteric MEK Inhibitors: Discovery and Optimization Efforts toward XL518 (GDC-0973). *ACS Med. Chem. Lett.* **3**, 416-421 (2012).
10. Devaraj, N. K., Weissleder, R. & Hilderbrand, S. A. Tetrazine-Based Cycloadditions: Application to Pretargeted Live Cell Imaging. *Bioconjugate Chem.* **19**, 2297-2299 (2008).
11. Li, J. & Sha, Y. *Molecules* **13**, 1111-1119 (2008).
12. Wang, K., Sachdeva, A., Cox, D. J., Wilf, N. W., Lang, K., Wallace, S., Mehl, R. A. & Chin, J. W. Optimized orthogonal translation of unnatural amino acids enables spontaneous protein double-labelling and FRET. *Nat. Chem.* **6**, 393-403 (2014).
13. Elliott, T. S., Townsley, F. M., Bianco, A., Ernst, R. J., Sachdeva, A., Elsasser, S. J., Davis, L., Lang, K., Pisa, R., Greiss, S., Lilley, K. S. & Chin, J. W. Proteome labeling and protein identification in specific tissues and at specific developmental stages in an animal. *Nat. Biotech.* **32**, 465-472 (2014).
14. Gottlieb, H. E., Kotlyar, V. & Nudelman, A. NMR Chemical Shifts of Common Laboratory Solvents as Trace Impurities. *J. Org. Chem.* **62**, 7512-7515 (1997).
15. Some of the 13-C NMR signals of this compound showed a bad signal to noise ratio which is caused by well known extensive signal broading associated with C-F couplings. An increase of the number of scans didn't lead to significant improvments of the spectra quality due to the low solubility of the compound. The affected signals were therefore analyzed by HSQC and HMBC.

6. NMR-spectra

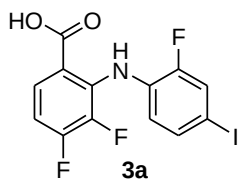

3a

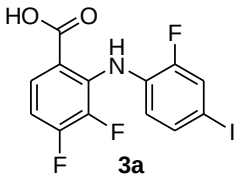
HO
O
H
N
F
F
F
I

3a

176
168
160
152
144
136
128
120
112
104
96
88
80
72
64
56
48
40
32
24
16
8
0
Chemical Shift (ppm)

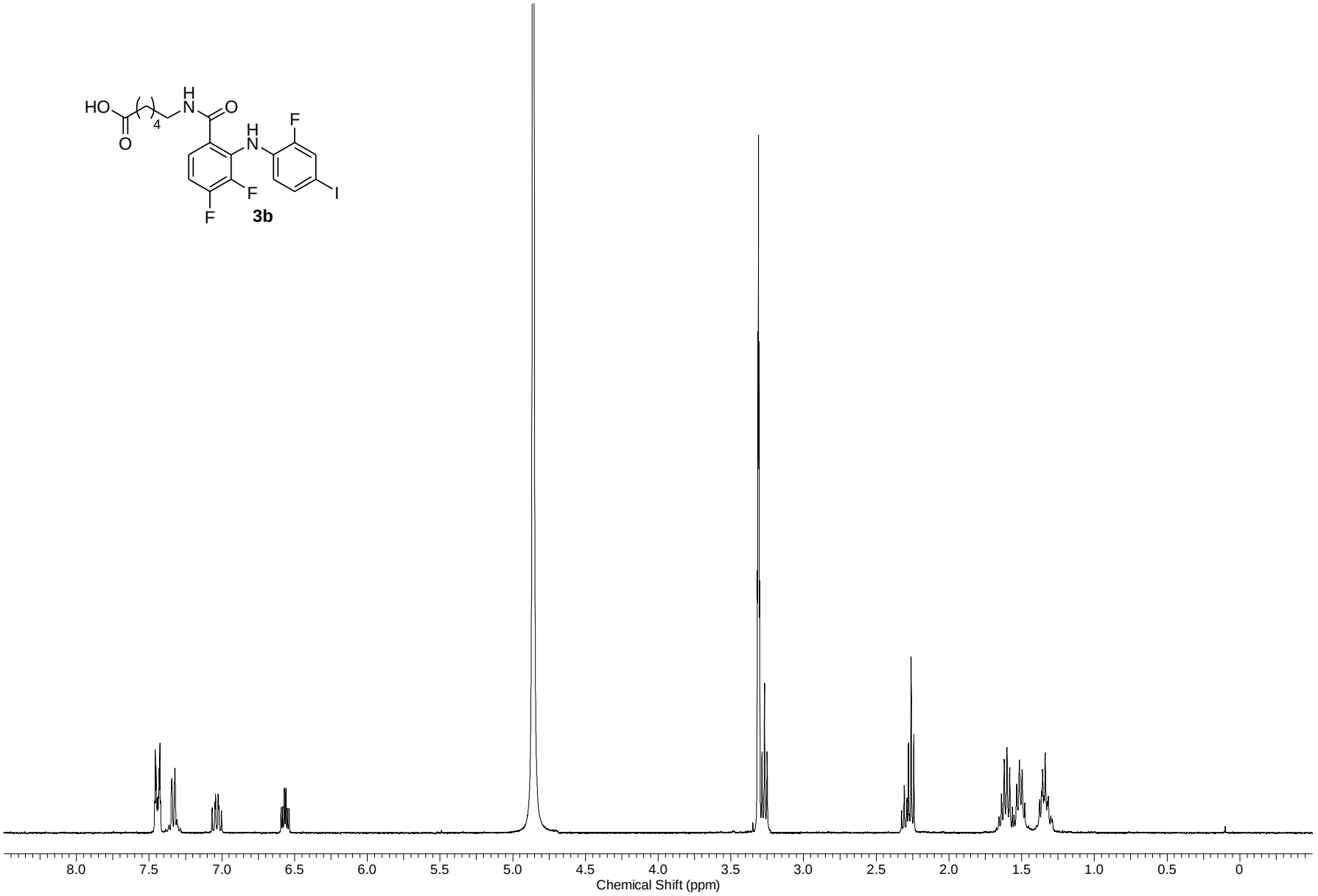
HO
O
4
H
N
O
H
N
F
F
F
I
3b
8.0
7.5
7.0
6.5
6.0
5.5
5.0
4.5
4.0
3.5
3.0
2.5
2.0
1.5
1.0
0.5
0
Chemical Shift (ppm)

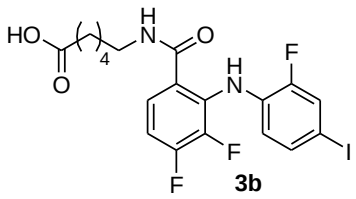
HO
O
4
H
N
O
H
N
F
F
F
I

3b

176
168
160
152
144
136
128
120
112
104
96
88
80
72
64
56
48
40
32
24
16
8
0
Chemical Shift (ppm)

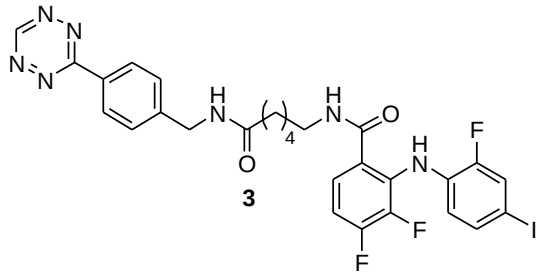
N
N
N
N
H
N
4
H
N
O
O
F
H
N
F
F
I

3

10.5
10.0
9.5
9.0
8.5
8.0
7.5
7.0
6.5
6.0
5.5
5.0
4.5
4.0
3.5
3.0
2.5
2.0
1.5
1.0
0.5
0
Chemical Shift (ppm)

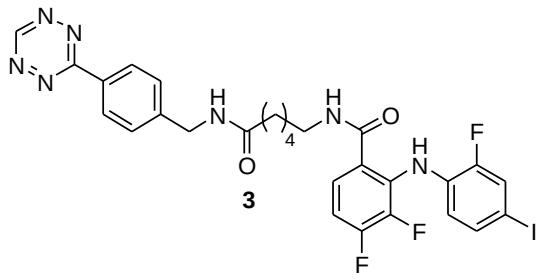
N
N
N
N
H
N
4
H
N
O
O
H
N
F
F
F
I

3

176
168
160
152
144
136
128
120
112
104
96
88
80
72
64
56
48
40
32
24
16
8
0
Chemical Shift (ppm)

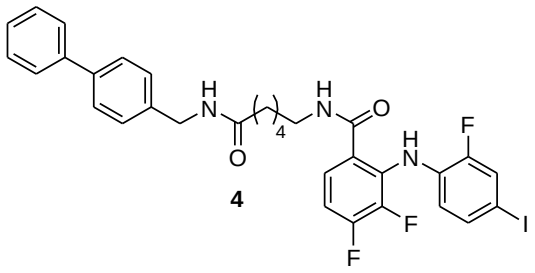
H
N
O
4
H
N
O
H
N
F
F
F
I

4

9.0
8.5
8.0
7.5
7.0
6.5
6.0
5.5
5.0
4.5
4.0
3.5
3.0
2.5
2.0
1.5
1.0
0.5
0
Chemical Shift (ppm)

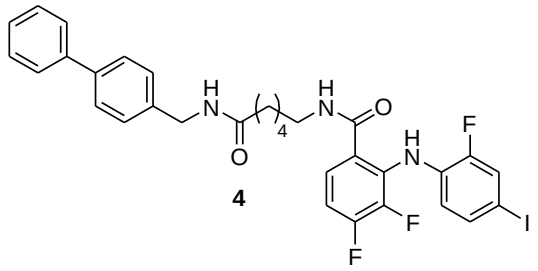
H
N
O
4
H
N
O
H
N
F
F
F
I

4

176
168
160
152
144
136
128
120
112
104
96
88
80
72
64
56
48
40
32
24
16
8
0
-8
Chemical Shift (ppm)

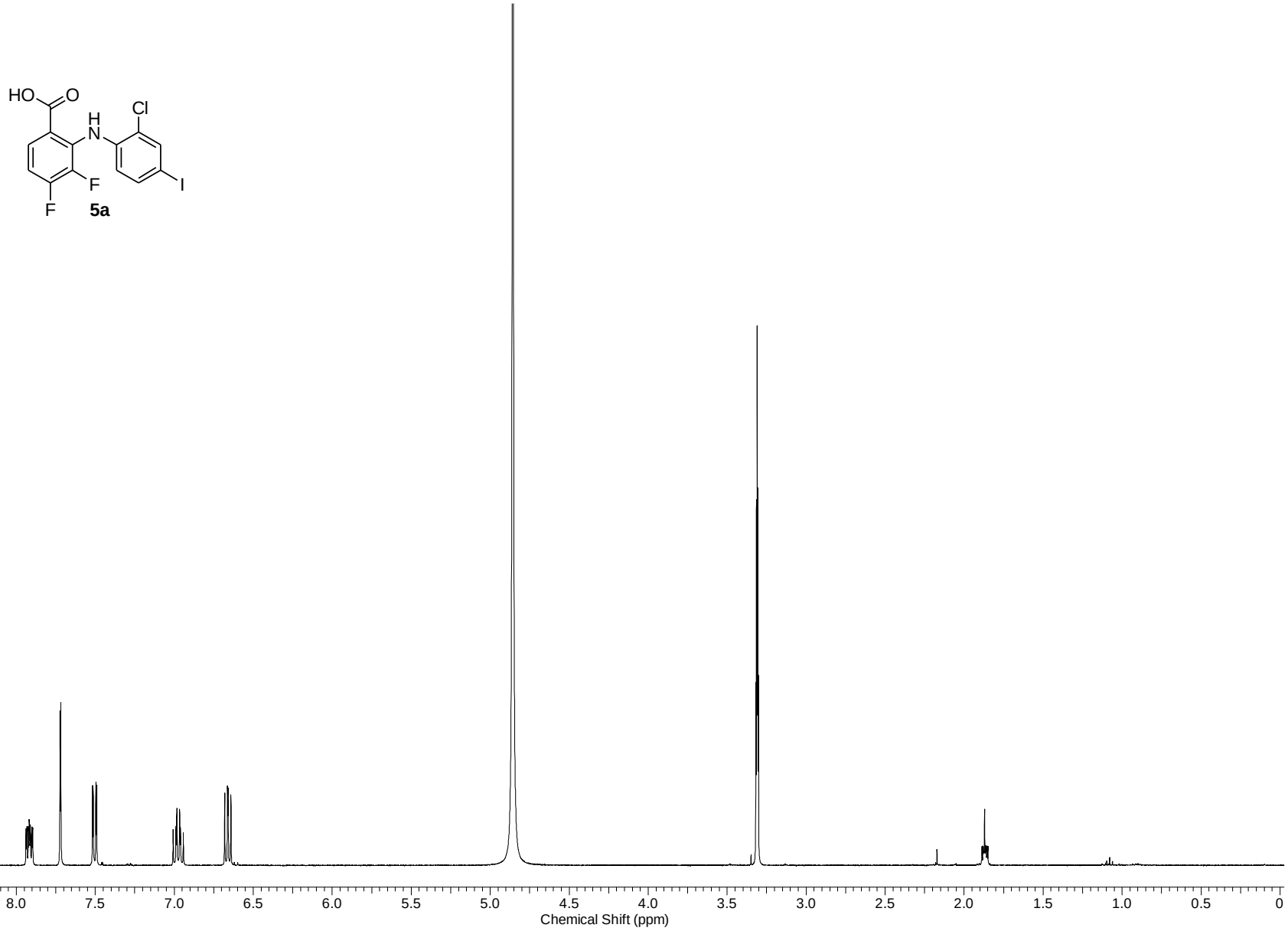
HO
O
H
N
Cl
F
F
I
5a
8.5
8.0
7.5
7.0
6.5
6.0
5.5
5.0
4.5
4.0
3.5
3.0
2.5
2.0
1.5
1.0
0.5
0
Chemical Shift (ppm)

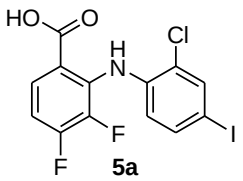
HO
O
H
N
Cl
F
F
I

5a

176
168
160
152
144
136
128
120
112
104
96
88
80
72
64
56
48
40
32
24
16
8
0
Chemical Shift (ppm)

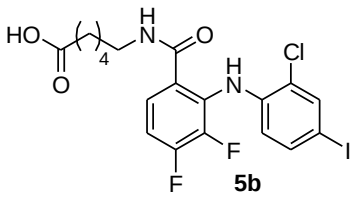
HO
O
4
H
N
O
H
N
Cl
F
F
I

5b

8.0
7.5
7.0
6.5
6.0
5.5
5.0
4.5
4.0
3.5
3.0
2.5
2.0
1.5
1.0
0.5
0
Chemical Shift (ppm)

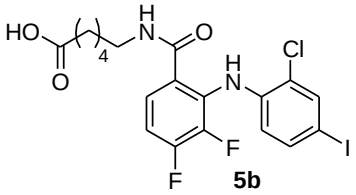
HO
O
4
H
N
O
H
N
Cl
F
F
I

5b

176
168
160
152
144
136
128
120
112
104
96
88
80
72
64
56
48
40
32
24
16
8
0
Chemical Shift (ppm)

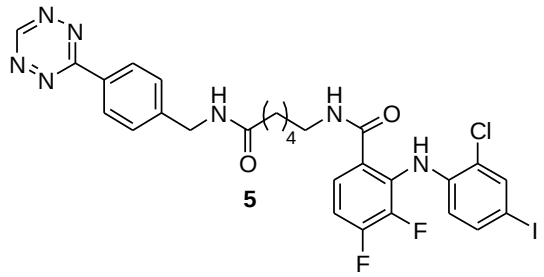
N
N
N
N
H
N
4
H
N
O
O
Cl
H
N
F
F
I

5

10.5
10.0
9.5
9.0
8.5
8.0
7.5
7.0
6.5
6.0
5.5
5.0
4.5
4.0
3.5
3.0
2.5
2.0
1.5
1.0
0.5
0
Chemical Shift (ppm)

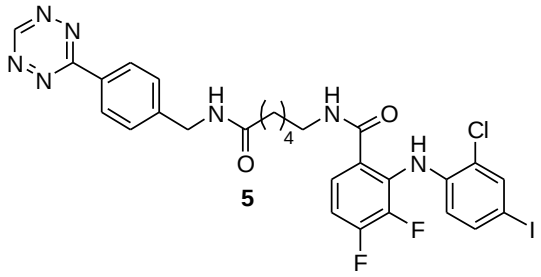
N
N
N
N
H
N
4
H
N
O
O
Cl
H
N
F
F
I

5

176
168
160
152
144
136
128
120
112
104
96
88
80
72
64
56
48
40
32
24
16
8
0
Chemical Shift (ppm)

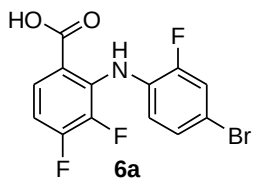
HO
O
H
N
F
F
F
Br

6a

8.0
7.5
7.0
6.5
6.0
5.5
5.0
4.5
4.0
3.5
3.0
2.5
2.0
1.5
1.0
0.5
0
-0.5
Chemical Shift (ppm)

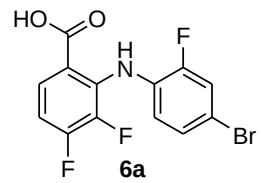
HO
O
H
N
F
F
F
Br

6a

176
168
160
152
144
136
128
120
112
104
96
88
80
72
64
56
48
40
32
24
16
8
0
Chemical Shift (ppm)

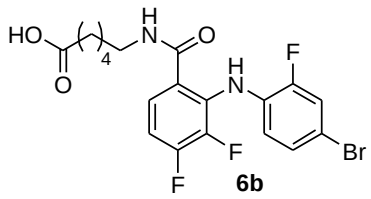
HO
O
4
H
N
O
H
N
F
F
F
Br

6b

8.0
7.5
7.0
6.5
6.0
5.5
5.0
4.5
4.0
3.5
3.0
2.5
2.0
1.5
1.0
0.5
0
Chemical Shift (ppm)

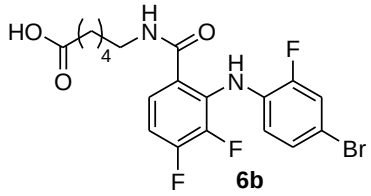
HO
O
4
H
N
O
H
N
F
F
F
Br

6b

176
168
160
152
144
136
128
120
112
104
96
88
80
72
64
56
48
40
32
24
16
8
0
Chemical Shift (ppm)

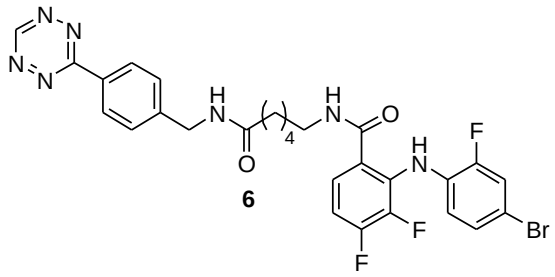
N
N
N
N
H
N
4
H
N
O
O
H
N
F
F
F
Br

6

10.5
10.0
9.5
9.0
8.5
8.0
7.5
7.0
6.5
6.0
5.5
5.0
4.5
4.0
3.5
3.0
2.5
2.0
1.5
1.0
0.5
0
Chemical Shift (ppm)

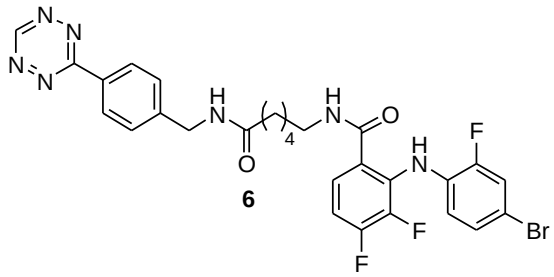
N
N
N
N
H
N
4
H
N
O
O
H
N
F
F
F
Br

6

176
168
160
152
144
136
128
120
112
104
96
88
80
72
64
56
48
40
32
24
16
8
0
Chemical Shift (ppm)

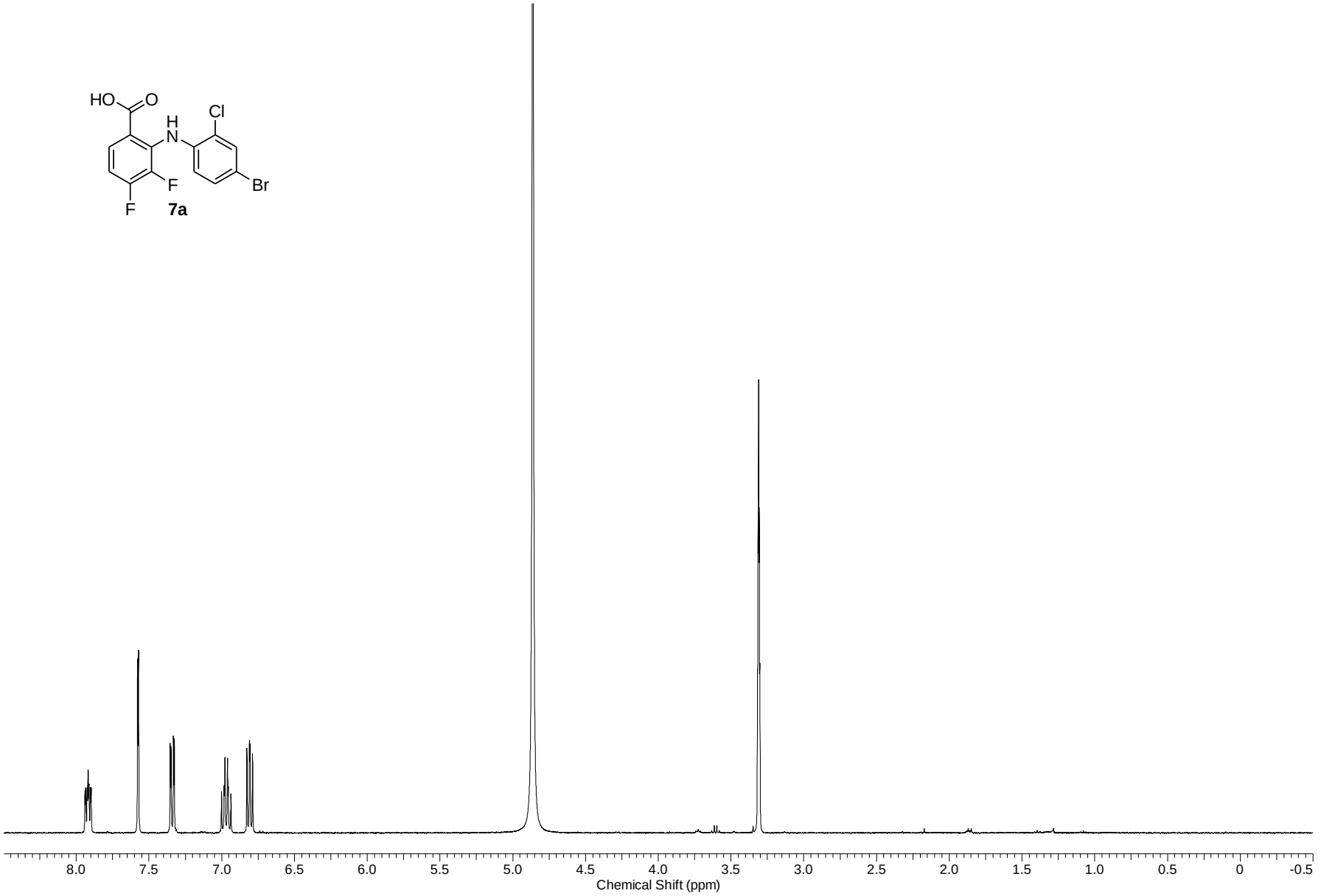
HO
O
H
N
Cl
F
Br
F
7a
8.0
7.5
7.0
6.5
6.0
5.5
5.0
4.5
4.0
3.5
3.0
2.5
2.0
1.5
1.0
0.5
0
-0.5
Chemical Shift (ppm)

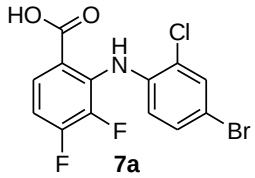
HO
O
H
N
Cl
F
F
Br

7a

176
168
160
152
144
136
128
120
112
104
96
88
80
72
64
56
48
40
32
24
16
8
0
Chemical Shift (ppm)

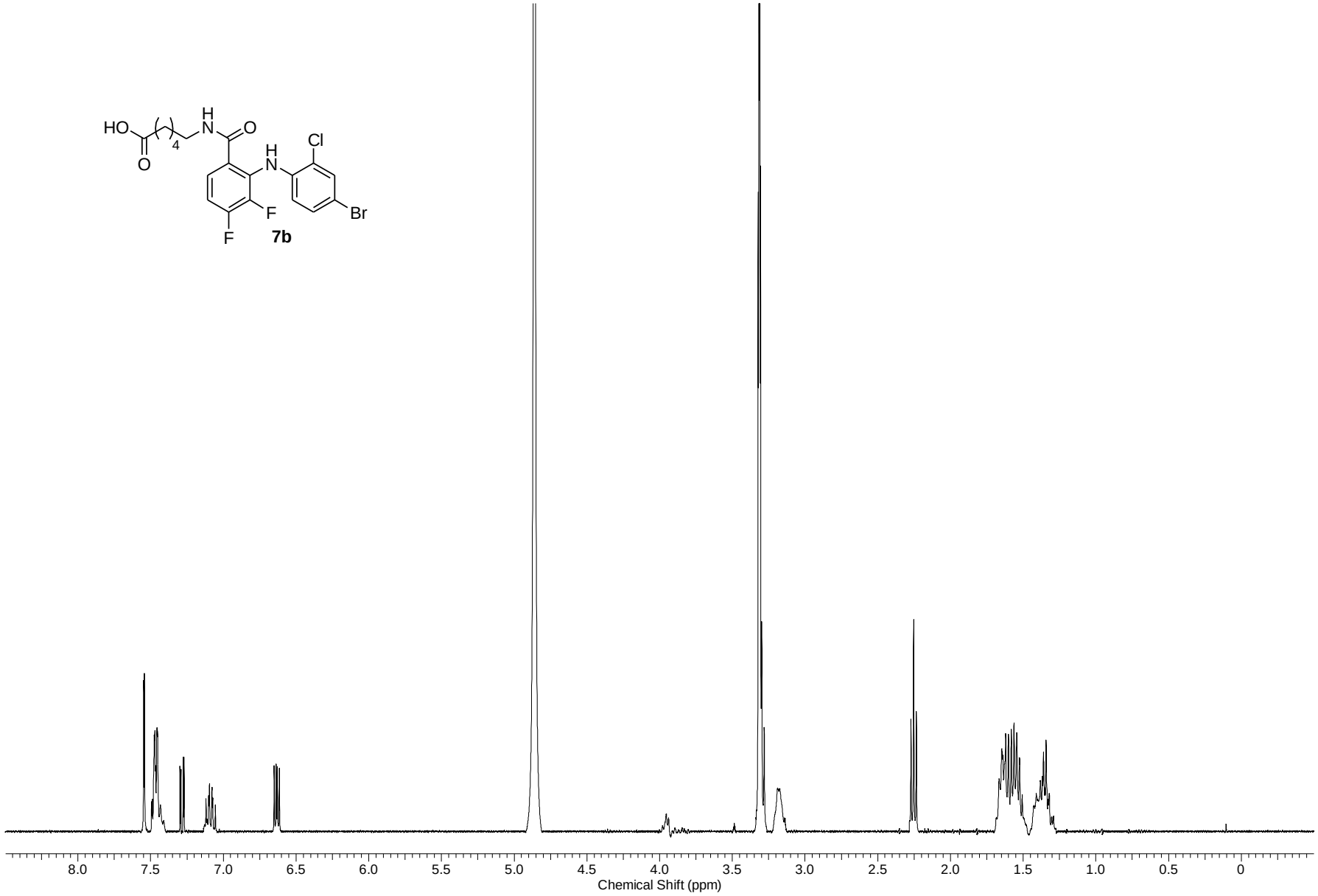
HO
O
4
H
N
O
H
N
Cl
F
F
Br
7b
8.0
7.5
7.0
6.5
6.0
5.5
5.0
4.5
4.0
3.5
3.0
2.5
2.0
1.5
1.0
0.5
0
Chemical Shift (ppm)

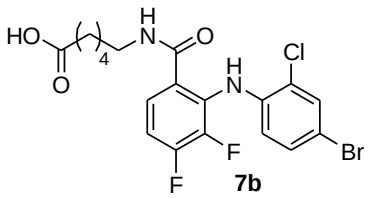
HO
O
4
H
N
O
H
N
Cl
F
F
Br

7b

176
168
160
152
144
136
128
120
112
104
96
88
80
72
64
56
48
40
32
24
16
8
0
Chemical Shift (ppm)

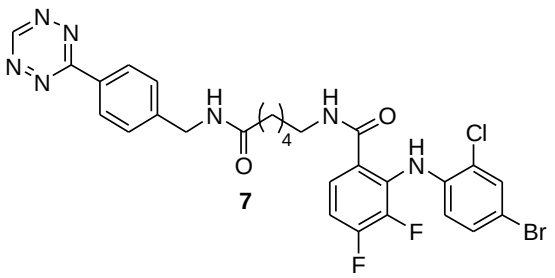
N
N
N
N
H
N
4
H
N
O
O
O
H
N
Cl
F
F
Br

7

10.5
10.0
9.5
9.0
8.5
8.0
7.5
7.0
6.5
6.0
5.5
5.0
4.5
4.0
3.5
3.0
2.5
2.0
1.5
1.0
0.5
0
Chemical Shift (ppm)

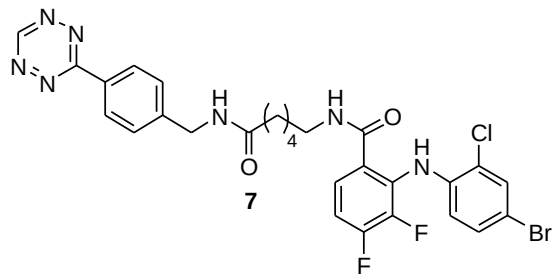
N
N
N
N
H
N
4
H
N
O
O
H
N
Cl
F
F
Br

7

176
168
160
152
144
136
128
120
112
104
96
88
80
72
64
56
48
40
32
24
16
8
0
Chemical Shift (ppm)

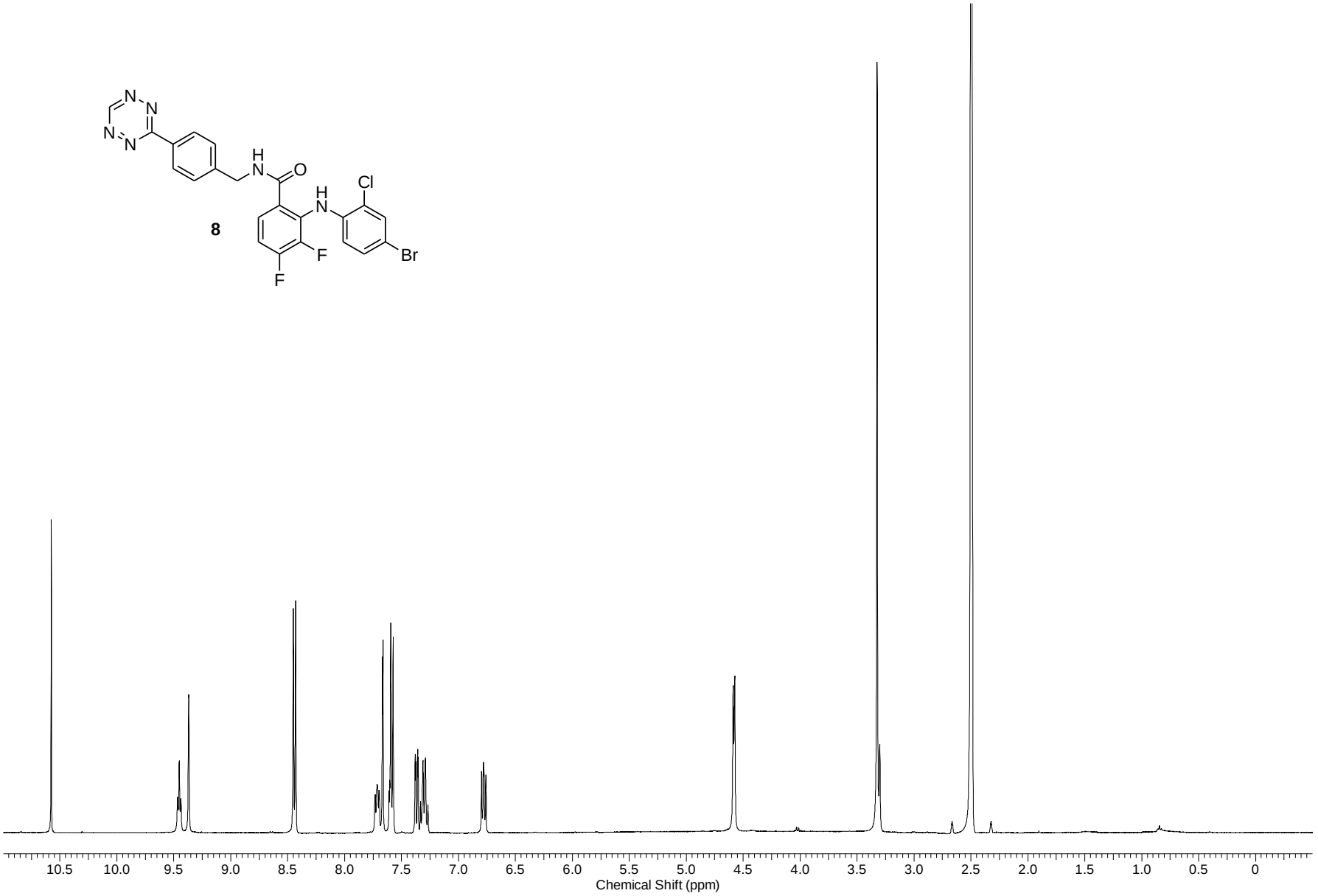
8
Chemical Shift (ppm)

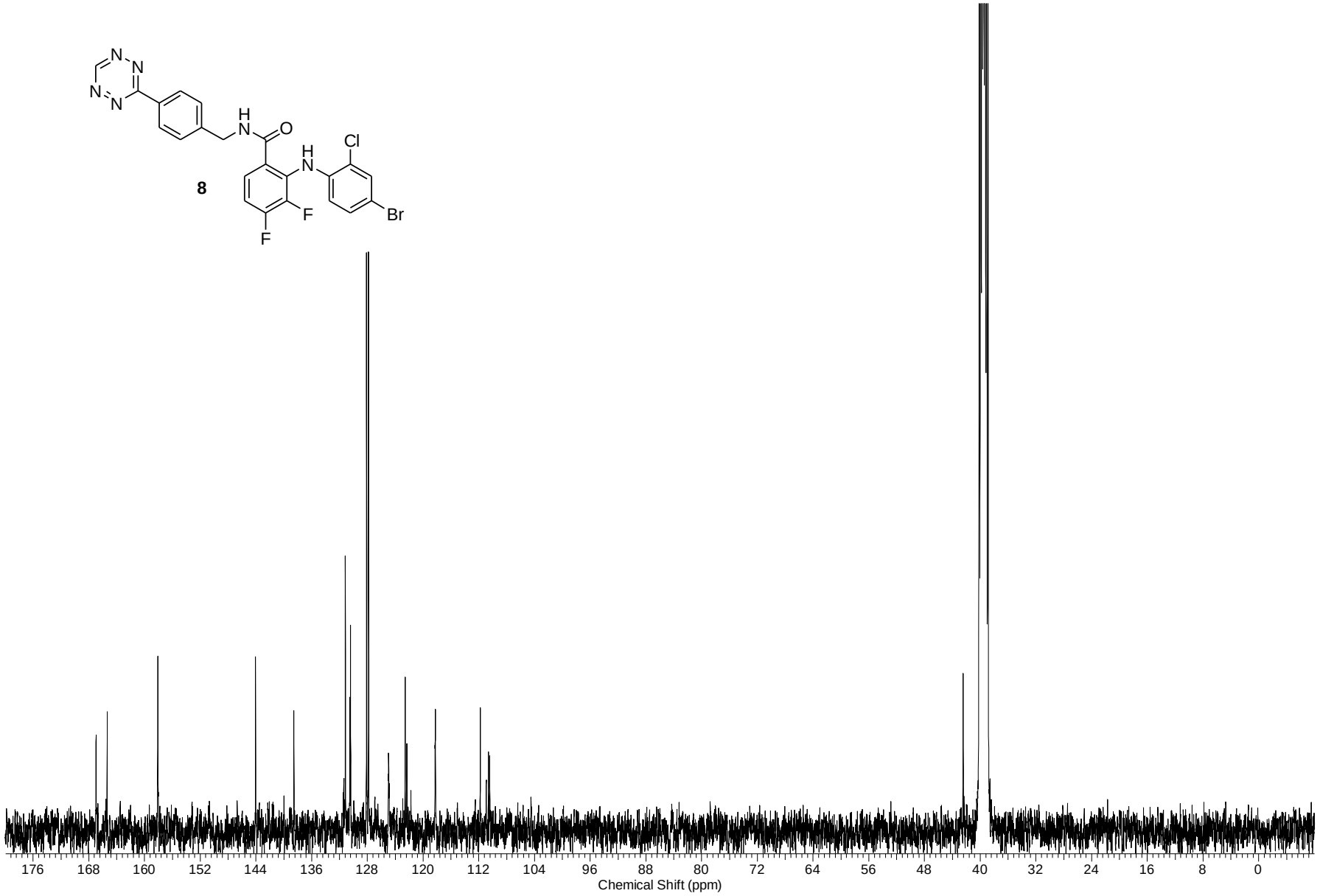
8
Chemical Shift (ppm)

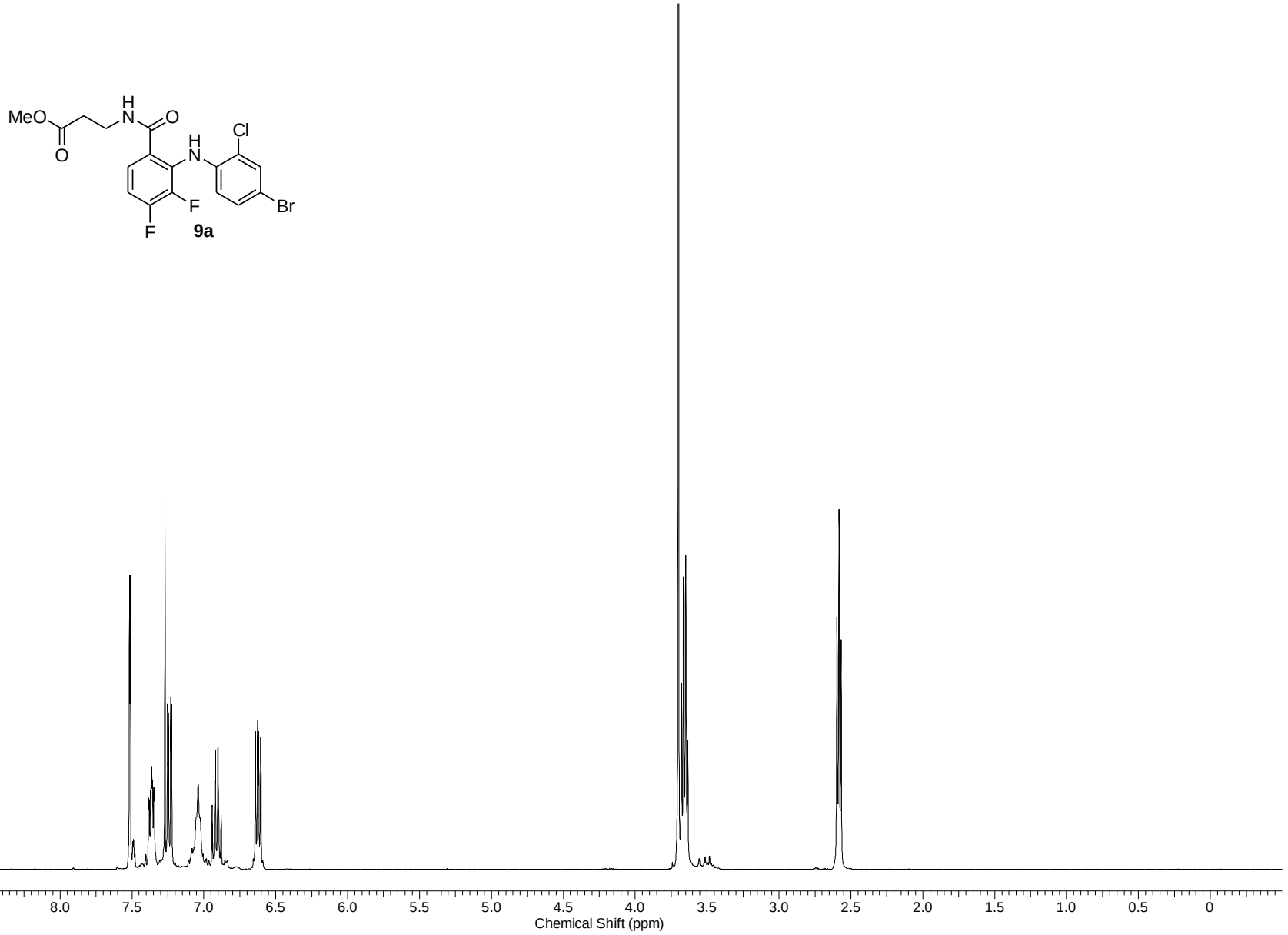
MeO
O
H
N
O
H
N
Cl
F
F
Br
9a
8.5
8.0
7.5
7.0
6.5
6.0
5.5
5.0
4.5
4.0
3.5
3.0
2.5
2.0
1.5
1.0
0.5
0
Chemical Shift (ppm)

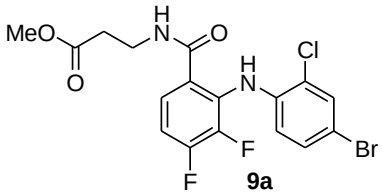
MeO
O
H
N
O
H
N
Cl
F
F
Br

9a

176
168
160
152
144
136
128
120
112
104
96
88
80
72
64
56
48
40
32
24
16
8
0
Chemical Shift (ppm)

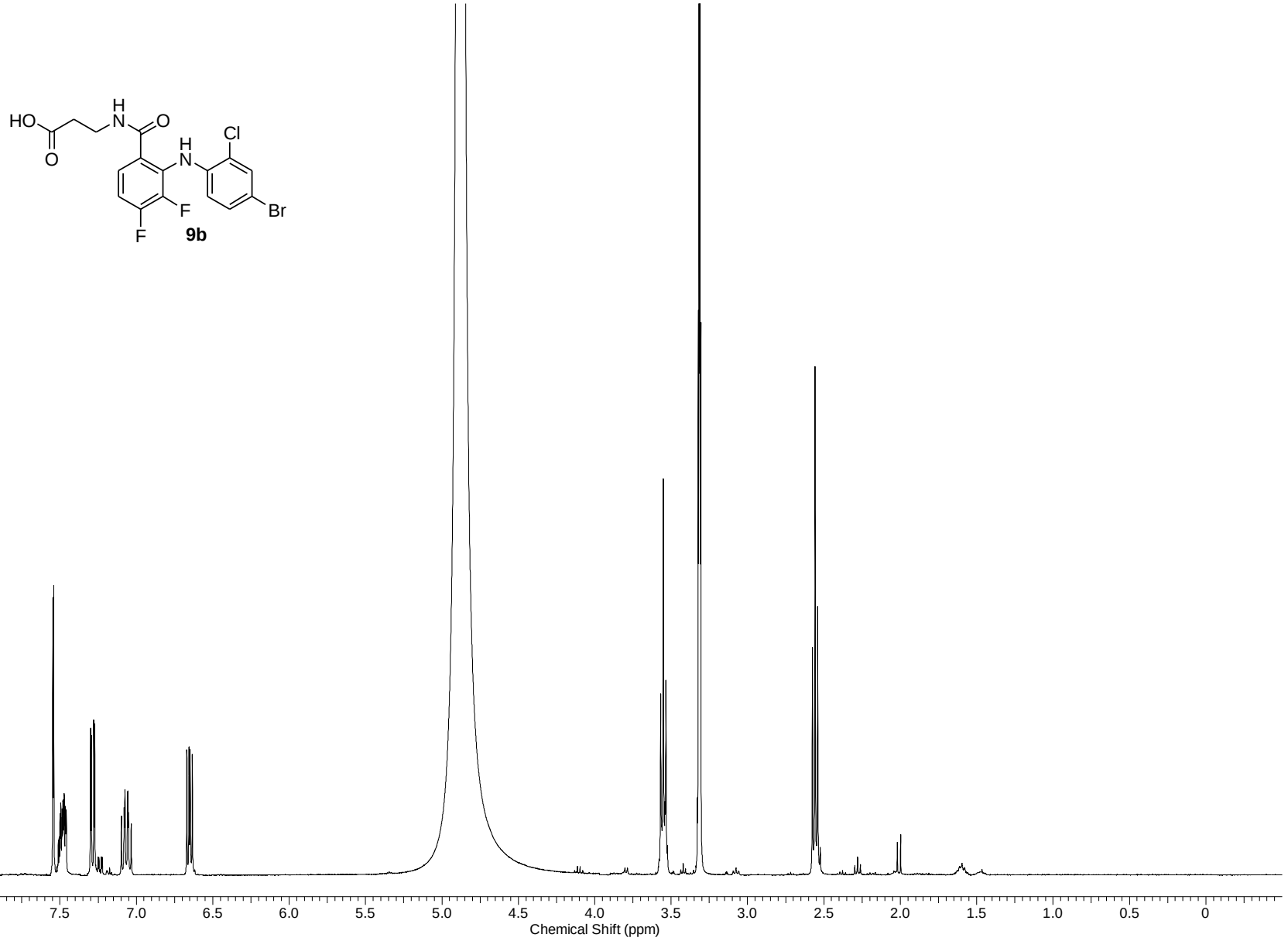
HO
O
H
N
O
H
N
Cl
F
F
Br
9b
8.0
7.5
7.0
6.5
6.0
5.5
5.0
4.5
4.0
3.5
3.0
2.5
2.0
1.5
1.0
0.5
0
Chemical Shift (ppm)

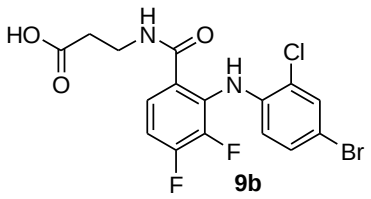
HO
O
H
N
O
H
N
Cl
F
F
Br

9b

176
168
160
152
144
136
128
120
112
104
96
88
80
72
64
56
48
40
32
24
16
8
0
Chemical Shift (ppm)

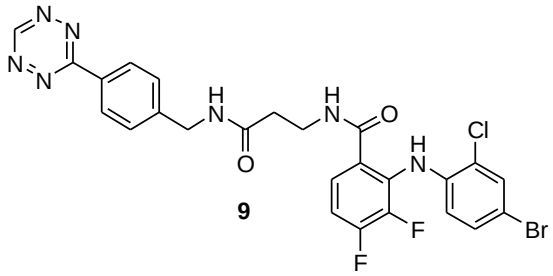
N
N
N
N
H
N
O
H
N
O
H
N
Cl
F
F
Br

9

10.5
10.0
9.5
9.0
8.5
8.0
7.5
7.0
6.5
6.0
5.5
5.0
4.5
4.0
3.5
3.0
2.5
2.0
1.5
1.0
0.5
0
Chemical Shift (ppm)

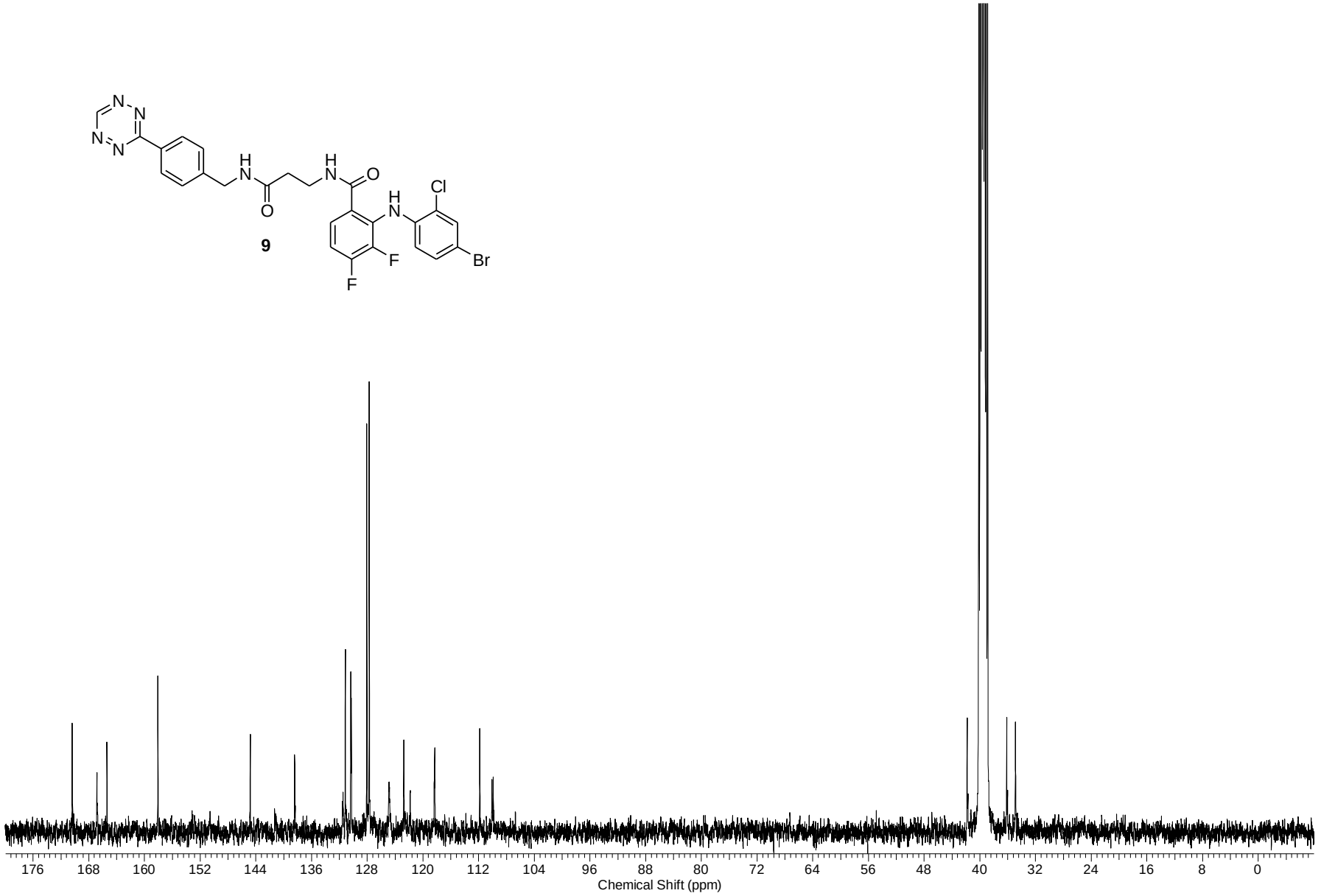
N
N
N
N
H
N
O
H
N
O
H
N
Cl
F
F
Br
9
176
168
160
152
144
136
128
120
112
104
96
88
80
72
64
56
48
40
32
24
16
8
0
Chemical Shift (ppm)

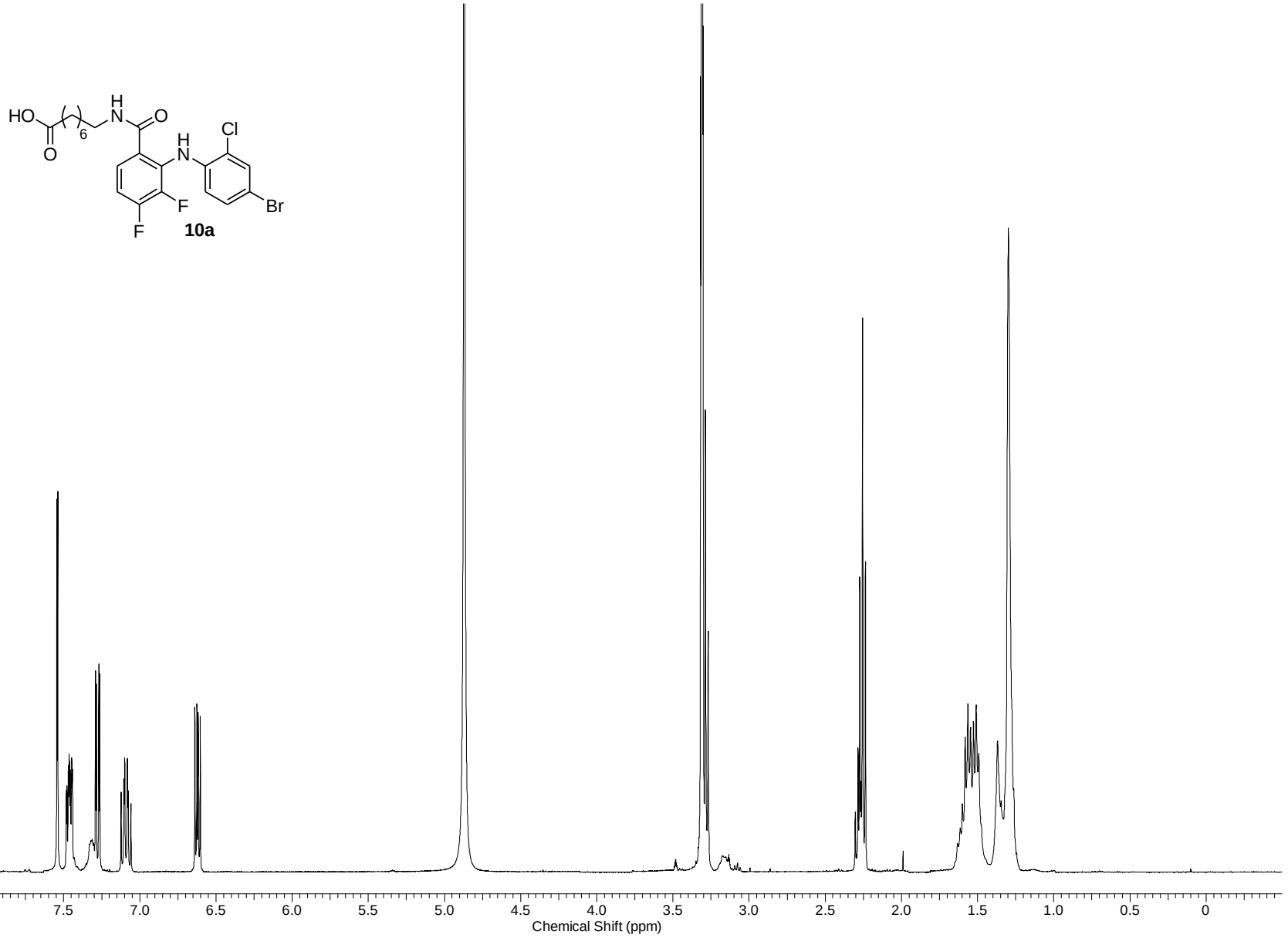
HO
O
6
H
N
O
H
N
Cl
F
F
Br
10a
8.0
7.5
7.0
6.5
6.0
5.5
5.0
4.5
4.0
3.5
3.0
2.5
2.0
1.5
1.0
0.5
0
Chemical Shift (ppm)

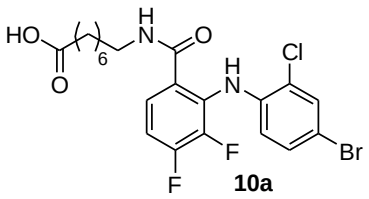
HO
O
6
H
N
O
H
N
Cl
F
F
Br

10a

176
168
160
152
144
136
128
120
112
104
96
88
80
72
64
56
48
40
32
24
16
8
0
Chemical Shift (ppm)

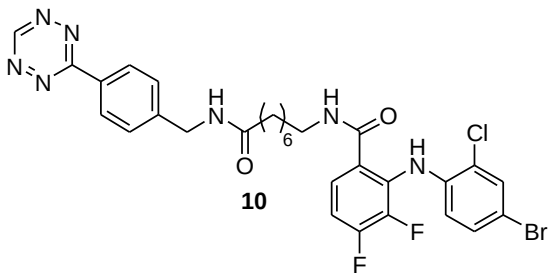
N
N
N
N
H
N
6
H
N
O
O
H
N
Cl
F
F
Br

10

10.5
10.0
9.5
9.0
8.5
8.0
7.5
7.0
6.5
6.0
5.5
5.0
4.5
4.0
3.5
3.0
2.5
2.0
1.5
1.0
0.5
0
Chemical Shift (ppm)

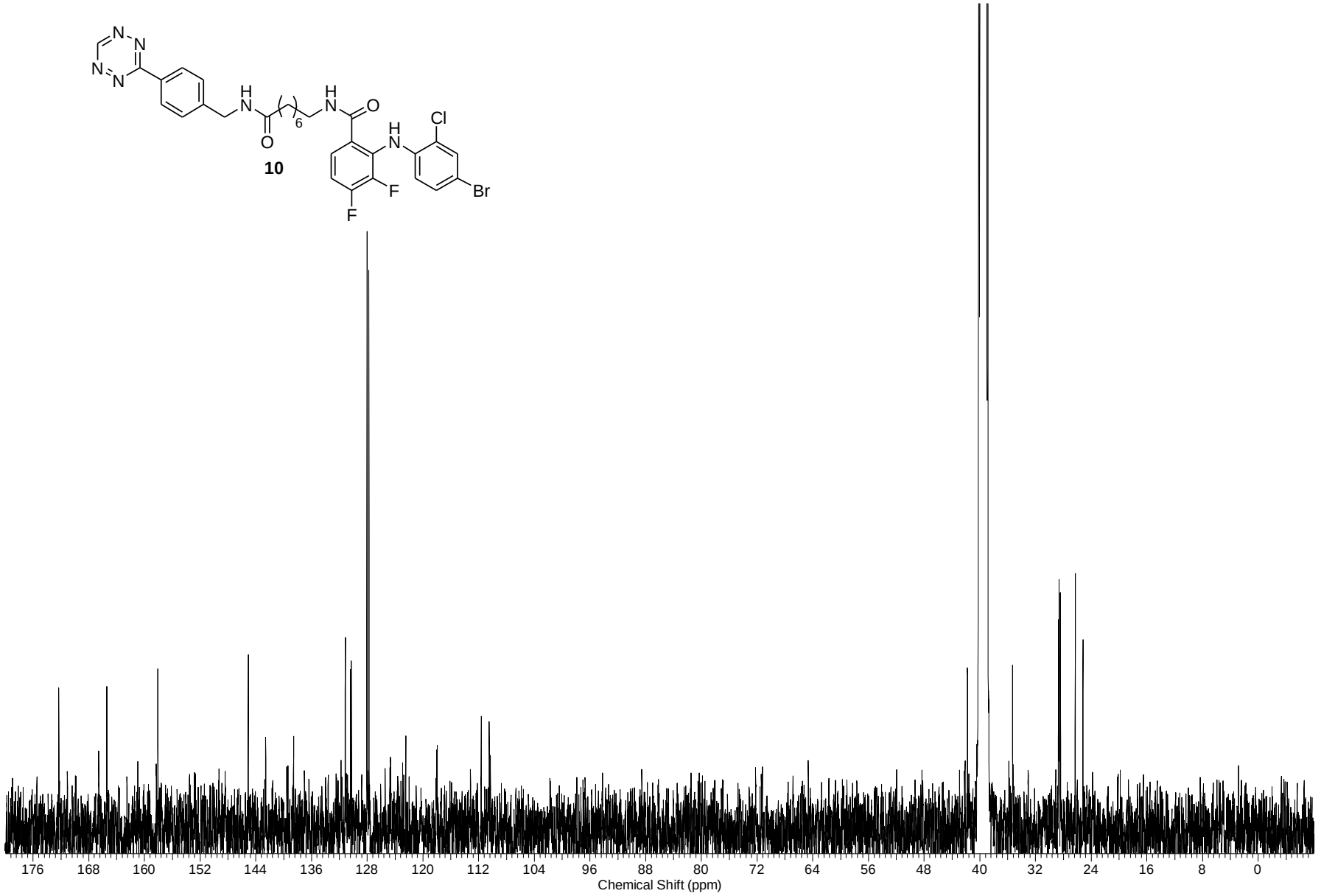
10
Chemical Shift (ppm)

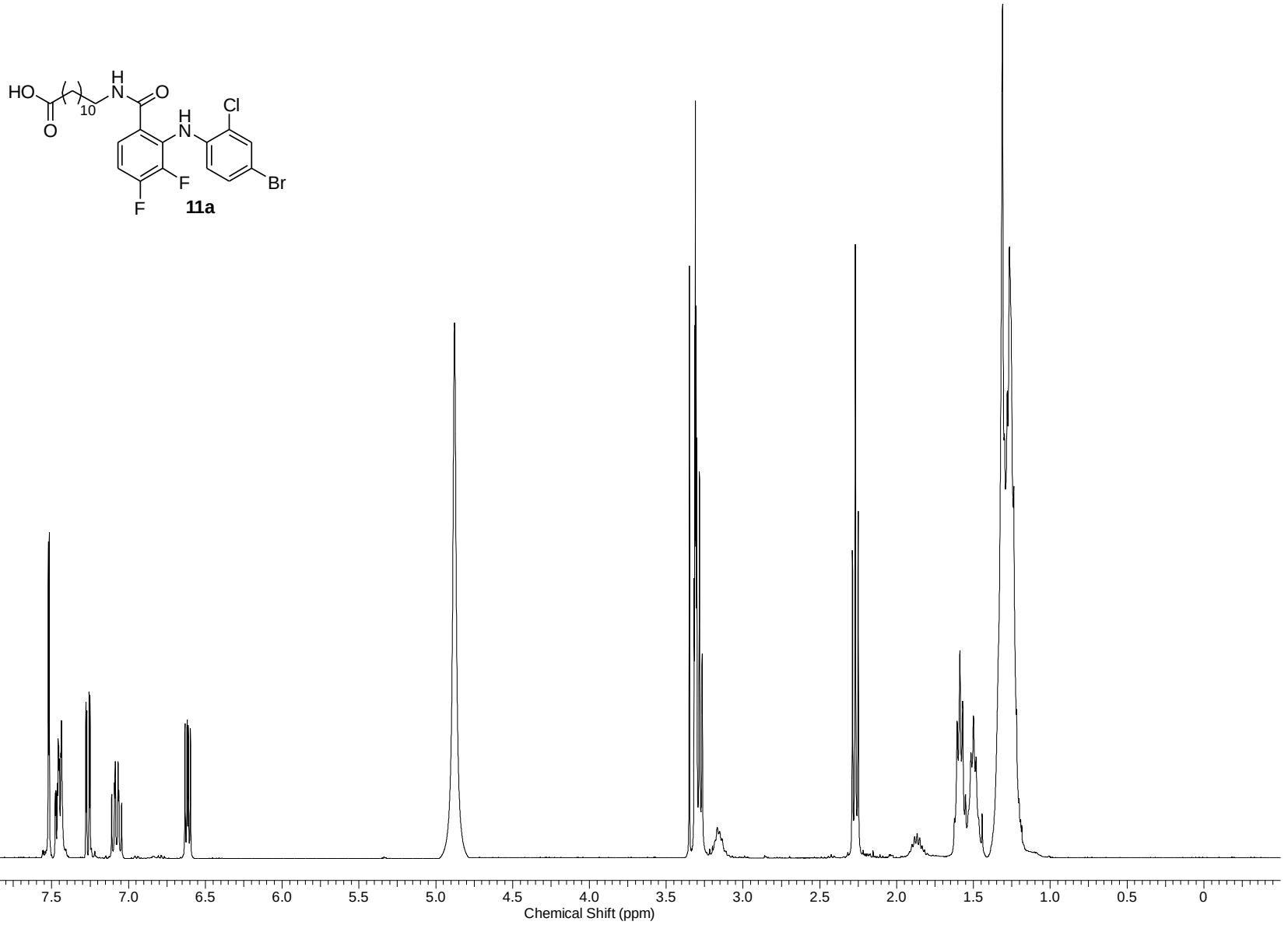
HO
O
10
H
N
O
H
N
Cl
F
F
Br
11a
8.0
7.5
7.0
6.5
6.0
5.5
5.0
4.5
4.0
3.5
3.0
2.5
2.0
1.5
1.0
0.5
0
Chemical Shift (ppm)

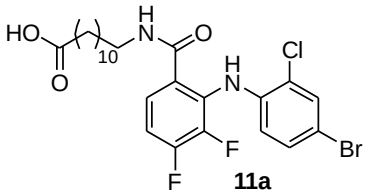
HO
O
10
H
N
O
H
N
Cl
F
F
Br

11a

176
168
160
152
144
136
128
120
112
104
96
88
80
72
64
56
48
40
32
24
16
8
0
Chemical Shift (ppm)

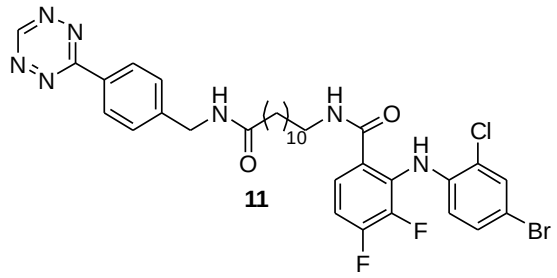
N
N
N
N
H
N
10
H
N
O
O
O
Cl
H
N
F
F
Br

11

10.5
10.0
9.5
9.0
8.5
8.0
7.5
7.0
6.5
6.0
5.5
5.0
4.5
4.0
3.5
3.0
2.5
2.0
1.5
1.0
0.5
0
Chemical Shift (ppm)

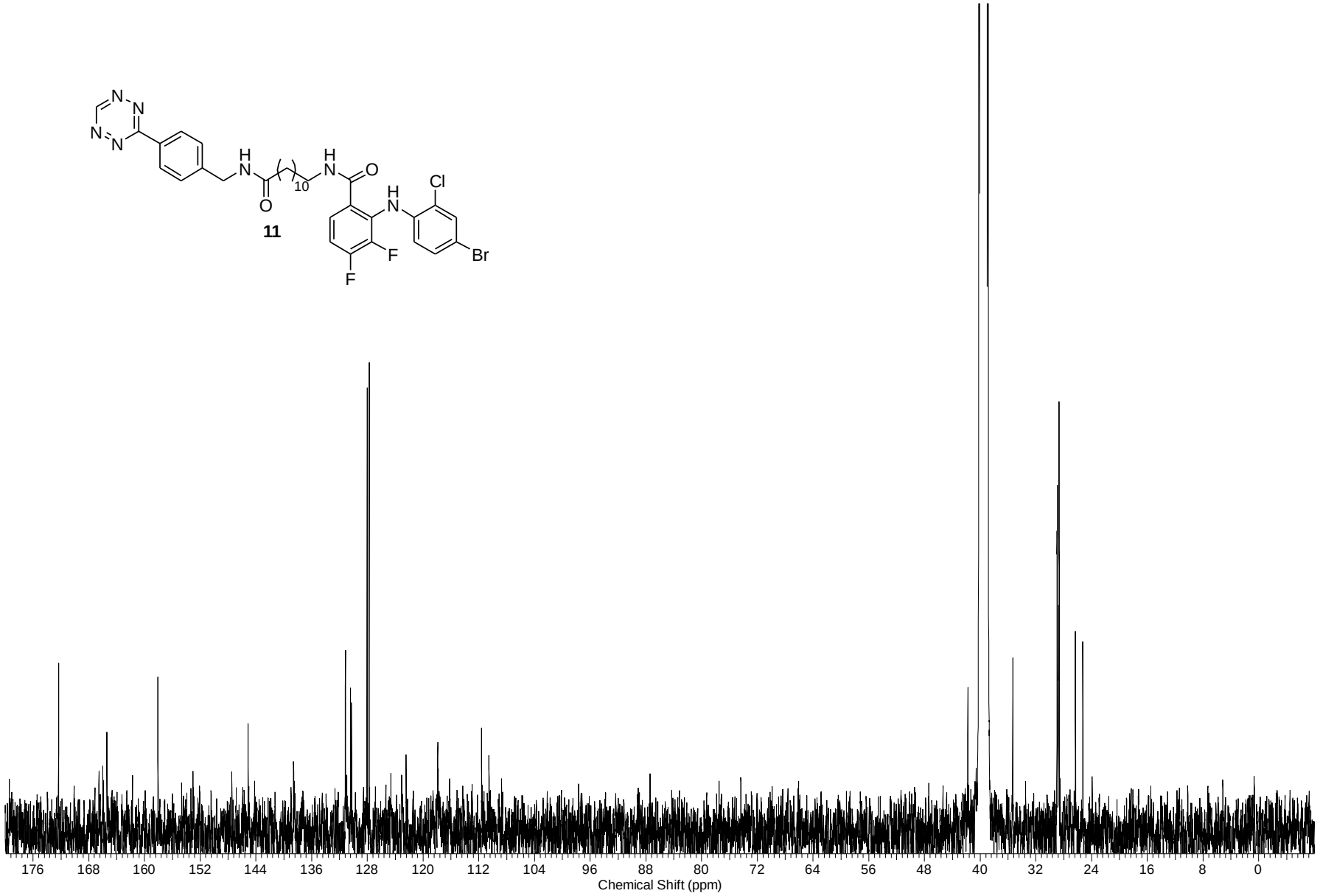
N
N
N
N
H
N
10
H
N
O
O
H
N
Cl
F
F
Br
176
168
160
152
144
136
128
120
112
104
96
88
80
72
64
56
48
40
32
24
16
8
0
Chemical Shift (ppm)

11

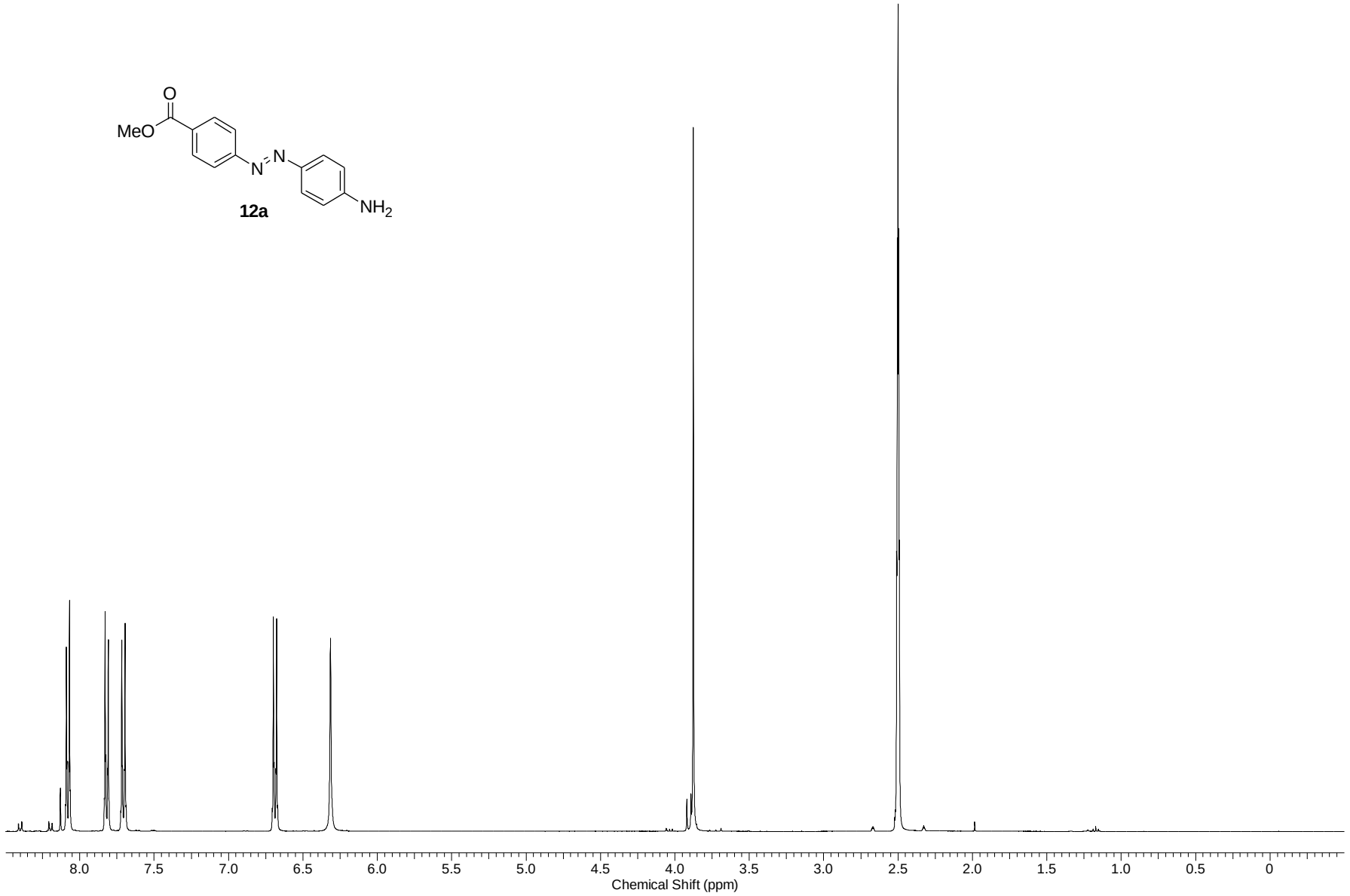
O
MeO
N
N
NH2
12a
8.0
7.5
7.0
6.5
6.0
5.5
5.0
4.5
4.0
3.5
3.0
2.5
2.0
1.5
1.0
0.5
0
Chemical Shift (ppm)

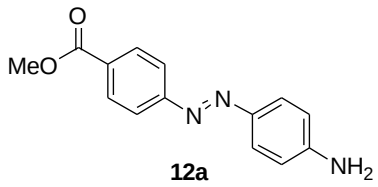
O
MeO
N
N
NH2

12a

176
168
160
152
144
136
128
120
112
104
96
88
80
72
64
56
48
40
32
24
16
8
0
Chemical Shift (ppm)

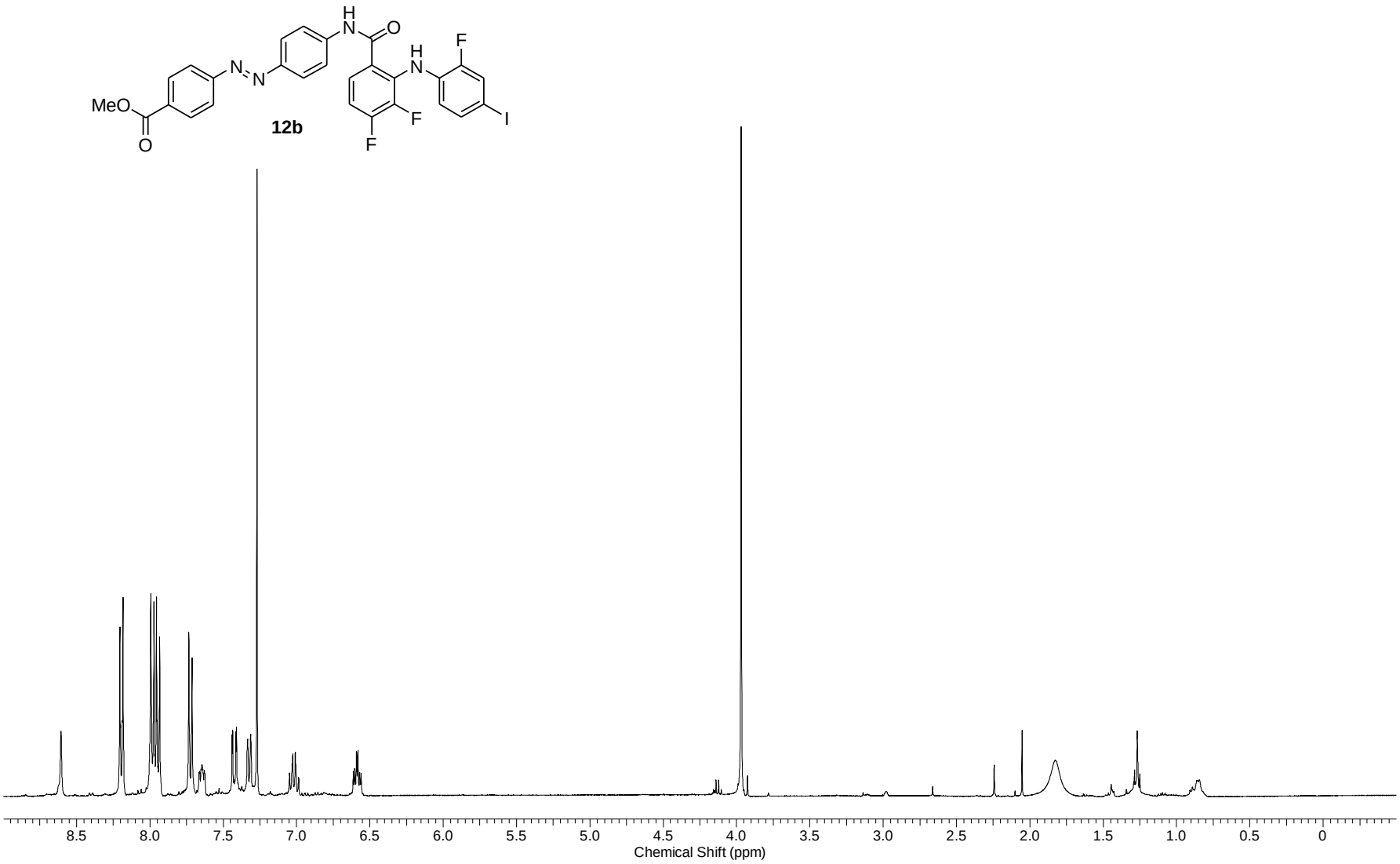
MeO
O
N
N
H
N
O
H
N
F
F
F
I
12b
8.5
8.0
7.5
7.0
6.5
6.0
5.5
5.0
4.5
4.0
3.5
3.0
2.5
2.0
1.5
1.0
0.5
0
Chemical Shift (ppm)

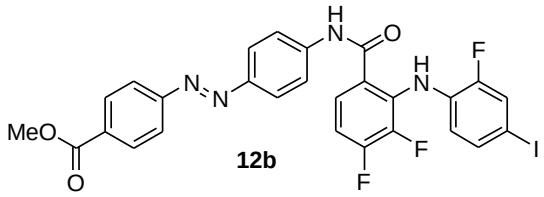
MeO
O
N
N
H
N
O
H
N
F
F
F
I

12b

176
168
160
152
144
136
128
120
112
104
96
88
80
72
64
56
48
40
32
24
16
8
0
Chemical Shift (ppm)

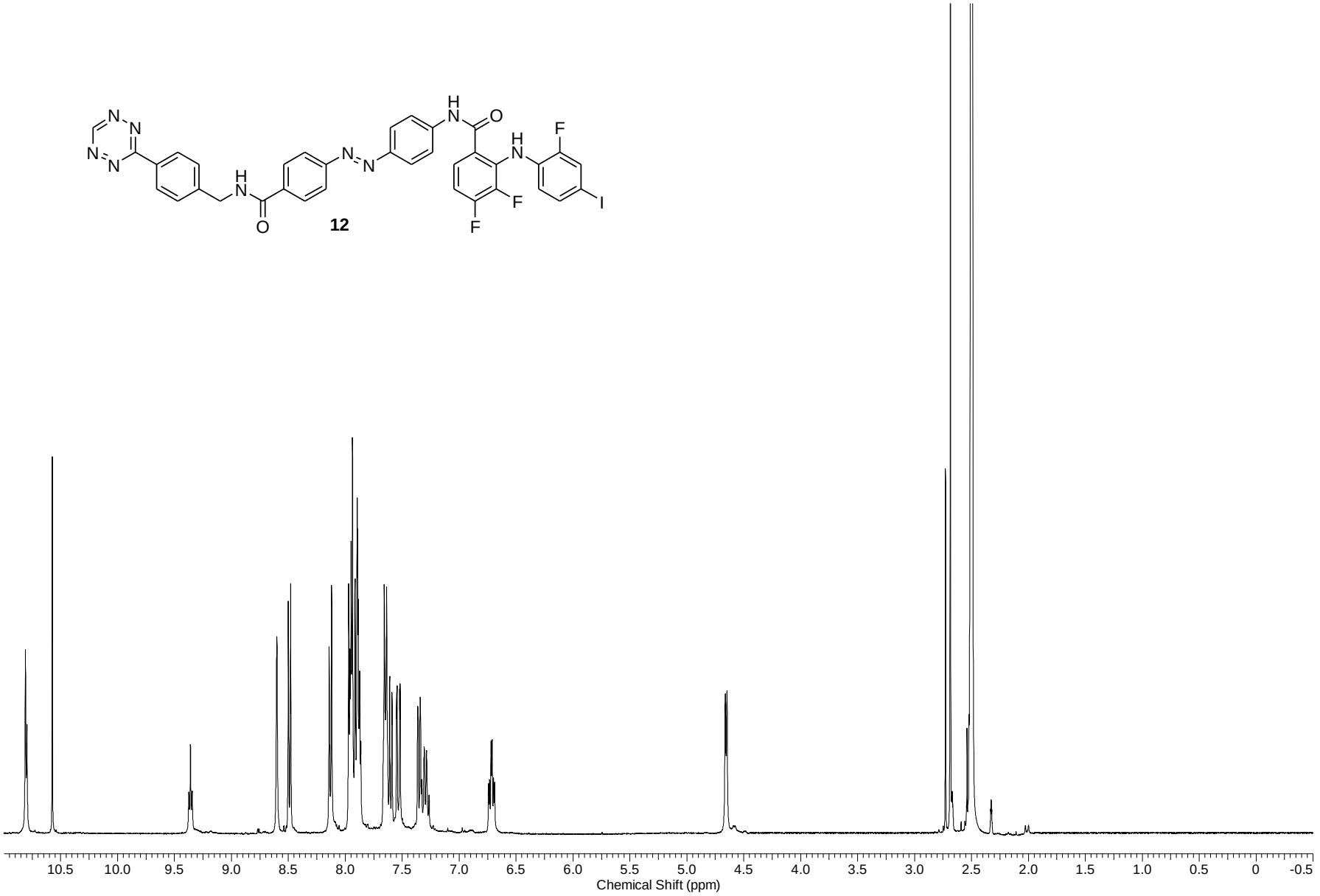
12
10.5
10.0
9.5
9.0
8.5
8.0
7.5
7.0
6.5
6.0
5.5
5.0
4.5
4.0
3.5
3.0
2.5
2.0
1.5
1.0
0.5
0
-0.5
Chemical Shift (ppm)

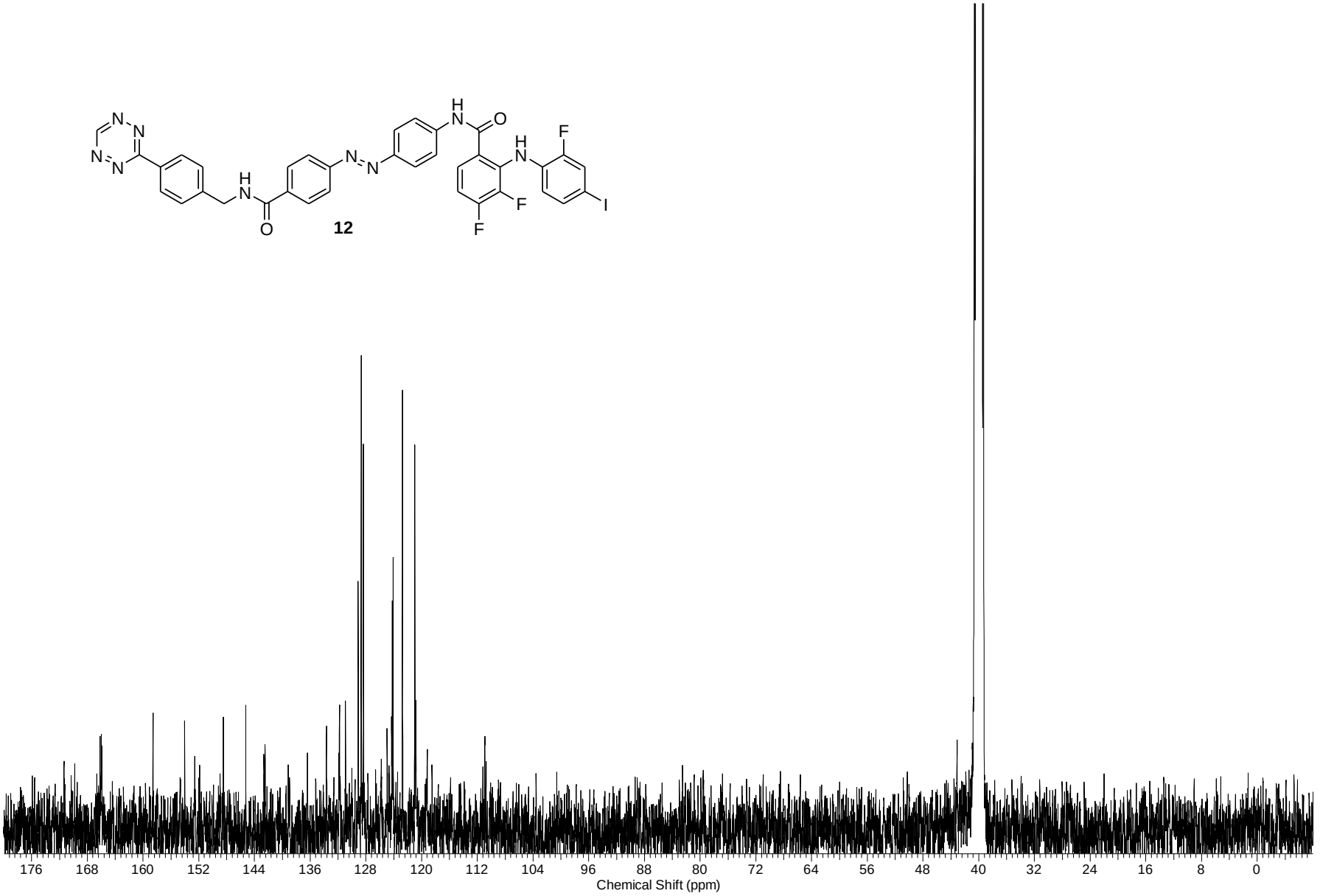
12
176
168
160
152
144
136
128
120
112
104
96
88
80
72
64
56
48
40
32
24
16
8
0
Chemical Shift (ppm)

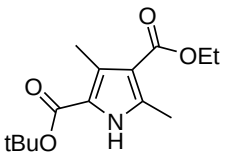
O
OEt
O
N
H
tBuO

15c

9.0
8.5
8.0
7.5
7.0
6.5
6.0
5.5
5.0
4.5
4.0
3.5
3.0
2.5
2.0
1.5
1.0
0.5
0
Chemical Shift (ppm)

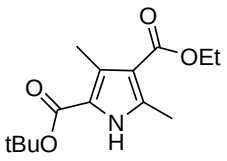
O
OEt
O
N
H
tBuO

15c

176
168
160
152
144
136
128
120
112
104
96
88
80
72
64
56
48
40
32
24
16
8
0
Chemical Shift (ppm)

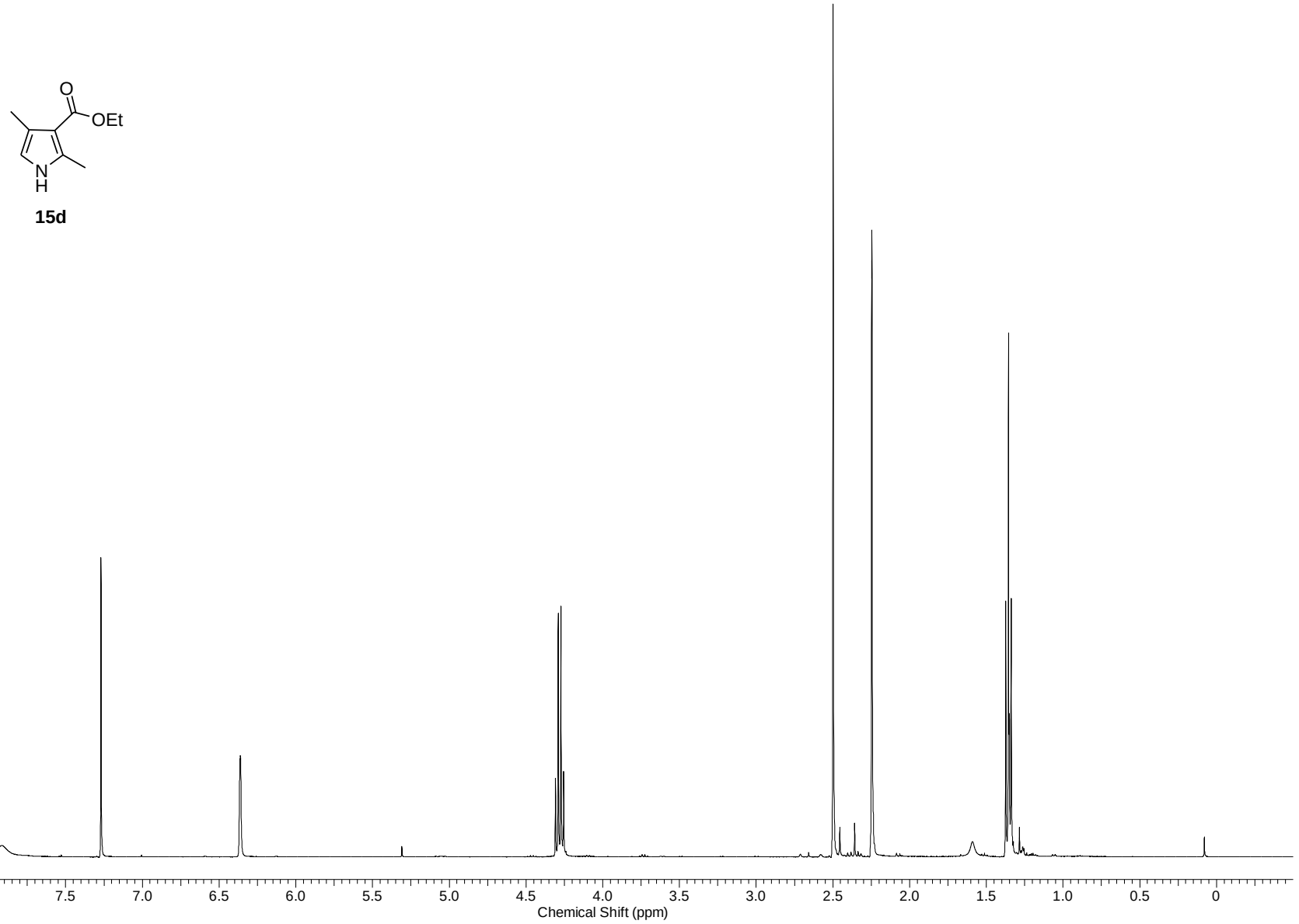
O
OEt
N
H
8.0
7.5
7.0
6.5
6.0
5.5
5.0
4.5
4.0
3.5
3.0
2.5
2.0
1.5
1.0
0.5
0
Chemical Shift (ppm)

15d

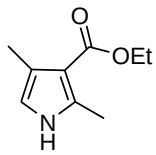
O
OEt
N
H

15d

176
168
160
152
144
136
128
120
112
104
96
88
80
72
64
56
48
40
32
24
16
8
0
Chemical Shift (ppm)

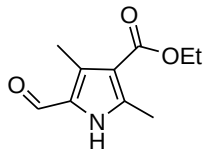
O
OEt
O
N
H

15e

10.5
10.0
9.5
9.0
8.5
8.0
7.5
7.0
6.5
6.0
5.5
5.0
4.5
4.0
3.5
3.0
2.5
2.0
1.5
1.0
0.5
0
Chemical Shift (ppm)

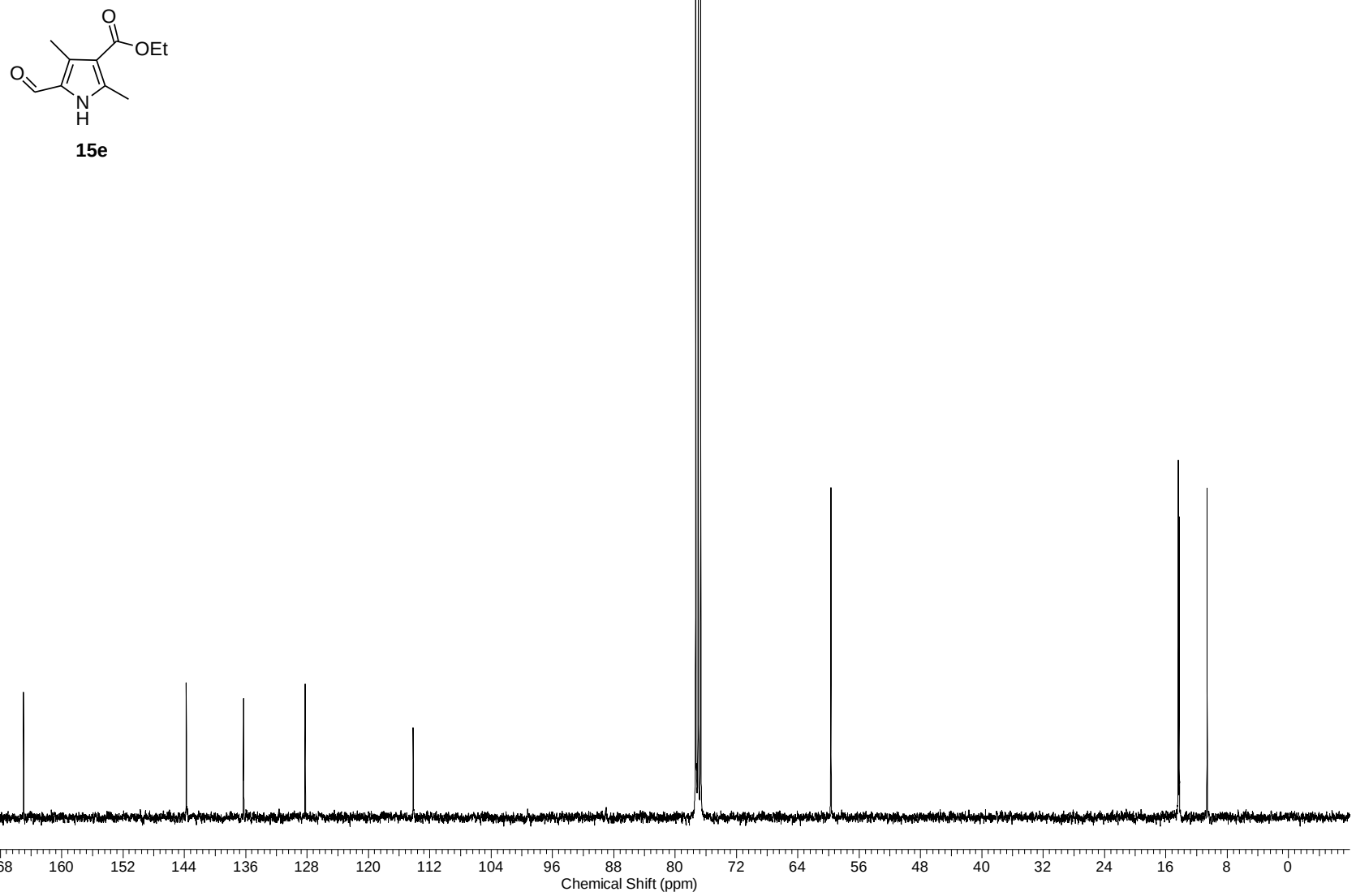
O
OEt
O
N
H
176
168
160
152
144
136
128
120
112
104
96
88
80
72
64
56
48
40
32
24
16
8
0
Chemical Shift (ppm)

15e

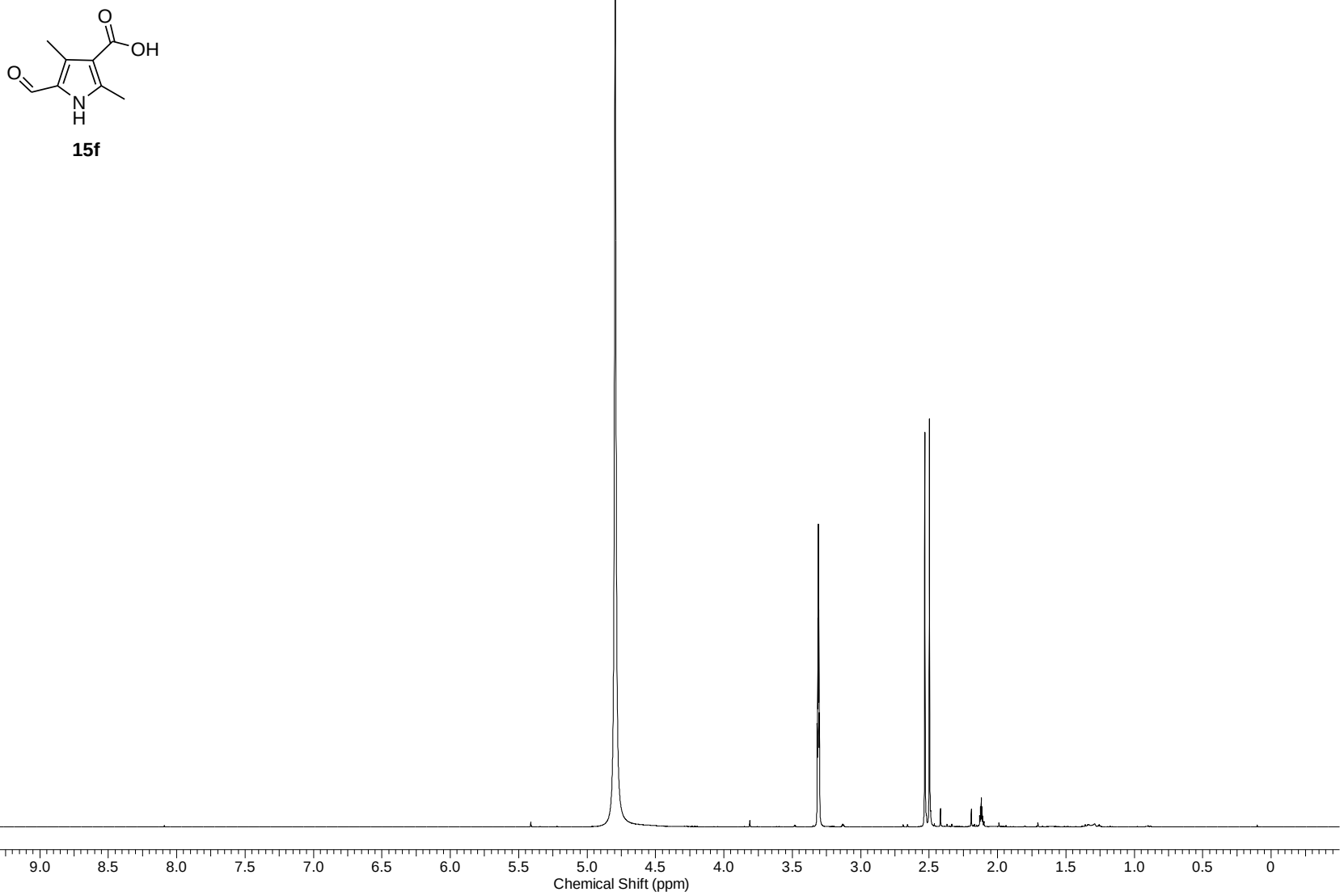
O
OH
O
N
H
9.5
9.0
8.5
8.0
7.5
7.0
6.5
6.0
5.5
5.0
4.5
4.0
3.5
3.0
2.5
2.0
1.5
1.0
0.5
0
Chemical Shift (ppm)

15f

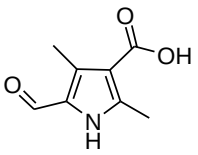
O
OH
O
N
H

15f

176
168
160
152
144
136
128
120
112
104
96
88
80
72
64
56
48
40
32
24
16
8
0
Chemical Shift (ppm)

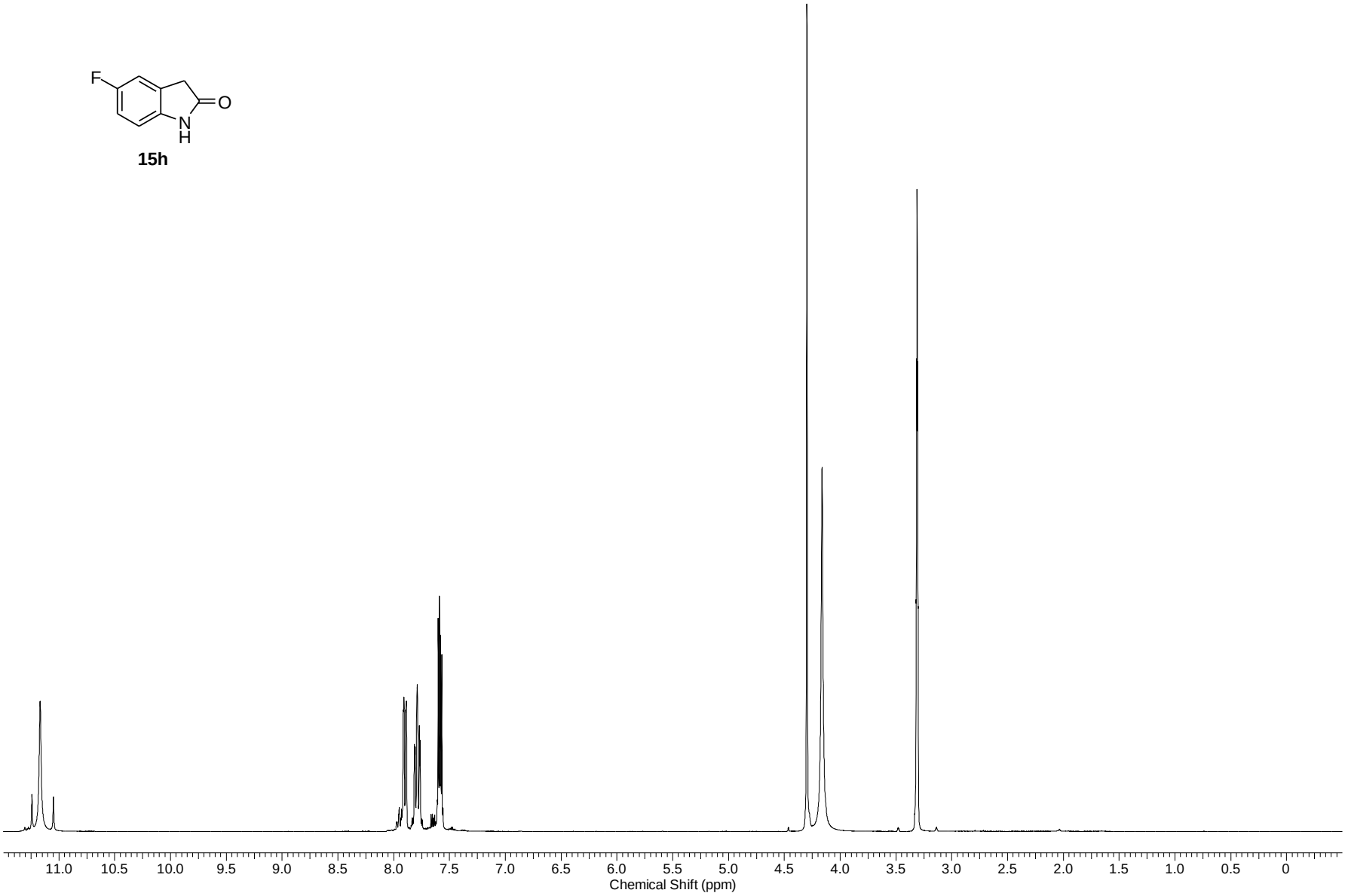
F
O
N
H
15h
11.0
10.5
10.0
9.5
9.0
8.5
8.0
7.5
7.0
6.5
6.0
5.5
5.0
4.5
4.0
3.5
3.0
2.5
2.0
1.5
1.0
0.5
0
Chemical Shift (ppm)

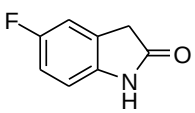
F
O
N
H

15h

184
176
168
160
152
144
136
128
120
112
104
96
88
80
72
64
56
48
40
32
24
16
8
0
Chemical Shift (ppm)

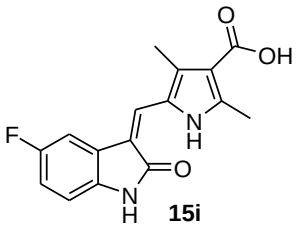

15i

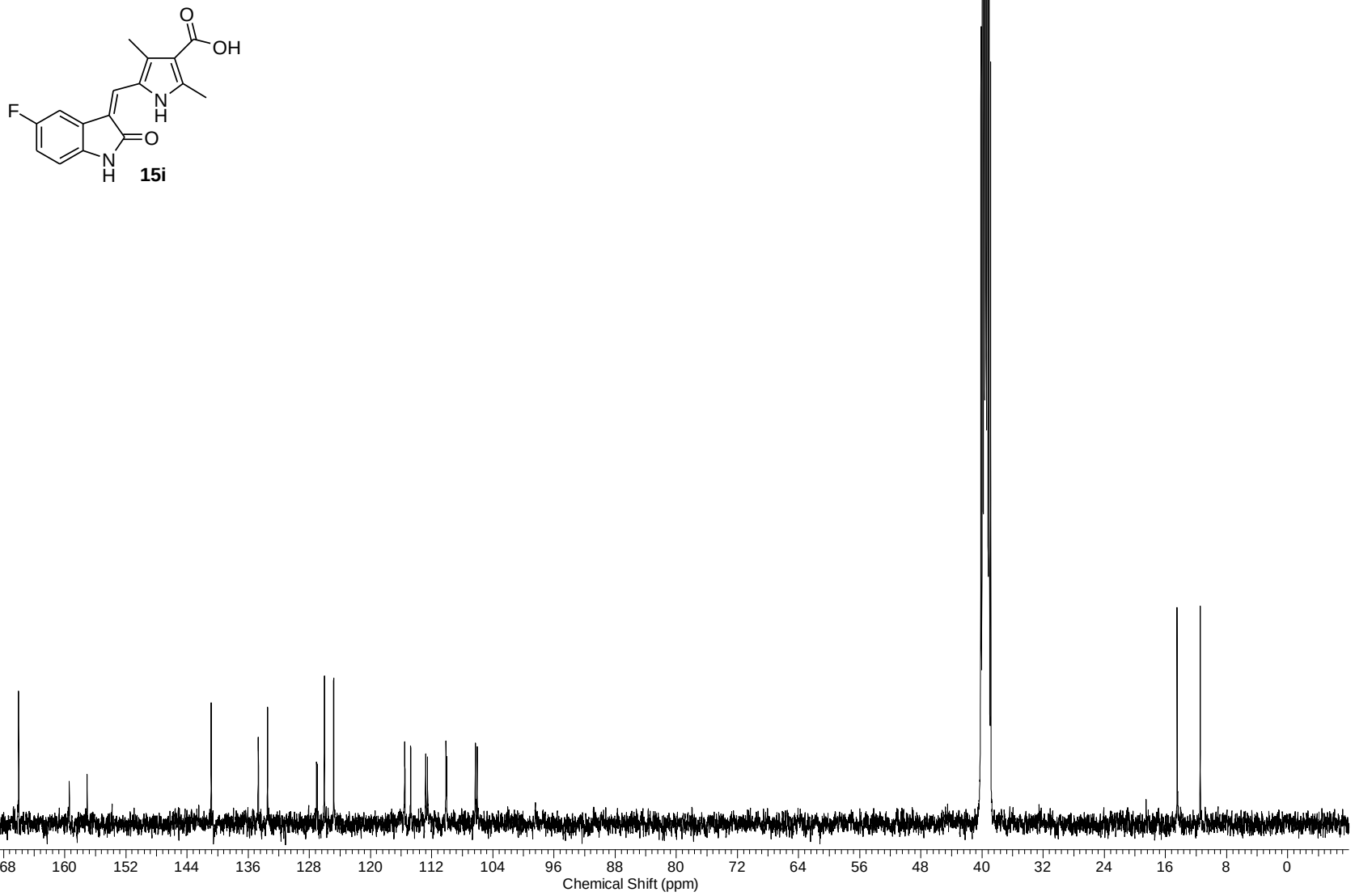
O
OH
F
N
H
O
N
H
15i
176
168
160
152
144
136
128
120
112
104
96
88
80
72
64
56
48
40
32
24
16
8
0
Chemical Shift (ppm)

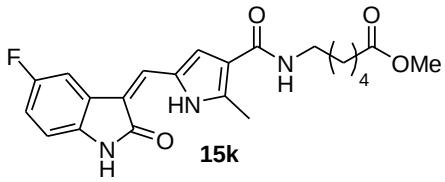

15k

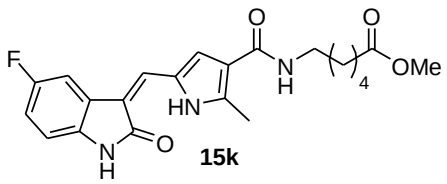
F
O
N
H
HN
O
O
N
H
4
OMe

15k

176
168
160
152
144
136
128
120
112
104
96
88
80
72
64
56
48
40
32
24
16
8
0
Chemical Shift (ppm)

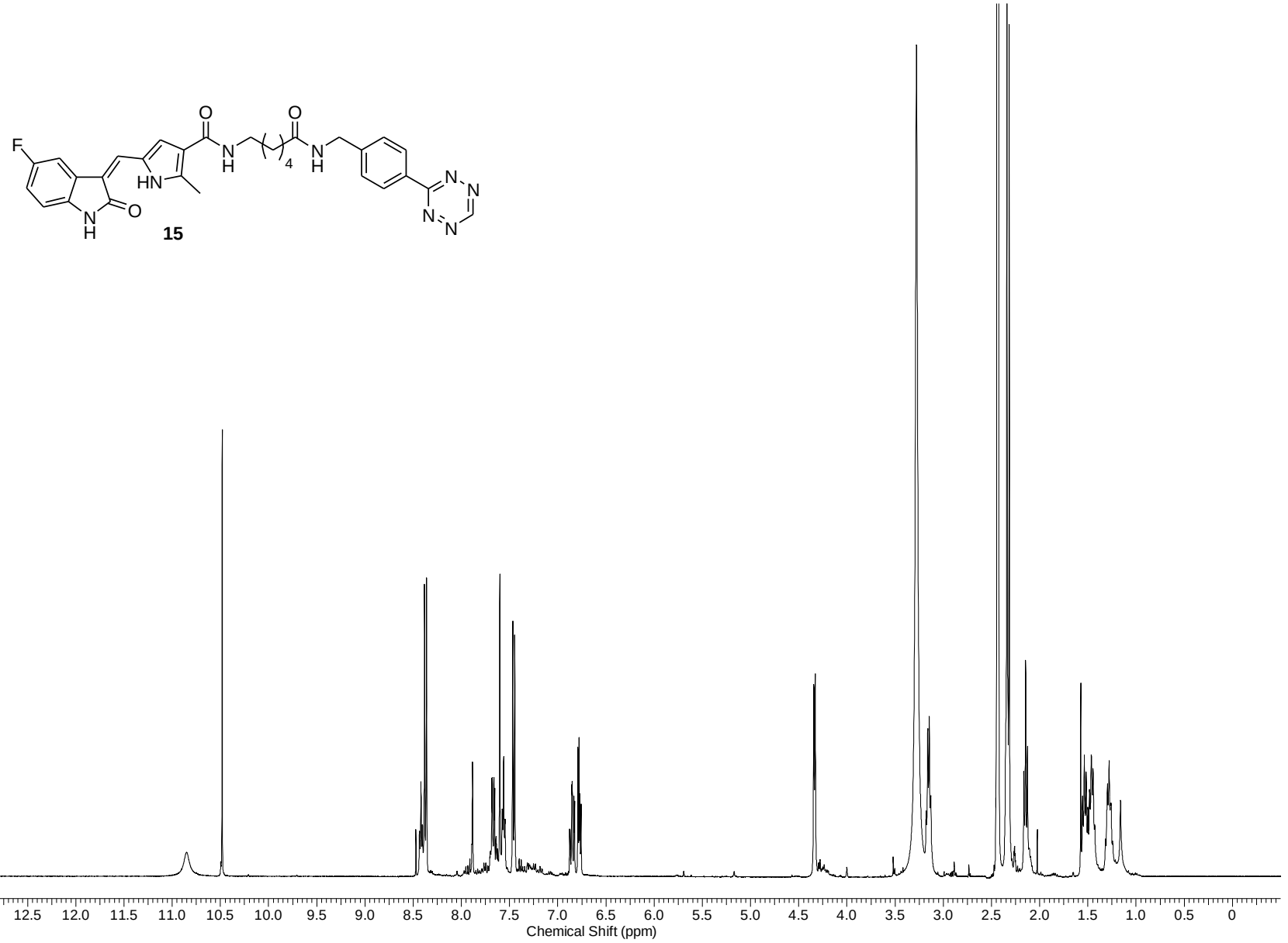
F
O
N
H
HN
O
N
H
4
O
N
H
N
N
N
N
15
13.5 13.0 12.5 12.0 11.5 11.0 10.5 10.0 9.5 9.0 8.5 8.0 7.5 7.0 6.5 6.0 5.5 5.0 4.5 4.0 3.5 3.0 2.5 2.0 1.5 1.0 0.5 0
Chemical Shift (ppm)

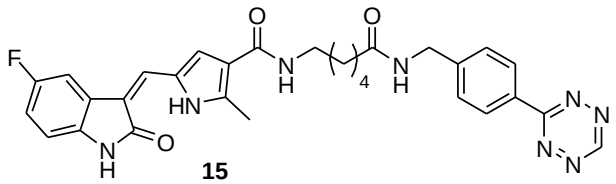
F
O
N
H
HN
O
N
H
4
O
N
H
N
N
N
N

15

176
168
160
152
144
136
128
120
112
104
96
88
80
72
64
56
48
40
32
24
16
8
0
-8
Chemical Shift (ppm)